A Re-Analysis of Nutrient Mass Balances in the Hartbeespoort Dam

Alexandra Carroll
Student number: 546875

Supervised by Prof. C. Curtis

School of Geography, Archaeology and Environmental Studies
University of the Witwatersrand
2019

DECLARATION OF PLAGERISM

I Alexandra Carroll (Student number: 546875) am a student registered for the degree of Master of Science (Coursework and Research Report) in Environmental Science in the academic year 2020.

I hereby declare the following:

- I am aware that plagiarism (the use of someone else's work without their permission and/or without acknowledging the original source) is wrong.
- I confirm that the work submitted for assessment for the above degree is my own unaided work except where I have explicitly indicated otherwise.
- I have followed the required conventions in referencing the thoughts and ideas of others.
- I understand that the University of the Witwatersrand may take disciplinary action against me if there is a belief that this is not my own unaided work or that I have failed to acknowledge the source of the ideas or words in my writing.

Signature:  Date: 21 May 2020

ACKNOWLEDGMENTS

To my supervisor, Prof. Chris Curtis, I greatly appreciate your insightful guidance and highly regarded knowledge over the last three years.

To Renette Krommenhoek, thank you for providing me with sound statistical advice.

To my mother, Wendy Carroll, and brother, Grant Carroll, thank you for your patience and support.

To my father, David Carroll, thank you for inspiring in me a love of science and a drive for understanding, discernment and learning.

ABSTRACT

The Hartbeespoort Dam, located 40 km west of Tshwane on the Crocodile River, has recently been described as the most eutrophic dam in Africa. The dam is situated in one of the most economically active areas of South Africa and receives a high nutrient input from 11 wastewater treatment plants, leaking sewers and urban and agricultural runoff. The Metsi a Me programme, which ran from 2006 to 2016, aimed to mitigate in-lake nutrient stocks using biomanipulation, including the physical removal of water hyacinth and algae. This study reassesses the debate regarding nutrient stocks and fluxes in the Hartbeespoort Dam. Using Department of Water and Sanitation water quality and flow data, the annual input and output fluxes of total nitrogen (TN) and total phosphorus (TP) to the Hartbeespoort Dam from 2010 to 2018 were calculated, which formed the principal focus of this study. Through literature review and previous studies the relative importance of nutrient removal from biomass harvesting in relation to retained nutrients was assessed. Between 2010 and 2017, the range of P to the Hartbeespoort Dam from rivers was 578 to 610 t/a and the range of N was 4437 to 4687 t/a. On average, the P inflow flux increased by 54.2 to 77.8 t/a and the N inflow flux increased by 368 to 465 t each year, a reversal of a long-term decreasing trend. A generous estimation of the total annual nutrient removal from hyacinth and algae harvesting combined is 1% of the nutrient influx. Much of the nutrient flux to the dam is sedimented. A summary of the flux calculations of this study is shown on the diagram on the next page. Thus, the upgrading of WWTWs in the catchment and the refurbishing of leaking and overflowing sewers is the most appropriate long-term solution to the eutrophication problem at the Hartbesspoort Dam.

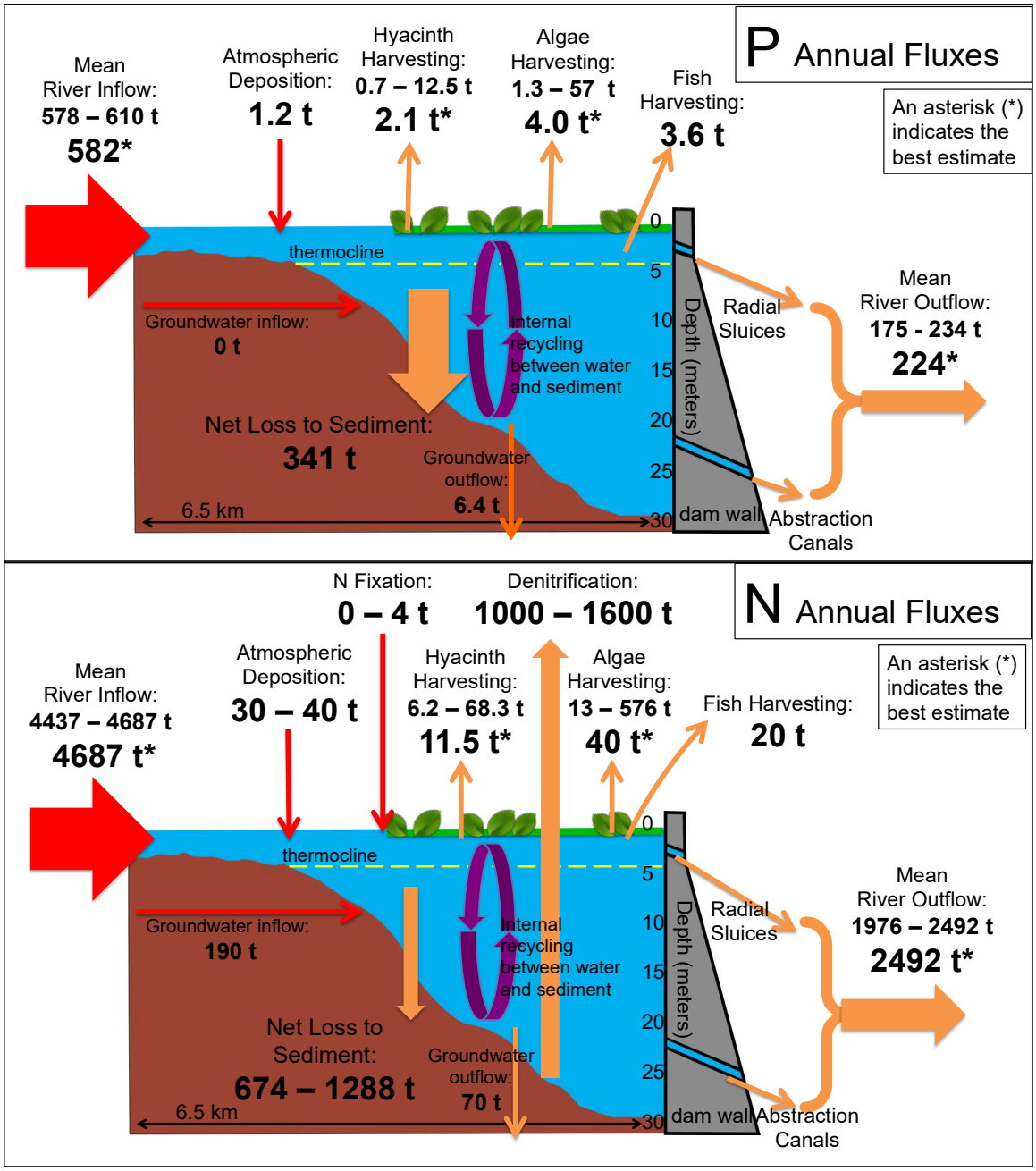

Conceptual diagram of annual P (above) and N (below) fluxes in the Hartbeespoort Dam during 2010 to 2017. Red arrows represent nutrient inputs. Orange arrows represent nutrient outputs. Widths of input and output arrows represent approximate relative flux contributions. Purple arrow represents recycling.

TABLE OF CONTENTS

DECLARATION OF PLAGERISM i

ACKNOWLEDGMENTS ii

ABSTRACT iii

LIST OF FIGURES viii

LIST OF TABLES x

CHAPTER 1: INTRODUCTION 1

1.1. Background 1

1.1.1. The Hartebeespoort Dam and the Integrated Biological Remediation Programme 1

1.1.2. An Introduction to Eutrophication 2

1.2. Problem statement 3

1.3. Aim and objectives 4

CHAPTER 2: LITERATURE REVIEW 5

2.1. Water scarcity in South Africa 5

2.2. Overview of Eutrophication 6

2.2.1. Global understanding of eutrophication 6

2.2.2. Eutrophication research in South Africa 6

2.2.3. Stratification 7

2.3. Strategies for controlling eutrophication 8

2.3.1. Reduction of inputs 8

2.3.2. Removal of in-lake nutrients 8

2.3.3. Controlling eutrophication symptoms (i.e. algae) 9

2.3.4. Biomanipulation 9

2.4. The 'P-Only' control debate 10

2.5. Mass balances and pollution load determination models and tools 11

2.6. Eutrophication modeling at the Hartbeespoort Dam 12

2.7. Study area 14

2.7.1. Land use 14

2.7.2. Climate 15

2.7.3. Geology and hydrology 15

2.8. Data available from the Department of Water and Sanitation 15

CHAPTER 3: METHODS 19

3.1. Calculation of a mass balance 19

3.2. River inputs and outputs 19
3.2.1. Sampling locations 20
3.2.2. N and P definitions 24
3.2.3. DWS laboratory methods 24
3.2.3.(a). Total phosphate as P (P) (mg/L) 25
3.2.3.(b). Orthophosphate as P (PO_4) (mg/L) 25
3.2.2.(c). Nitrate plus nitrite ($NO_3 + NO_2 – N$) (mg/L) 25
3.2.3.(d). Kjeldahl nitrogen ($NH_4 – N$) (mg/L) 26
3.2.4. Date format of flow data corrections 26
3.2.5. Flow rate 27
3.2.5.(a). Spot flow values 27
3.2.5.(b). Daily Average flow values 28
3.2.5.(c). "Two-Weekly" flow values 28
3.2.5.(d). Comparison of the three flux calculation methods 30
3.2.6. Seasonal inflow and outflow calculations 30
3.2.7. Annual inflow and outflow calculations 31
3.2.8. Standard deviation calculations 32
3.2.9. Missing data 32
3.2.10. Statistical analysis 33
3.2.11. Flow vs. concentration plots 33
3.3. Other flux contributors 34
3.3.1. Water hyacinth biomass output 34
3.3.1 (a) Hyacinth density 35
3.3.1 (b) Hyacinth dry matter composition 35
3.3.1 (c) Hyacinth N or P dry weight composition 36
3.3.2. Algae biomass output 36
3.3.2 (a) Algal biomass output Method 1 37
3.3.2 (b) Algal biomass output Method 2 39
3.3.3. Fish biomass output 40
3.3.3.(a). N removal from fish biomass estimation method 41
3.3.3.(b). P removal from fish biomass estimation method 41
3.3.4 Denitrification output 42
3.3.5. Atmospheric deposition inputs 42
3.3.6. N fixation input 43
3.3.7. Groundwater input and output 43
3.3.8 Sedimentation 44

CHAPTER 4: RIVER FLUX RESULTS 46
4.1. Annual P and N river inflows and outflows 46
4.2. Impact of flow on inflow flux 47
4.3. Impact of flow on outflow flux 51
4.4. P seasonal time series and trends 55
4.5. N Seasonal time series and trends 59
4.6. How representative is the flow on sampling days? 63

4.7. Does flow affect concentration at inflow sites? 67

4.8. Can water chemistry of the Left Canal be used to infill missing data of the Right Canal and vice versa? 70

CHAPTER 5: OTHER FLUX CONTRIBUTORS 72

5.1. Water hyacinth biomass output 72

5.2. Algae biomass output 72

5.3. Fish biomass output 73

5.4. Denitrification output 74

5.5. Atmospheric deposition input 75

5.6. N Fixation input 76

5.7. Groundwater Input and Output 76

5.8. Sedimentation and mass balances 77

CHAPTER 6: CONCLUSIONS AND LIMITATIONS 79

6.1. Overview of mass balances 79

6.2. Sources of nutrient influxes 79

6.3. Trends 80

6.4. Flux uncertainties 81

6.5. Limitations of the study 82

6.6. The way forward 83

CHAPTER 6: REFERENCES 84

CHAPTER 7: APPENDIX 95

7.1. Breakdown of seasonal P fluxes and trends of individual sites 95

7.2. Time series of N and P inflow and outflow using Daily Average flow values 99

7.3. Did flow increase over the study time period? 102

7.4. Relationship between orthophosphate (OP) and total phosphorus (TP) 103

LIST OF FIGURES

Fig. 3.2.1.(a): Map of Hartbeespoort Dam catchment area and river sampling sites. 21

Fig. 3.2.1.(b): Satellite photograph of river outflow sampling locations (represented by yellow markers) in relation to the Hartbeespoort Dam wall (represented by a red marker). 22

Fig. 3.2.1.(c): Photograph of inflow site on the Crocodile River. 22

Fig. 3.2.1 (d): Photograph of outflow site on Crocodile River. Dam wall visible in the distance. 23

Fig. 3.2.1 (e): Photograph of right canal from above. 23

Fig. 4.2.1: Mean P flux (t/a) of the different flow calculation methods at the inflow site on the Crocodile River. Bars represent means. Error bars represent standard deviations. 49

Fig. 4.2.2: N flux (t/a) of the different flow calculation methods at the inflow site on the Crocodile River. Bars represent means. Error bars represent standard deviation. ... 50

Fig. 4.3.1: Mean P outflow flux (t/a) of the various flux calculation methods. Bars represent means, error bars represent standard deviation and letters indicate significant differences. 53

Fig. 4.3.2: Comparison of the mean outflow N flux (t/a) of the various flux calculation methods. Bars represent means, error bars represent standard deviation and letters indicate significant differences. 54

Fig. 4.4.1: Seasonal river flux of P into and out of the Hartbeespoort Dam (t/season) from June 2010 until February 2018. Calculations based on Spot Flow values. Error bars represent standard deviations. 56

Fig. 4.4.2: Seasonal river TP fluxes into and out of the Hartbeespoort Dam (t/season) from June 2010 until February 2018. Calculations based on Two-Weekly Flow values. Error bars represent weighted standard deviations. 57

Fig. 4.4.3: Annual P (t/a) inflow, outflow and difference (inflow minus outflow) for hydrological years (October – September) at the Hartbeespoort Dam using two-weekly values. 58

Fig. 4.5.1: Seasonal N river fluxes into and out of the Hartbeespoort Dam (t/season) from June 2010 until February 2018. Calculations based on spot flow values. Error bars represent standard deviations. Outflow trend line not significant. 60

Fig.4.5.2: Seasonal N river fluxes into and out of the Hartbeespoort Dam in tons per season from June 2010 until January 2018. Calculations based on two-weekly flow values. Error bars represent weighted standard deviations. 61

Fig 4.5.3: Annual N (t/a) inflow, outflow and difference (inflow minus outflow) for hydrological years (October – September) at the Hartbeespoort Dam using two-weekly values. 62

Fig. 4.6.1: Distribution of the complete raw flow dataset from 2 June 2010 until 25 April 2018 at inflow site on the Crocodile River. *n* = 309 946. 65

Fig. 4.6.2: Distribution of Spot flow values used to calculate nutrient fluxes at inflow site on the Crocodile River. *n* = 178 66

Fig. 4.6.3: Distribution of Daily Average flow values used to calculate nutrient fluxes at inflow Site on the Crocodile River. *n* = 177 66

Fig. 4.6.4: Distribution of Two-Weekly flow values used to calculate nutrient fluxes at inflow Site on the Crocodile River. *n* = 178 67

Fig. 4.7.1: Relationship between Spot flow (m^3/s) and P concentration (mg/L) at the inflow site on the Crocodile River. Straight line represents linear relationship (not significant). 68

Fig. 4.7.2: Relationship between Spot flow (m^3/s) and P concentration (mg/L) at The inflow site on the Magalies River. Straight line represents linear relationship (significant). 69

Fig. 4.8.1: Box-and-whisker plots comparing the data spread of P concentration (mg/L) (A) and N concentration (mg/L) (B) of the left and right canals on days where both sites were measured on the same day. 71

Fig. 5.8.1: Conceptual diagram of annual P (above) and N (below) fluxes in the Hartbeespoort Dam during 2010 to 2017 78

LIST OF TABLES

Table 2.8.1: Available data for river stations before the inflow into the Dam (as of 30 May 2018) 16

Table 2.8.2: Available data for river stations at the outflow from the Dam (as of 30 May 2018) 17

Table 2.8.3: Available data for stations on the Dam (as of 30 May 2018)..... 18

Table 3.3.1: Cubic metres of water hyacinth removed each year by the Metsi a Me programme as reported in response to Parliamentary question 2936 of 7 October 2015. Years assumed to span from April to March the following year. 35

Table 3.3.2.1: Cubic metres of algae "soup" removed each year by the Metsi a Me programme as reported in response to Parliamentary question 2936 of 7 October 2015. Years assumed to span from April to March the following year. 36

Table 3.3.3.1: Kilograms of fish removed each year by the Metsi a Me programme as reported in response to Parliamentary question 2936 of 7 October 2015. 40

Table 3.3.3.2: Mean annual yield fish biomass removed by anglers from the Hartbeespoort between 1982 and 1984 (NIWR, 1985) 41

Table 4.1.1: Annual river P inflow and outflow of the Hartbeespoort Dam using the three flux calculation methods for hydrological years 2010-2011 until 2016-2017..... 46

Table 4.1.2: Annual N inflow and outflow using the three flux calculation methods for hydrological years 2010-2011 until 2016-2017 47

Table 4.2.1: Descriptive statistics of the various P flux calculation methods of the inflow site on the Crocodile River 49

Table 4.2.3: Descriptive statistics of the various N flux calculation methods of site 90164 on the Crocodile River 50

Table 4.2.2: Pairwise comparison of *p*-values for the various P flux calculation methods at the inflow site on the Crocodile River (no significant differences). 51

Table 4.2.4: Pairwise comparison of *p*-values for the various N flux calculation methods at the inflow site on the Crocodile River (no significant differences). 51

Table 4.3.1: Descriptive statistics of the various P outflow flux calculation methods based on monthly averages 53

Table 4.3.3: Descriptive statistics of the various N outflow flux calculation methods based on monthly averages 54

Table 4.3.2: Pairwise comparison of *p*-values for the various P outflow flux calculation methods ("*" indicates significant difference). 55

Table 4.3.4: Pairwise comparison of *p*-values for the various N outflow flux calculation methods ("*" indicates significant difference). 55

Table 4.4.1: Descriptive statistics of seasonal P inflow and outflow (Spot flow method) 56

Table 4.4.2: Descriptive statistics of seasonal P inflow and outflow (Two-Weekly flow method) 57

Table 4.4.3: Sen's Slope and seasonal Mann-Kendall *p*-values of inflow and outflow P fluxes for the various flux calculation methods (asterisk indicates statistical significance) 59

Table 4.5.1: Descriptive statistics of seasonal N inflow and outflow (Spot flow method) 60

Table 4.5.2: Descriptive statistics of seasonal N inflow and outflow (Two-Weekly flow) 61

Table 4.5.3: Sen's Slope and seasonal Mann-Kendall *p*-values of inflow and outflow N fluxes for the various flux calculation methods (asterisk indicates statistical significance) 63

Table 4.6.1: Descriptive statistics of the complete raw flow dataset and flow values of the various flux calculation methods of inflow site 90164 on the Crocodile River, and Kolmogorov-Smirnov test *p*-values ('*' indicates significant difference) 64

Table 4.7.1: Descriptive statistics of P concentrations (mg/L) at river inflow sites from June 2010 until April 2018 69

Table 4.7.2: Descriptive Statistics of flow (m^3/s) at inflow the inflow site on the Magalies River from June 2010 until April 2018 70

Table 5.1: Total, average annual and largest annual yield estimates of P and N removed from the Harbeespoort from water hyacinth removal during the Metsi a Me programme 72

Table 5.2: Total, average annual and largest annual yield estimates of P and N removed from the Harbeespoort from algae removal during the Metsi a Me programme 73

Table 5.3.1: N and P removal estimates from fish biomass harvesting from Anglers and the Metsi a Me programme in the Hartbeespoort Dam 73

Table 5.4.1: Denitrification rates from the literature. Range of tons removed from Hartbeespoort Dam given in brackets. 74

Table 5.5.1: Atmospheric deposition P fluxes from the literature. Range of flux to the Hartbeespoort Dam given in brackets 75

Table 5.5.2: Atmospheric deposition N fluxes from the literature. Range of flux to the Hartbeespoort Dam given in brackets 75

Table 5.6.1: N fixation rates from the literature. Range flux to the Hartbeespoort Dam given in brackets. 76

Table 5.7.1: Groundwater flow and N/P flux estimations of inflows and outflow 76

CHAPTER 1: INTRODUCTION

1.1. Background

1.1.1. The Hartebeespoort Dam and the Integrated Biological Remediation Programme

The Hartbeespoort Dam is located about 37 km west of Pretoria on the Crocodile River in the North West Province of South Africa and was completed in 1925 (Chutter and Rossouw, 1991). The dam was originally intended to be used solely for irrigation but as the population of the area grew it subsequently also became used for recreation and as a source of drinking water (Chutter and Rossouw, 1991). The largest river that sustains the dam, the Crocodile River, has its source in the Witwatersrand mountain range. The upper reaches of the Crocodile River catchment are densely settled. High levels of urbanisation as well as dysfunctional sewerage systems, result in sewage and industrial discharges to the Crocodile River from Johannesburg, Midrand and Krugersdorp (RHP, 2005). Water researcher Professor Antony Turton has recently described the Hartbeespoort Dam as the most eutrophic dam on the continent (Bega, 2016). The initial findings of the Green Drop 2014 assessment showed that regress in the performance of South African municipal treatment facilities is evident from 2014 (Mashitisho, 2017). In Gauteng, 40 out of 58 wastewater treatment works (WWTWs) took up a higher risk position than their 2013 assessments and 477 out of 824 WWTWs in the country are classed as having high or critical risk (Mashitisho, 2017). In addition, aging sewerage infrastructure and frequently blocked and broken pipelines cause overspill into storm water drains (Crafford and Mitchell, 2016; Bwapwa, 2018) Eutrophication can be briefly summarised as an oversupply of plant nutrients into an environment causing excessive growth of certain plants and algae, typically phytoplankton but also hyacinth and reeds (Rossouw *et al*., 2008). This is associated with a loss of biodiversity and ecosystem health as well as the increasing dominance of potentially toxic cyanobacteria (Rossouw *et al.*, 2008).

In aquatic ecosystems that are subjected to nutrient enrichment, the reduction or removal (harvesting) of plant and/or animal biomass in order to reduce nutrient stocks and associated nutrient recycling is widely advocated as a strategy to alleviate the problem (Hart and Harding, 2015). The Hartbeespoort Dam Integrated Biological Remediation

Programme (HDIBRP), also known as “Harties Metsi a Me”, which ran from 2006 until 2016, aimed to rehabilitate the dam using this strategy and had a strong food-web restructuring approach. The multi-pronged approach involved fish removal, algae and hyacinth biomass harvesting, sediment dredging, construction of floating wetlands and vermiculture. According to the project leader, Petrus Venter:

> “The vision of the Harties Metsi a Me programme is the restoration of the Hartbeespoort Dam ecosystem to a level where it will be able to function naturally again including coping with reasonable levels of incoming nutrients.” (HDRP, 2012)

As early as 1985 it was determined that removal of water hyacinth and algae from the dam would serve a purely aesthetic purpose and would be unlikely to improve the impacts of eutrophication (NWIR, 1985). Several recent studies support the argument that biomanipulation is an ineffective method of reducing nutrient stocks in the Hartbeespoort Dam (Hart and Harding, 2015; Hart and Mathews, 2018). These studies concluded that the trophic status of the Hartbeespoort Dam is too high for biomanipulation to have a significant effect on nutrient stocks. In addition, Hart (2006) concluded that "as far as can be generalised, prospects of applying classical biomanipulation as a management tool to ameliorate consequences of eutrophication in local reservoirs are weak". Nevertheless, biomanipulation is cited as a strategy for controlling eutrophication at the Hartbeespoort Dam in the Metsi a Me management plans. One of the aims of the study is to investigate whether biomass harvesting is an effective method of reducing the in-lake nutrient volumes. Using nutrient budgets, volumes of nutrients removed from the dam through algae and hyacinth biomass harvesting are compared with the incoming nutrient flux.

1.1.2. An Introduction to Eutrophication

Eutrophication is regarded as the greatest threat globally to freshwater and coastal marine ecosystems (Smith and Schindler, 2009). In addition, eutrophic water bodies lose their

usefulness and safety as domestic and industrial water supplies because of secondary metabolites produced by cyanobacterial blooms that can poison humans, livestock and aquatic foodwebs (Wilson and Chislock, 2013). In South Africa, nutrient enrichment of inland water bodies is widespread and severe (Hart and Harding, 2015). Much of the water stored in reservoirs in South Africa is eutrophic (highly enriched with nutrients) or hypertrophic (grossly enriched with nutrients) (Hart and Harding, 2015). It has been estimated that between 41% and 76% of reservoir-stored water is affected, with the higher value considered to be more realistic (Hart and Harding, 2015).

Fluxes of phosphorus (P) and nitrogen (N) are major components of the many different biophysical and chemical pollutants that cause eutrophication (Rossouw *et al.*, 2008). This means that ecologically intact ecosystems can exist despite high levels of nutrient enrichment but once structural stability is lost, the water body is likely to swing to a state dominated almost entirely by phytoplankton (Rossouw *et al*., 2008). Phytoplankton blooms associated with eutrophication limit light penetration, preventing aquatic flora in the littoral zone from photosynthesising (Chislock *et al*., 2013). Oxygen shortages in the water column caused by the decomposition of algae and aquatic weeds causes loss of aquatic organisms (Khan and Mohammed, 2014). In addition, during times of environmental disturbance, cyanobacteria tend to dominate the phytoplanktonic assemblage in terms of biovolume (Harding and Paxton, 2001). Cyanobacteria have the ability to produce a range of extremely potent biological toxins (Harding and Paxton, 2001). The term "algae" refers to both macroalgae (i.e. seaweeds) and microalgae (cyanobacteria, photosynthetic bacteria and microscopic algae between 5 and 50 μm) (Zamalloa *et al*., 2011). This paper will use the term algae to refer to microalgae.

1.2. Problem statement

The Hartbeespoort Dam is known to receive 350 tons of P annually from eleven wastewater treatment plants in addition to diffuse source nutrients (Mitchell and Crafford, 2016). Although the Hartbeespoort Dam has been studied extensively, much of the work done in earlier studies, particularly regarding nutrient stocks in the dam, is not freely

available and has been a topic of debate among researchers. This study will attempt to reassess and clarify the debate regarding nutrient stocks and fluxes in the Hartbeespoort Dam.

1.3. Aim and objectives

The aim of this study is to perform N and P mass balance calculations on the Hartbeespoort Dam and calculate the retained (i.e. inflow minus outflow) nutrients in the dam. Through literature review and previous studies, the relative importance of nutrient outputs from biomass harvesting in relation to retained nutrients will be assessed in order to determine whether biomass harvesting serves a functional purpose in managing eutrophication by reducing nutrient mass in the dam.

The objectives are:

1. Using Department of Water and Sanitation (DWS) flow and water quality data, calculate the annual input flux of dissolved N and P to the Hartbeespoort Dam from the Crocodile and Magalies Rivers from 2010 to 2018.
2. Using DWS flow and water quality data, calculate the annual flux of dissolved N and P leaving the Hartbeespoort Dam from where surface water exits the dam from 2010 to 2018.
3. Using literature data, estimate the annual input flux of N and P to the Hartbeespoort Dam from atmospheric deposition, groundwater, and N fixation.
4. Using literature data, estimate the annual output flux of N and P from the Hartbeespoort Dam from biomass removal of water hyacinth, algae and fish and from sediment storage to evaluate the impact of biomass removal.

CHAPTER 2: LITERATURE REVIEW

2.1. Water scarcity in South Africa

South Africa has a semi-arid climate with low rainfall and high evapotranspiration (King *et al.*, 2011). Development in South Africa is described as being a "hostage to hydrology" because only a small portion of rainfall is converted to stream flow that can be easily accessed (Turton, 2008). In 2010, 97% of the total available water yield was already being utilised (Claassen, 2010). According to the Department of Water and Sanitation (DWS) in their 2018 master plan, South Africa will be at a 17% water deficit if nothing is done soon (Balzer, 2018). Currently, there may not be enough water to supply projects that will promote economic growth in South Africa. In addition, a growing population and climate change pose risks to water security (Turton, 2012).

Water scarcity is the lack of or inability to access water (Schyns *et al.*, 2015). This can be caused by a physical scarcity, when there is not enough water of sufficient quality to meet the demands of a population or economic scarcity, and when there is a lack of investment in water infrastructure and human capital in a country (Turton, 2012). South Africa currently experiences a combination of natural and economic water scarcity (Turton, 2012). Pollution is one of the greatest threats to water security globally (Vörösmarty *et al.*, 2010). Eutrophication is a natural process in most water bodies that takes place on the timescale of centuries or more (Gong and Xie, 2001). Natural eutrophication is caused by sedimentation, which decreases the depth of the water column and increases the littoral area, resulting in a gradual increase of nutrients and biomass (Laws, 2000). Cultural eutrophication, caused by anthropological activities, speeds up the natural eutrophication process (Gong and Xie, 2001). Cultural eutrophication is the leading cause of poor water quality for many freshwater and coastal marine ecosystems, and is a growing problem for developing countries such as South Africa (Smith and Schindler, 2009).

2.2. Overview of Eutrophication

2.2.1. Global understanding of eutrophication

Climate warming and eutrophication are predicted to become increasingly important threats to the world's ecosystems (Binzer *et al.*, 2015). Population increase and land-use intensification are drivers of eutrophication and their associated toxic algae blooms (Schindler *et al.*, 2016). The largest group of toxins produced by cyanobacteria are known as microcystins, which are known to cause sub-acute liver toxicity in humans and animals who come into contact with cyanobacterial blooms as they float to the surface of the water (Harding and Paxton, 2001; Zhang *et al*., 2015). Toxins are commonly known from the cyanobacteria genera *Anabaena, Aphanizomenon, Cylindrospermopsis, Microcystis, Nodularia, Nostoc* and *Oscillatoria* (Harding and Paxton, 2001).

Globally, much research has been devoted to predicting whether a water body has the tendency to develop problematical algae blooms (Borsuk *et al.*, 2004; Kuo *et al.*, 2007). While this approach may be useful in managing eutrophication symptoms, it remains an "end-of-pipe" means of living with the problem (Gupta, 2000). Prevention of the causes of the problem can be challenging and costly, however prevention remains a central tenet of pollution control (Gupta, 2000). In addition, eutrophication management strategies need to be assessed on a reservoir-by-reservoir basis (Mattson *et al.*, 2004).

2.2.2. Eutrophication research in South Africa

South African research has made a number of important, global contributions to the understanding of eutrophication and cyanobacterial toxicology. A notable example was by Hoffmann (1976), which confirmed prior research that suggested that coagulation, flocculation, sedimentation, filtration and chlorination purification methods are not able to completely remove algae toxins from water, posing a risk to consumers. In addition, the Institute for Water Quality Studies has provided valuable data on the trophic and cyanobacterial status of many South African reservoirs. This includes research on the Hartbeespoort Dam, Vaal Dam and Orange River (Harding and Paxton, 2001).

Most impaired reservoirs in South Africa are impacted by wastewater effluents (Harding, 2008). The extent of eutrophication in South Africa has increased since it was first noted in the 1970s (Rossouw *et al.*, 2008). The death of large numbers of crocodiles along the Olifants River has raised public interest on the deterioration of water quality in South Africa (Oberholster, 2009; Ashton, 2010). A combination of acid mine drainage and nutrient loading are the causes of the observed deterioration of water quality in the Olifants River in the Gauteng, Mpumulanga and Limpopo provinces (Dabrowski and de Klerk, 2013). Despite the scale of eutrophication problems in South Africa, cultural eutrophication is reversible (Walmsley, 2000). Transparent research and monitoring as well as explicit policies and legislation are pre-requisites to bring eutrophication under control in South Africa (Walmsley, 2000).

2.2.3. Stratification

Stratification can be defined as "the development of relatively stable light and warm layers above colder deeper layers within a body of water" (Huttula, 2012). Stratification is an important concept for understanding eutrophication. A stratified water body has a relatively warm and oxygenated layer of water near the surface, termed the epilimnion (Boehrer and Schultze, 2008). The hypolimnion, at the deeper levels of the water body, is colder and low in dissolved oxygen (Boehrer and Schultze, 2008). A thin layer of water between the epilimnion and the hypolimnion is the thermocline, where a rapid decrease in temperature and dissolved oxygen may take place (Boehrer and Schultze, 2008). The epilimnion is maintained because of light penetration and mixing caused by wind. Stratification is more pronounced during months of warmer temperatures when there is extended duration and intensity of sunlight (Boehrer and Schultze, 2008). Thermal stratification ultimately results in nutrient stratification, with the deeper layers being nutrient-rich and the upper layers nutrient-poor (Harding and Paxton, 2001). Thermal mixing occurs seasonally when the epilimnion becomes as cold or colder than the hypolimnion, causing the bottom waters to mix with the surface (Huttula, 2012). In addition, during periods of heavy rainfall, a large influx of water can cause the water body to be mixed (Huttula, 2012). Mixing of a stratified water body is known as overturn. Turbulence is considered to reduce cyanobacterial blooms. Cyanobacteria have

relatively long growth-response times and turbulence in deep waters is thought to mix algal cells out of the light-rich epilimnion for long enough that they do not survive (Harding and Paxton, 2001).

2.3. Strategies for controlling eutrophication

2.3.1. Reduction of inputs

The first, and arguably most important, strategy used to control eutrophication is regulating and reducing nutrient sources (Jiang *et al.*, 2011). This includes constructing sewage treatment facilities to purify domestic waste, adopting strategies to control industrial effluent, developing eco-agriculture and assisting farmers to reduce fertiliser and pesticide use (Jiang *et al.*, 2011). However, it can be difficult to regulate and monitor non-point sources of nutrients, such as agricultural areas (Chislock *et al.*, 2013). Removing N and P from water at wastewater treatment facilities can also be costly (Howarth *et al.*, 2011). Removing both P and N from sewage in Winnipeg, Manitoba, Canada is estimated to cost four- to eightfold more than removing P alone (Schindler, 2012). In addition, internal loading of sediments may prevent water quality improvements and the full response of lakes may take decades (Chislock *et al.*, 2013; Schindler, 2006). Diverting excess nutrients may also be an effective method of controlling eutrophication. Studies conducted on Lake Washington showed that when sewage was diverted from the lake, the lake recovered rapidly, disproving theories that once a lake becomes eutrophic, it is unrecoverable (Edmondson, 1970; Schindler, 2006).

2.3.2. Removal of in-lake nutrients

Eutrophication in reservoirs can also be controlled by reducing nutrients that are already in the reservoir (Jiang *et al.*, 2011). These types of methods do not control the primary cause of the problem and are generally found to be ineffective, costly and/or impractical for large, complex ecosystems (Chislock *et al.*, 2013). For example, aerating the hypolimnion of a reservoir to increase the oxygen concentration of the deep water and thus suppress P release from sediments is one strategy used to control eutrophication (Jiang *et al.*, 2011). However, external loading may mask the aeration effect on nutrient

recycling (Garrell *et al.*, 1977). Sediment dredging, removing the nutrient-rich top layers of sediment, has also been found to produce mixed results in managing eutrophication, depending on the dredging method (Peimin *et al.*, 2000). Theoretical analysis has shown that lake bottoms act as a sink of nutrients, and not a source of nutrients in the long-term, even though there is sometimes a flux of nutrients from the sediment into the water column (Peimin *et al.*, 2000).

2.3.3. Controlling eutrophication symptoms (i.e. algae)

Sometimes, harmful algae bloom control is employed instead of nutrient control in managing eutrophication. Examples of this type of strategy includes the application of algaecides and herbicides; and shading water bodies with opaque liners to prevent photosynthesis (Chislock *et al.*, 2013). Algaecides reduce algae blooms temporarily but they also harm non-target aquatic organisms and pose a threat to humans, livestock and wildlife (Chislock *et al.*, 2013).

2.3.4. Biomanipulation

Biomanipulation, the alteration of a food web to restore ecosystem health, is also an alternative to improve water quality in eutrophic reservoirs (Chislock *et al.*, 2013). Biomanipulation involves removing secondary consumers (planktivorous fishes) from the reservoir in order that generalist grazers, such as *Daphnia*, control phytoplankton (Chislock *et al.*, 2013). This is achieved either through the introduction of piscivorous fishes or through harvesting (Chislock *et al.*, 2013). It is important to note that fish-centric biomanipulation will only have an effect on water quality in the time-range of weeks to months and is most effective in small, easily managed systems (i.e. ponds) (Chislock *et al.*, 2013). Fish-centric biomanipulation may also reduce total algal biomass but is unlikely to suppress blooms of blue-green algae (Carpenter *et al.*, 1995). Benthivorous fish, such as carp, are known to uproot hydrophytes and re-suspend sediment, increasing turbidity and possibly releasing 'trapped' P from the sediment to be released into the water column (Zambrano *et al.*, 2001). However, the effect of carp on turbidity is neither linearly related to carp biomass nor necessarily great (Zambrano *et al*., 2001; Hart and Harding, 2015). The purported improvements in water quality at the

Hartbeespoort Dam following food web management benefit a minor fraction of reservoir-stored water as the habitat area suitable for rooted macrophytes is spatially constrained by water level fluctuations (Hart and Harding, 2015). In newly constructed reservoirs, constructing a stable ecosystem by the introduction of large aquatic plants is also used as a strategy to suppress algae blooms and purify polluted water (Jiang *et al*., 2011). Near-shore plant communities are established in the construction of stable ecosystem projects along with mussels, snails or other benthic organisms to create a suitable living environment for aquatic animals (Jiang *et al.*, 2011).

In many cases, biomanipulation, aeration, dredging, aquatic plant harvesting and other methods are used to accelerate the removal of P or internal nutrient loading (Schindler, 2006). It is generally agreed, however, that these strategies are too costly to pursue in large lakes and should not be adopted unless reduction of external loading of P can simultaneously be reduced (Schindler, 2006).

2.4. The 'P-Only' control debate

Eutrophication management tools focus primarily on P reduction (Rossouw *et al.*, 2008). This is because in the majority of cases there is a direct relationship between the concentration of total phosphorus (TP) and the photosynthetic pigment *chlorophyll-a* (Rossouw *et al.*, 2008). The question of whether N or P or both should be controlled to manage eutrophication was thought to have been settled by Schindler in 1974 with the use of long-term experiments on small lakes in Ontario, Canada (Schindler, 1974). Schindler (1974) argued that the subsidence of phytoplankton blooms was proportional to the reduction of P. This 'P-Only' approach for controlling harmful cyanobacteria blooms was based on the assumption that N-fixation by N_2-fixing-cyanobacteria would supply the N input needed for blooms to form, thus making the control of N inputs unnecessary (Paerl and Otten, 2013). However, N-fixation has been shown to be insufficient in meeting ecosystem and phytoplankton demands as wind and turbulence can disrupt N-fixation, N fixation has a high energy requirement, other factors such as iron and/or other trace metals may be limiting and oxygen in the water column can prohibit the anaerobic

process of N-fixation (Paerl and Otten, 2013). In addition, controlling only P and ignoring N inputs can result in N being transported downstream to estuaries and coastal marine ecosystems, which are more N limited than P limited (Howarth *et al.*, 2011). P-only reduction is likely to fail in lakes with rapid recycling of P between sediments and water and where non-N_2-fixing cyanobacteria, such as *Microcystis*, *Planktolyngbya* or *Oscillatoria*, are the dominant phytoplankton (Conley, 2009). However, it is significantly more costly to remove both N and P from sewage (Howarth *et al.*, 2011). During the period 1984 to 1989, the Hartbeespoort Dam saw a five-fold reduction in mean annual total phosphate concentration, however there was a limited change in chlorophyll concentration during that period (Chutter and Rossouw, 1991). This suggests that because the dam already had a low TN:TP ratio, a reduction in total phosphorus caused an increase in chlorophyll yield per unit of total phosphorus (Chutter and Rossouw, 1991).

2.5. Mass balances and pollution load determination models and tools

Mass balances are a biogeochemistry tool used to study how living systems influence and are controlled by the chemistry, physics and geology of the earth. Input/ output mass balance models are only applicable to long-term average conditions of water bodies, and are not appropriate to examine short-term variation (Uttormark and Hutchin, 1980). Mass balances attempt to account for all material entering and leaving a system in order to account for fluxes that are unknown or difficult to account for (Himmelblau and Riggs, 2012). Both point and non-point sources are responsible for nutrient flux. Point sources can be measured and quantified with greater ease than non-point sources (Beaulac and Reckhow, 1982). Direct *in situ* measurements are more reliable for nutrient flux estimates; however, they are a more expensive and time-consuming method of estimating flux (Beaulac and Reckhow, 1982).

A less time- and cost-intensive method of determining nutrient flux than *in situ* measurements involves using export coefficient values reported in the literature (Beaulac and Reckhow, 1982; Dabrowski *et al*., 2013). Export coefficients are "estimates of the amount of pollution loaded into a system per unit area of a particular land-use"

(Dabrowski *et al*., 2013). Export coefficients are useful in making predictions of how projected land use change will affect water quality (Beaulac and Reckhow, 1982). However, a lack of a relationship between stormflow and export make the use of export coefficients challenging (Coser, 1989). South Africa faces an additional challenge in using export coefficients to estimate loading. The South African Nutrient Export Coefficient Database (SANED), developed in 2007 for DWA, does not make considerations for the effect of topography, geology, soil type or vegetation on the export of pollutants from a land area (Harding, 2015). This renders its use in runoff modeling extremely limited (Harding, 2015). The Measured Annual Nutrient Loads from Agricultural Environments (MANAGE) is a database applicable to the USA that provides a clear example of the type of N and P export studies that would be required locally (Harding, 2015).

A number of programmes exist for estimating and modeling nutrient loads to water bodies using flow and water quality data. FLUX 32 is a free software that requires complete daily average flow record for the period of interest, water quality readings as concentrations for a variable and instantaneous flow for the corresponding water quality data to estimate loading. LOADEST is similar to FLUX 32 in that it requires flow and water quality data but is less user friendly because of the input file formats. In addition, the Nutrient Enrichment Assessment Protocol (NEAP) was a freely available web-based watershed-scale phosphorus loading and lake response modeling software (Rossouw *et al.*, 2008). It was designed for use in South Africa and was widely used from 2004 until 2009. It was discontinued as the WRC did not extend the project (Harding, 2015). NEAP allowed "the user to determine the manner in which the annual mean concentration of phosphorus is likely to change in response to an increase or decrease in the loading of this element" (Newcombe, 2009).

2.6. Eutrophication modeling at the Hartbeespoort Dam

A 2010 report used ecological informatics models to predict cyanobacteria and algae bloom events. *Microcystis aeruginosa* blooms were monitored over a five-year period in

the Hartbeespoort Dam (Van Ginkel *et al.*, 2010). Using multivariate analysis, the study found that temperature was the most important factor in the development of cyanobacterial blooms (Van Ginkel *et al.*, 2010). Other important factors were: "dissolved inorganic phosphorous (DIP), dissolved inorganic nitrogen (DIN), DIP:DIN ratio, total phosphorous, total nitrogen, and Chl-*a* concentration" (Van Ginkel *et al.*, 2010). The study concluded that modeling methods are capable in assisting with managing eutrophication. This would help protect water users from potentially toxic events (Van Ginkel *et al.*, 2010).

A 2007 report published by the WRC reviewed factors that influenced cyanobacterial growth in the Hartbeespoort Dam as well as the options used to control the bloom (Owuor *et al.*, 2007). Water and sediment samples were taken and historical data from the Department of Water Affairs and Forestry (DWAF) and others analysed. Water sampling was done at 1, 2, 5, 10, 15 and 20 metre depth and an integrated surface to 5 metre sample was taken. Temperature, dissolved oxygen, electrical conductivity and light penetration were measured every 0.1 metre until total light extinction. Sediment samples were taken for algal identification and quantification using an Ekmann Grab Sampler. The report found that changes in nitrate, phosphate and temperature contributed to unacceptably high cyanobacterial blooms and recommended continuous monitoring, as is already being done, to help predict blooms (Owuor *et al.*, 2007). In 2016, the DWS used the company CyanoLakes (cyanolakes.com) to predict cyanobacteria blooms in South African Dams (Matthews, 2016). Using remote sensing, satellite images, which are captured every two to three days, are utilised by CyanoLakes to estimate algal and cyanobacterial biomass in lakes and dams (Matthews, 2016). The use of remote sensing is significantly less labour- and cost-intensive than traditional methods of monitoring for toxic cyanobacterial blooms, which involves collecting and analysing water samples from a single location on each dam twice per year (Matthews, 2016). In addition, because of the frequency at which satellite images are available, remote sensing allows seasonal and spatial patterns to be examined (Matthews, 2016). However, the DWS has since discontinued the use of CyanoLakes's services due to cost constraints.

2.7. Study area

2.7.1. Land use

The Hartbeespoort Dam is situated approximately 37 km west of Pretoria in the North West Province south of the Magaliesberg Mountain Range. The catchment area that drains to the dam is 4100 km^2 (WRC, 2012). Figure 3.2.1 (a) shows the catchment area of the dam. The dam is currently used to irrigate 15 000 hectares of cropland surrounding the Dam (Bega, 2016). The Hartbeespoort Dam is situated in one of the most economically active areas of South Africa. The Jukskei and Hennops rivers drain northern and western Johannesburg, southern Tshwane, northern Ekurhuleni, Mogale City and Randburg (Mitchell and Crafford, 2016). Since the start of gold mining in the late 1900s, industrial effluent and urbanisation have impacted the Jukskei and Hennops rivers and the Hartbeespoort Dam currently receives large volumes of return flows from 11 WWTWs and diffuse sources (Mitchell and Crafford, 2016). The three largest WWTWs in the Hartbeespoort Dam catchment are: Northern Works, which is situated in the Jukskei River catchment and has a design capacity of 450 ML/day, Olifantsfontein, which is situated in the Hennops River catchment and has a design capacity of 105 ML/day; and Sutherland Ridge, which is situated in the Hennops River catchment and has a design capacity of 65 ML/day (Mitchell and Crafford, 2016). Effluent from each of these three WWTWs is estimated to contribute approximately 12% of the total nutrient load to the Hartbeespoort Dam (Mitchell and Crafford, 2016).

The Skeerpoort River, a tributary of the Magalies River, is contained within the Cradle of Humankind, which is a World Heritage Site comprised of dolomitic caves where the fossilized remains of important hominids have been found (RHP, 2005). Because of this, development in the Skeerpoort catchment is restricted to a minimum and most of the catchment is a proclaimed nature reserve (RHP, 2005). Along the Magalies River, large volumes of water are extracted for agricultural use and bottling (RHP, 2005). The upper reaches of the Magalies River are classified as having fair river integrity, however the town of Magaliesburg and the return flows from the pig, chicken and flower farms in the area negatively impact on the water quality (RHP, 2005).

2.7.2. Climate

The upper Crocodile sub-management area has a mean annual precipitation of 668 mm and s-pan potential evaporation is 1702 mm per annum (WRC, 2012 Rain occurs predominantly during the summer months from November until March, with more than 75% of the yearly rainfall occurring during these months (WRC, 2012). December and January are the peak rainfall months (WRC, 2012). Because of the high evaporation potential, only a small portion of the rainfall is converted to stream flow that can be easily accessed. The area experiences cold winters (with daily average minima and maxima of 1 and 15°C respectively) and warm summers (with daily average maxima and minima of 10 and 30°C respectively) (DWAF, 2004).

2.7.3. Geology and hydrology

The Hartbeespoort Dam is built on the Brits Graben, which consists of two steeply dipping, SSE-NNW striking normal faults with horizontal displacement of 600m and vertical displacement of 50m (Judeel and Hartmann, 2008). These fault lines are a potential conduit for groundwater flow. However, the degree to which groundwater interacts with surface water at the Hartbeespoort Dam has not been investigated fully (Abiye et al., 2015). Acid mine drainage has a negligible effect on TDS load because the good to excellent quality dolomitic groundwater that flows into the dam is diluting mine water impact (Hobbs, 2017). The Hartbeespoort Dam is separated from the groundwater in winter (Davis, 2017). Two perennial rivers, the Crocodile and Magalies, as well as two minor streams (the Swartspruit and Leeuspruit) flow into the Dam. The gross storage capacity is 205 million m^3 (DWAF, 2009). The Hartbeespoort Dam has a high rate of flushing, 1.24 times per year (DHEC, 2004).

2.8. Data available from the Department of Water and Sanitation

Flow and water quality data can be obtained from the DWS Resource Quality Information Services (RQIS) website, which can be found at: http://www.dwa.gov.za/iwqs/. The data available from the DWS are summarised in Tables 4.1, 4.2 and 4.3 below. Parameters that were of interest to this study were drawn

from water quality data made available from the DWS RQIS website. Water quality readings are taken approximately every two weeks or once a month in some cases. Flow readings were available in a "raw" format where a reading is taken every 12 minutes, although days with fewer than 120 flow readings are frequent. Water quality data from sites on the dam itself have sporadic entries from the 1960s, 1970s and 1980s, with the exception of the monitoring site closest to the dam wall (site 90240).

Table 2.8.1: Available data for river stations before the inflow into the dam (as of 30 May 2018)

Sample Site	**Flow Data**	**Water Quality Data**
90164 (A2H12) Crocodile River	Daily average flow rate (m^3/s) 1922 to 31 March 2018	Fortnightly dissolved concentrations of: NH_4, NO_3+NO_2, Kjeldahl nitrogen, total phosphate, and orthophosphate. 1976 to January 2018 (3439 entries in total) (From 2010 until the most current entry 195 water chemistry entries were available)
192731 Crocodile River	N/A	Every second month dissolved concentrations of: NH_4, NO_3+NO_2, and orthophosphate. February 2012 to September 2017 (9 entries in total)
90165 (A2H13) Magalies River	Daily average flow rate (m^3/s) 1922 to 31 March 2018	Fortnightly dissolved concentrations of: NH_4, NO_3+NO_2, Kjeldahl nitrogen, total phosphate, and orthophosphate. 1976 to September 2017 (1742 entries in total) (From 2010 until the most current entry, 197 water chemistry entries were available)
90202 (A2H58) Swartspruit	Daily average flow rate (m^3/s) 1982 to 31 March 2018	Monthly dissolved concentrations of: NH_4, NO_3+NO_2, Kjeldahl nitrogen and orthophosphate. 1982 to November 2017 (466 entries in total) (From 2010 until the most current entry, 99 water chemistry entries were available)

Table 2.8.2: Available data for river stations at the outflow from the Dam (as of 30 May 2018)

Sample Site	**Flow Data**	**Water Quality Data**
90212 (A2H81) Left Canal	Daily average flow rate (m^3/s) 1956 to 31 March 2018	Fortnightly concentrations of: NH_4, NO_3+NO_2, Kjeldahl nitrogen, total phosphate and orthophosphate. 1962 until September 2017 (1712 entries in total). From 2010 until the most current entry 190 water chemistry entries were available.
90213 (A2H82) Right Canal	Daily average flow rate (m^3/s) 1971 to 31st March 2008	Fortnightly concentrations of: NH_4, NO_3+NO_2, Kjeldahl Nitrogen, Total Phosphate, and Orthophosphate. 1962 to June 2008 (317 entries in total) From 1965 until 1983, 1984 until 1992, and 1995 until 2000 no data were available
85109 (A2H117) Right Canal	Daily average flow rate (m^3/s) 1989 to 28th February 2018	Fortnightly concentrations of: NH_4, NO_3+NO_2, Kjeldahl nitrogen, total phosphate, and orthophosphate. June 2008 to December 2015 (150 entries in total)
(A2H83) Weir downstream of Hartbeespoort	Daily average flow rate (m^3/s) 1956 to 31st March 2018	Fortnightly concentrations of: NH_4, NO_3+NO_2, Kjeldahl nitrogen, total phosphate, and orthophosphate. 1962 to September 2017

Table 2.8.3: Available data for stations on the Dam (as of 30 May 2018)

Sample Site	**Flow Data**	**Water Quality Data**
90240 (A2R1) Close to the Dam wall (Spillway)	Daily average spill (m^3/s) 1922 to 31st March 2018	Fortnightly concentrations of: NH_4, NO_3+NO_2, Kjeldahl nitrogen, total phosphate, and orthophosphate. 1968 to November 2017 (9725 entries in total) Most of the sample entries have as many as eight repetitions within an hour for a given date.
90242 (A2R1.3)	N/A	Monthly concentrations of: NO_3+NO_2.1962 until 1965 (26 entries in total)
90247 (A2R1.8)	N/A	Weekly concentrations of: NH_4, NO3+NO_2, Kjeldahl nitrogen, total phosphate and orthophosphate. 1980 to 1983 (213 entries in total)
90244 (A2R1.5)	N/A	Monthly concentrations of: NO_3+NO_2.1962 to 1965 (26 entries in total)
90241 (A2R1.2)	N/A	Monthly concentrations of: NH_4, NO_3+NO_2, and orthophosphate. 1962 to 1979 (35 entries in total) From 1966 until 1978 no data is available
90246 (A2R1.7)	N/A	Weekly concentrations of: NH_4, NO_3+NO_2, Kjeldahl nitrogen, total phosphate and orthophosphate. 1980 to 1983 (132 entries in total)
(A2R1.10)	N/A	Weekly concentrations of: NH_4, NO_3+NO_2, Kjeldahl nitrogen, total phosphate and orthophosphate. 1980 to 1983 (222 entries in total)
(A2R1.4)	N/A	Monthly concentrations of: NO_3+NO_2. 1962 to 1965 (26 entries in total)

CHAPTER 3: METHODS

3.1. Calculation of a mass balance

Annual inputs and outputs were calculated. The sum of the annual inputs was assumed to be equal to the sum of the annual outputs plus the sediment accumulation in the dam, shown by Formula 1. The river inputs and outputs were calculated precisely, while the rest of the components of the mass balance were estimated from the literature.

$$\Sigma \text{ annual inputs}_{(N \text{ or } P)} = \Sigma \text{ annual outputs}_{(N \text{ or } P)} + \Delta \text{ annual storage}_{(N \text{ or } P)} \quad \ldots\ldots\ldots\ldots\ldots\ldots\ldots\ldots (1)$$

Where:

Inputs are river, atmospheric deposition and groundwater (as well as nitrogen fixation in the case of N).

Outputs are river, biomass removal (water hyacinth, algae and fish) and groundwater (as well as denitrification in the case of N).

Storage is sediment accumulation within the dam.

3.2. River inputs and outputs

Section 3.2 describes the methods used to meet Objectives 1 and 2 of the study (i.e. calculations of river inputs and outputs), which formed the principal focus of this study. River outputs and inputs were calculated using Formula 2 with water quality and flow data from DWS. Water quality readings occur at two weekly intervals while flow readings occur at 12-minute intervals. Time series using intermittent weekly or monthly grab sampling is widely used to calculate fluxes (Kirchner *et al.*, 2004). Over the time period from June 2010 until April 2018 examined in this study, there were approximately 180 N and 180 P observations for each site. June 2010 was selected as the starting date as there was a gap in TP readings on the Crocodile River from July 2008 until May 2010.

$$\text{Flux (g/s)} = \text{N or P concentration (mg/L)} \times \text{flow rate } (m^3/s) \quad \ldots\ldots\ldots\ldots\ldots\ldots\ldots\ldots (2)$$

3.2.1. Sampling locations

The sampling locations used to determine nutrient inflow and outflow fluxes are shown in Figure 3.2.1.(a) It is well documented in the literature that the Crocodile River is the major river contributing nutrients to the Hartbeespoort Dam, with the Magalies River contributing less than 1% of the nutrient inputs from rivers (NWIR, 1985; DHEC, 2004; Roux *et al.*, 2010; Botha, 2015; Mitchell and Crafford, 2016). These findings were confirmed in this study (see Section 7.1 in Appendix). Although the Swartspruit River also contributes nutrients to the Hartbeespoort, the data available from DWS on the Swartspruit were limited. From 2010 to 2018, monthly Total Oxidised Nitrogen (TON) (i.e. nitrate plus nitrite) and orthophosphate readings were available; however, no monthly TP or Kjeldahl nitrogen readings were available. In addition, nutrient influx from the Swartspruit River has been documented to be a minor nutrient contributor. Mitchell and Crafford (2016) estimated the Swartspruit contributes 0.79% of the annual P load to the Hartbeespoort. Thus the Swartspruit nutrient flux was not included in mass balance calculations.

A satellite photograph of the river outflows is shown in Figure 3.2.2.(b). The outflow of water from the dam consists of two portions: the canals, which release irrigation and compensation water from a port located 20 m below the full supply level; and the radial sluices that draw water from a depth of approximately 2 m (NWIR, 1985). The sampling site of the water released from the radial sluices was Site 90214 on the Crocodile River. Site 90212 on the Left Canal and Site 85109 on the Right Canal were the sampling sites of the irrigation and compensation water.

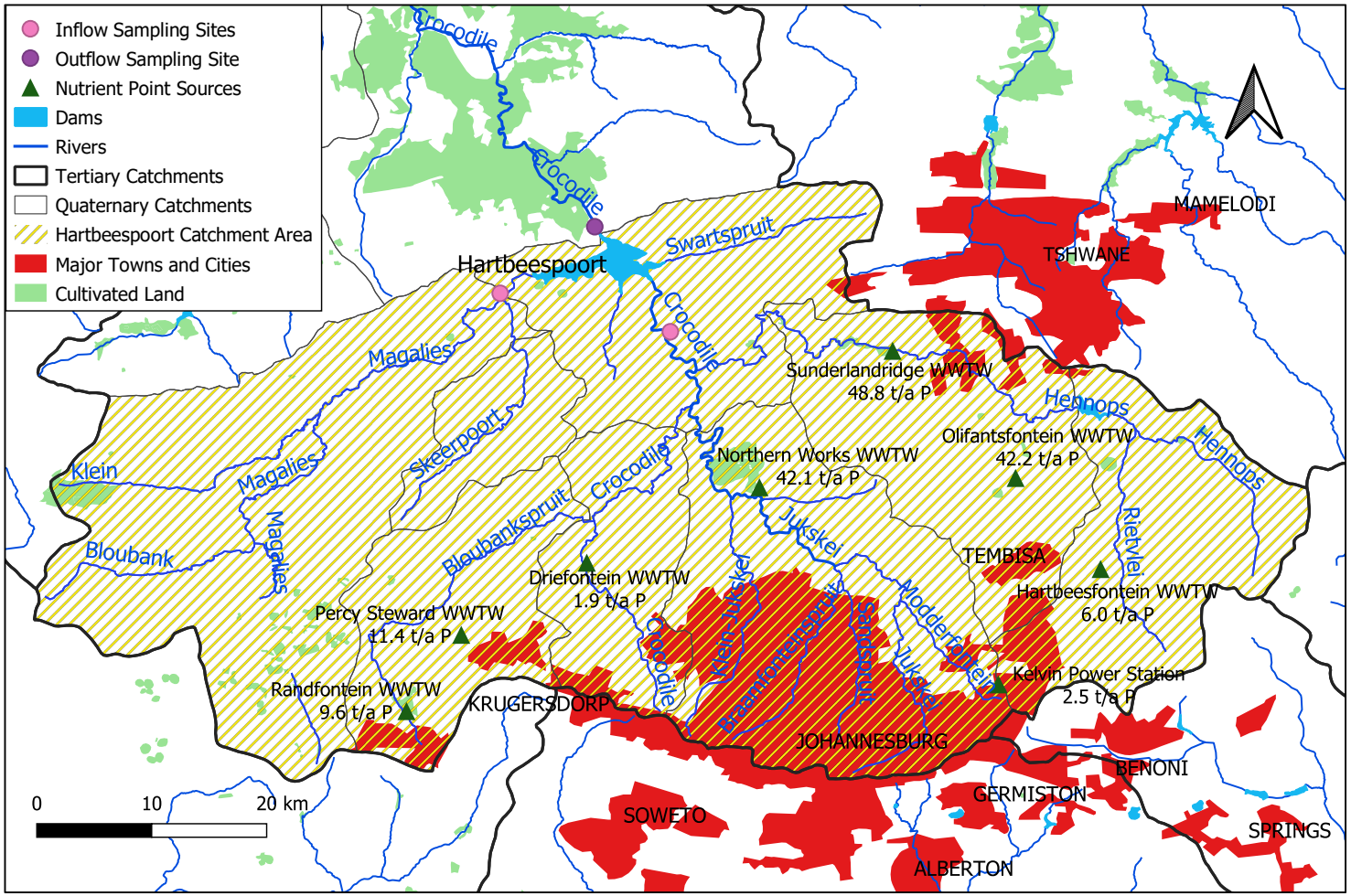

Fig. 3.2.1.(a): Map of Hartbeespoort Dam catchment area and river sampling sites. Nutrient point source effluent P flux estimates from Mitchell and Crafford (2016). GIS shapefiles from: http://www.waterresourceswr2012.co.za. Shapefiles used: LandUse – major towns and cities_poly, irrigation-nlc96, dams500g_wgs84, dter, dquat, wriall500_primary, wriall500_secondary.

Fig. 3.2.1.(b): Satellite photograph of river outflow sampling locations (represented by yellow markers) in relation to the Hartbeespoort Dam wall (represented by a red marker).

Fig. 3.2.1.(c): Photograph of inflow site on the Crocodile River.

Fig. 3.2.1 (d): Photograph of outflow site on Crocodile River. Dam wall visible in the distance.

Fig. 3.2.1 (e): Photograph of right canal from above.

3.2.2. N and P definitions

This study estimated total phosphorus (TP) and total nitrogen (TN) fluxes. In this study N will be used to refer to TN and P will be used to refer to TP. To calculate river N fluxes, 'nitrate plus nitrite' and 'Kjeldahl nitrogen' values from DWS were added together. Formula 3 thus describes the components that make up N water quality observations. If an observation date had a nitrate plus nitrite value but not a Kjeldahl nitrogen value or vice versa, the observation date was removed. TP values from DWS were used to calculate P fluxes. Orthophosphate (OP) values were evaluated as a proxy for TP, as used by Harding (2015). TP is the sum of all phosphorus compounds while OP is the soluble, inorganic fraction of phosphorus (Murphy, 2007). OP is considered to comprise about 90% of the TP content of wastewater effluents (Harding, 2015). When TP data are not available, estimate ratios of OP:TP can be used to estimate TP (Harding, 2015). There were 10% more readings available for OP than TP from 2010 to 2018. However, the variability of OP contained in TP was high (see Section 7.4 in Appendix). The standard deviation of OP/TP was 18%, with observations as high as 99% and as low as 0.7%. Thus it was decided that OP would be an unreliable proxy for TP in this study.

$$TN = NO_3 + NO_2 + NH_4 + \text{Organic N} \quad \ldots\ldots(3)$$

3.2.3. DWS laboratory methods

The Analytical Methods Manual (DWAF, 1992) outlines the procedures used by the DWS at the Hydrological Research Institute in analytical laboratories to determine organic, trace metal, toxicity, biological and bacteriological concentrations in water samples. The DWS analytical procedures of N and P water quality concentrations used by the DWS are outlined below. The procedures use a Technicon Autoanalyzer TRAACS 800 or similar equipment and colorimetric detection.

3.2.3.(a). Total phosphate as P (P) (mg/L)

DWS method number 0015003 – automated determination of total phosphorus as phosphomolybdate

In the acid hydrolysis step, 0.5 ml of digestion mixture (peroxodisulphate) is added to 10 ml of sample to convert all forms of phosphorus to orthophosphate. The sample and a series of standard solutions and two blank samples are autoclaved at 103 kPa for 30 minutes in test tubes with screw tops and Teflon linings. In the colorimetric step, a mixture of ammonium molybdate solution, sulphuric acid solution and antimony potassium tartrate solution as well as absorbic acid solution are added to each test tube. In an acid medium, a solution containing phosphorus and molybdate ions form 1,2-molybdophosphoric acid (Jarvie, 2002). Ascorbic acid is then used to reduce 1,2-molybdophosphoric acid to the phosphomolybdenum blue complex (Jarvie, 2002). The intensity of the blue colour produced, measured at 880 nm, is proportional to the amount of orthophosphate incorporated into the phosphomolybdenum blue complex (Jarvie, 2002).

3.2.3.(b). Orthophosphate as P (PO_4) (mg/L)

DWS method number 0015004 – automated determination of dissolved orthophosphate as phosphomolybdate

Samples are filtered through a prewashed 0.45 μm membrane filter to remove solids. Following filtration the orthophosphate method follows the colorimetric step described in Section 3.2.2(a) above.

3.2.2.(c). Nitrate plus nitrite (NO_3 + NO_2 – N) (mg/L)

DWS Method number 0007107 – automated determination of dissolved nitrate by cadmium reduction (NO_3 – N) (mg/l)

Nitrate is reduced to nitrite in a copper coated cadmium tube in an ammonium chloride buffer solution. A colour reagent (sulphanilamide hydrochloride) and deionised water are added to each sample. The nitrate is determined by diazotizing with sulfanilamide and coupling with N-(1-naphthyl)-ethylenediamine dihydrochloride to form a colour azo dye

(Zhang *et al.*, 1997). The absorbance of the azo dye is measured at 540 nm and is linearly proportional to the concentration of nitrate plus nitrite (Zhang *et al.*, 1997).

3.2.3.(d). Kjeldahl nitrogen (NH_4 – N) (mg/L)

DWS method number 0007003 – automated determination of dissolved Kjeldahl nitrogen

This method determines the sum of the ammonium originally present plus the organic nitrogen (DWAF, 1992). Ten millilitres of sample and 2 ml of digestion mixture (concentrated sulphuric acid combined with deionised water mercury (II) oxide, potassium sulphate – the latter two compounds accelerate the digestion process) are pipetted into a digestion tube to convert organic N to ammonium sulphate while inorganic compounds are not reduced. The ammonium ions are then determined using the indophenol-blue method. This method involves reacting the ammonium in a mildly alkaline medium with hypochlorite to form monochloramine (Verdouw *et al.*, 1978). Monochloramine forms indophenol-blue in the presence of phenol and nitropruside (Verdouw *et al.*, 1978).

3.2.4. Date format of flow data corrections

Complete raw flow datasets (in m^3/s) from 2010 until April 2018 for all inflow and outflow sites were provided by e-mail from DWS. Microsoft Excel for Mac 2011 (Version 14.7.7) did not read the dates of these datasets correctly. In the format the data were sent, from the first to the 12th of each month, Excel recognised the month value as the day value and vise versa. From the 13th until the end of each month Excel recognised the date only as text. The dates had to be converted to read as correct dates before fluxes could be calculated.

To convert the dates of the complete raw flow datasets to the correct readable date values in Excel, the date column was transferred to the programme Textedit where forward virgules, spaces and colons were removed. Ten digit numbers remained for the first to the 12th of each month (two day values, two month values, two year values, two hour values and two minute values). The dates from the 13th to the end of each month had 12 digit

numbers as they contained four year values. These values were then imported back into Excel. The Micrsosft Excel formula shown in Formula 4 was applied to the values to read all dates in the correct format. Formula 5 shows an example of the formula being used. Since Excel read column A as numbers, numbers larger than 100 000 000 000 (i.e. the 12 digit numbers) would follow the [value_if_true] formula and numbers smaller than 100 000 000 000 (i.e. the 10 digit numbers) would follow the [value_if_false] formula.

=IF (logical_test, [value_if_true], [value_if_false])……..……..(4)

=IF(A:A>100000000000,DATE(MID(A2,5,4),MID(A2,3,2),LEFT(A2,2))+TIME(MID(A2,9,2),MID(A2,11,2),0),DATE(MID(A2,4,4),MID(A2,2,2),LEFT(A2,1))+TIME(MID(A2,8,2),RIGHT(A2,2),0))……..…..(5)

3.2.5. Flow rate

Three different methods were used to calculate flux inputs and outputs. The three methods, spot, daily average and two-weekly, have different *flow values* multiplied with N or P concentration. These three methods were used to investigate the possible effect of flow variation on water quality and flux estimates. Flow was measured every 12 minutes while N and P concentrations were measured once every two weeks. The limited matching of flow and concentration presents a challenge to flux calculations. While it is unclear which flow values are the most appropriate for flux calculation, the results of the different methods produce a range. The actual flux is likely to be in-between the lowest and highest flux.

3.2.5.(a). Spot flow values

The flow value from the complete raw flow dataset that matched most closely with the sampling date and time of the DWS water quality reading was used. The time interval of the complete raw flow dataset was 12 minutes, although days with fewer than 120 readings per day were frequent. The Microsoft Excel Formula 6 was used. Formula 7 shows an example of the formula being used to find the corresponding flow value for a water quality observation date and time on the Crocodile River.

= VLOOKUP(value, table, col_index, [range lookup]) ……..……(6)

= VLOOKUP(B3,A2H012!B2:C309949,2,TRUE) ……..…..(7)

value - the value to look for (water quality observation date and time)

table - the table from which to retrieve a value (all flow observations in column C in m^3/s and all the corresponding dates and times of the flow recording in column B of Excel page labeled A2H012. There were 309 949 rows in this table)

col_index – the column in the table from which to retrieve a value (flow observation in m^3/s)

range lookup – TRUE is approximate match, FALSE is exact match

3.2.5.(b). Daily Average flow values

Daily average flow rates (m^3/s) were available from DWS. In this flux calculation method, the daily average value that matched with the DWS water quality sampling date was used. Formula 6 was also used for daily average flow values. Formula 8 shows an example of the formula being used to find the corresponding flow value for a water quality observation date and time on the Crocodile River. Note that Excel page labeled '90164 DAF' contains all corresponding Daily Average Flow (DAF) dates and that there were 3043 rows in the table from which values were retrieved.

=VLOOKUP(B3,'90164 DAF'!A2:B3043,2,TRUE)……..……..(8)

3.2.5.(c). "Two-Weekly" flow values

For this flux calculation method, the raw flow observations between each water quality observation and the next were averaged. Because there are approximately two-weekly intervals between each water quality reading, this method was termed the "two-weekly flow" method. For this method, dates marking the end of each season, which will be referred to as "seasonal markers" in this study, were added to the water quality data. (31/8/relevant year 23:59 for end of winter, 30/11/relevant year 23:59 for end of spring, 31/5/relevant year 23:59 for end of autumn, 28/2/relevant year 23:59 for end of summer or 29/2/relevant year 23:59 for end of summer during a leap year). Seasonal markers

were added to ensure that flow was representative of seasons since the lag between two water quality sampling dates would often span across seasonal boundaries. The additional flow dates were added to prevent flow from the incorrect season being incorporated into seasonal flux calculations. The most recent available water quality observation after the added end of season date was assumed for these dates.

The average flow values were calculated by first using the Microsoft Excel Formula 9. Formula 10 shows an example of the formula being used to find the sum of the flows observations between the first water quality observation (i.e. 2 June 2010 09:45) and the second (i.e. 15 June 2010 12:27) for the inflow site on the Crocodile River. Formula 11 was then used to create a count of the number of flow observations between any two water quality observations. Formula 12 shows an example of the formula being used for the inflow site on the Crocodile River. The sum of the flow observations were divided by the count of the flow observations to obtain a flow rate averaged over the period between water quality observations (approximately two weeks) in m^3/s.

=SUMIFS (sum_range, range1, criteria1, [range2], [criteria2], ...)…….....(9)
=SUMIFS(B2:B310052,A2:A310052,">"&E2,A2:A310052,"<="&E3)……...(10)
=COUNTIFS (range1, criteria1, [range2], [criteria2], ...)…….…….……(11)
=COUNTIFS(A2:A310052,">"&E2,A2:A310052,"<="&E3)……..…….(12)
sum_range – the range to be summed (all flow observations of the complete raw dataset in m^3/s. There were 310 052 flow observations)
range1 – the first range to evaluate (the date and times of the flow readings)
criteria1 – the criteria to use on range 1 (bigger than the first water quality observation)
range2 - the second range to evaluate (the date and times of the flow readings)
criteria2 – the criteria to use on range 2 (smaller or equal to the date and time of the second water quality observation)
To calculate the sum of the flow between water quality observations if column A contains the date and time of flow readings, column B contains the discharge for the relevant date and time and column E has the dates with the water quality observations.

3.2.5.(d). Comparison of the three flux calculation methods

The representativeness of the flow values used in capturing the actual river flow at the Crocodile River inflow site was examined. This was necessary as the lack of concentration data sampling frequency to match that of the flow data meant there were approximately 24 flux observations each year. Ideally, the flow values used should be representative of the actual river flow. To determine how representative the flow values were, frequency histograms of flow values for the Spot, Daily Average and Two-Weekly methods were compared to the frequency histogram of the complete flow dataset (i.e. the dataset of flow readings taken every 12 minutes). The non-parametric Kolmogorov-Smirnov test was used to compare the distributions of the flow values of each flux calculation method against the complete raw flow dataset.

3.2.6. Seasonal inflow and outflow calculations

Although annual trends were of ultimate interest, seasonal plots are useful for looking at trends on a finer scale than annual plots. Seasonal plots were also useful for showing outliers caused by pollution events. Seasonal fluxes for the Spot and Daily Average flow methods were calculated by assigning each season a number from one to four using the Formula 13. Formula 14 shows an example of the formula being used. Seasonal fluxes in g/s for the relevant inflow and outflow sites were added together. Flux in g/s was converted to t/season using Formula 15. Seasonal fluxes of the Two-Weekly flow method were calculated differently. The elapsed time between one water quality observation and the next was calculated using the Formula 16. The time elapsed was converted to seconds using Formula 18. Formulas 17 and 19 show example of the formulas used. Fluxes in g/s were multiplied with the number of seconds elapsed between the water quality observations to get a flux in tons. The seasonal Two-Weekly flux was then summed by season using Formula 13.

=CHOOSE (index_num, value1, [value2], ...)……..……..(13)

=CHOOSE(MONTH(K3),4,4,1,1,1,2,2,2,3,3,3,4) …….……(14)

index_num – the value to choose (the month of a flux an observation date)

value – the value from which to choose (Spring was defined as September 1 to November 30 and assigned the number 3. Summer was defined as December 1 to February 28/29 and assigned the number 4. Autumn was defined as March 1 to May 31 and assigned the number 1. Winter was defined as 1 June until August 31 and assigned the number 2)

[flux (t/season) = $\left[\frac{\text{flux (g/s)}}{1000000}\right]$×[(60×60×24×91.25 (s) – in the case of the Spot and Daily average flow methods) or (time between samplings (s) – in the case of the Two-Weekly flow method)]……(15)

=TEXT (value, format_text)……..….(16)
=TEXT(B3-B2,"dd:hh:mm:ss")…….(17)
value – the number to convert (the difference between the date of one water quality observation and the next)
format_text – the number format to use

=SUM (number1, [number2], [number3], ...)……(18)
=SUM((LEFT(D3,2)*24*60*60),(MID(D3,4,2)*60*60),(MID(D3,7,2)*60))……(19)
number1 – the first value to sum (amount of seconds of the days between one water quality observation and the next)
number2 – the second value to sum (amount of seconds of the hours between one water quality observation and the next)
number3 – the third value to sum (amount of seconds of the seconds between one water quality observation and the next)

3.2.7. Annual inflow and outflow calculations

A hydrological year was defined as October until September the following year, as used by Mitchell and Crafford (2016). To calculate annual N and P fluxes using the Spot and Daily Average Method, average monthly fluxes in g/s of the inflow or outflow sites were added together. Monthly averages were used as water quality sampling of the respective inflow and outflow sites did not usually occur on the same day. Thus monthly averages

made it possible to add the fluxes of the respective inflow and outflow sites. These were then converted to monthly fluxes in tons by multiplying by the number of seconds in a month and dividing by 10^6 to convert grams to tons. Formula 20 shows how g/s was converted to t/month with 30 days, 24 hours per day, 60 minutes per hour and 60 seconds per minute. The monthly fluxes for each hydrological year were then added together. Two-Weekly mean flow values were multiplied with nutrient concentrations and seconds between each sampling to get a value in tons. The readings that fell within a hydrological year were summed.

$$[\text{flux (t/month)} = [\frac{\text{flux (g/s)}}{1000000}]\times[60\times60\times24\times30.417\text{ (s)}] \quad (20)$$

3.2.8. Standard deviation calculations

It was assumed that the sum of the inflow sites and outflow sites were representative of the whole population of the inflow and outflow respectively. Thus, the standard deviation of each seasonal flux was determined by calculating the variance of the flux in g/s at each site and then adding the variance of the inflow and outflow sites together before taking the square root of the sum of the variance. The square root in g/s was converted to tons per season using Formula 16.

3.2.9. Missing data

As shown in Table 2.8.2, the right canal had significantly fewer N and P concentration data than the left canal. The right canal had missing data from September 2010 until June 2012 and from June 2014 there were no readings except for six readings from late 2015. Because the water in the left and right canals both come from the same source - a port on the dam wall located 20 m below the full supply level, it was hypothesised that the left canal could be used to infill missing right canal concentration data. This was tested by comparing box plots of N and P concentration data of the left and right canals on days when both canals were sampled. The non-parametric Wilcoxon signed rank test was used to compare the median N and P concentrations of the left and right canals.

3.2.10. Statistical analysis

Statistical analysis was performed on XLSTAT, the statistical software and data analysis add on for Microsoft Excel (http://www.xlstat.com/en/). Time series analyses were used to examine trends in nutrient inputs and outputs over time.

Shapiro-Wilk normality tests were performed on each variable to assess whether the data followed normal distributions. Non-parametric tests are better suited to water quality studies because seasonality and missing data can prevent the assumptions of classical parametric tests to be met (van Belle and Hughes, 1984). Where data were not normally distributed the non-parametric Wilcoxon signed rank test was used to assess statistical significance between the medians of the inflow and outflow calculations. Where the data were normal, t-tests were used to assess statistical significance between fluxes of the means of the inflow and outflow.

Seasonal Mann Kendall trend tests were used to determine trends in inflow and outflow calculations. Trend tests were used to determine whether there were changes in annual fluxes over time. Pivot tables with averages of monthly fluxes in g/s were constructed for each site. The relevant inflow and outflow sites were then added together. The trend test was then performed on the monthly averages with a seasonality period of 12. If a month had a missing value in one of the relevant sites, that month was not included in the seasonal Mann-Kendall trend test, even if the other site(s) contained a value for that month.

3.2.11. Flow vs. concentration plots

Flow vs. concentration scatter plots were examined to investigate whether increased flow caused the increasing trends observed in seasonal and annual plots. If flow was not correlated with concentration then it was assumed to be unlikely that an increase in flow from 2010 to 2018 was the cause of an increase in nutrient flux. If flow was correlated with concentration then a change in flow was assumed to be linked to nutrient flux trends. In addition, the presence of a significant correlation between flow and concentration

indicated that agricultural runoff was the predominant source of nutrients in a river. This is because fertilisers and topsoil are transported to rivers during storm events, making high river flow events likely to have high nutrient concentrations in a catchment dominated by agricultural nutrient pollution. The absence of a significant correlation between flow and nutrient concentration was an indication that sewage was the most likely source of nutrients. This is because pollution events from leaking pipes and/or dysfunctional WWTWs are not dependent on the flow of the river. A Spearman Rank correlation test was used to determine if there was a correlation between the spot flow values and P concentration for the Crocodile and Magalies inflow sites.

3.3. Other flux contributors

Section 3.3 describes the methods used to meet Objectives 3 and 4 of the study (i.e. estimations of biomass, denitrification, sedimentation and groundwater outputs as well as atmospheric deposition, nitrogen fixation and groundwater inputs).

3.3.1. Water hyacinth biomass output

In response to Parliamentary question 2936 of 7 October 2015 (available at https://pmg.org.za/committee-question/1267) the cubic metres of water hyacinth removed by the Metsi a Me programme were reported and presented in Table 3.3.1. Hyacinth removal is reported in cubic metres, not kilograms or tonnes, making estimating N and P removal challenging as the density of hyacinth removed was unclear. Cubic metres of hyacinth removed needed to be converted to kilograms before the masses of N and P removed could be calculated. The mass of hyacinth removed was then multiplied with the concentrations of N and P in hyacinth using literature data. An estimation of how much N and P could be removed each year from the Hartbeespoort Dam through water hyacinth harvesting was calculated using Formula 21.

Table 3.3.1: Cubic metres of water hyacinth removed each year by the Metsi a Me programme as reported in response to Parliamentary question 2936 of 7 October 2015. Years assumed to span from April to March the following year.

	2007/ 2008	**2008/ 2009**	**2009/ 2010**	**2010/ 2011**	**2011/ 2012**	**2012/ 2013**	**2013/ 2014**	**2014/ 2015**	**2015/ 2016***	**TOTAL**
Hyacinths (m^3)	4 826	9 536	9 500	10 986	25 031	24 398	48 269	46 463	34 289	**213 296**

*Until July 2015

[N or P removed from hyacinth harvesting (t/a)] = [hyacinth harvested (m^3/a)] x [hyacinth density (t/m^3)] x [hyacinth dry matter composition (%)] x [hyacinth N or P dry weight composition (%)] ……(21)

3.3.1 (a) Hyacinth density

Two densities of water hyacinth were used to estimate the N and P removed by hyacinth harvesting, one representing a realistic density and the other representing the maximum density. Water hyacinth harvesting methods were not detailed in Metsi a Me progress reports, which made estimating tons of hyacinth removed imprecise. The first density value used was a literature-derived density of water hyacinth per cubic metre from Bagnall *et al.* (1984), who reported that a water hyacinth harvester with a 25 m^3 hold can carry 4200 kg of plant material. This was converted to 0.168 t/m^3. The second density value used assumes a maximum density of hyacinth per cubic metre of 1 t/m^3. As water hyacinth has a high water content, the 1 t/m^3 represents the theoretical upper limit of tons of hyacinth removed.

3.3.1 (b) Hyacinth dry matter composition

Eichhornia crassipes has a very high moisture content, like most other aquatic macrophytes. Manually cleared water hyacinth has a water content of about 95.8% (Akendo et al., 2008). However, Su *et al.* (2018) reported the dry matter component making up 9.84%, 9.5%, 6.2% and 9.4% of water hyacinth. Considering the moisture contents reported in the literature, this study assumes the water hyacinth removed had a

constant minimum dry matter composition of 4.2% and a maximum of 9.84% (i.e. a maximum constant water content of 95.8% and a minimum of 90.16%, respectively).

3.3.1 (c) Hyacinth N or P dry weight composition

Boyd (1976) measured concentrations of N and P in dried samples of water hyacinth grown in nutrient-enriched water and found that N composition ranged from 1.2 to 5.6% (average of 2.5%) and P concentrations ranged from 0.1 to 0.8% (average of 0.47%). Similarly, Su *et al.* (2018) reported P compositions of 0.28 and 0.53% dry weight and N compositions of 2.76 and 2.9% dry weight. Considering the N and P concentrations reported in the literature, this study assumed that the water hyacinth removed had a minimum P concentration of 0.28% and a maximum of 0.53% as well as a minimum N concentration of 2.5% and a maximum of 2.9%.

3.3.2. Algae biomass output

In response to Parliamentary question 2936 of 7 October 2015 (available at https://pmg.org.za/committee-question/1267) the cubic metres of algae "soup" removed by the Metsi a Me programme were reported and are presented in Table 3.3.2.1.

Table 3.3.2.1: Cubic metres of algae "soup" removed each year by the Metsi a Me programme as reported in response to Parliamentary question 2936 of 7 October 2015. Years assumed to span from April to March the following year.

	2007/ 2008	**2008/ 2009**	**2009/ 2010**	**2010/ 2011**	**2011/ 2012**	**2012/ 2013**	**2013/ 2014**	**2014/ 2015**	**2015/ 2016***	**TOTAL**
Algae (m^3)	6 040	5 207	4 445	360	1 570	14 515	9 690	15 335	9 008	**67 947**

*Until July 2015

Ololo (2013) found that *Microcystis aeruginosa* was the most dominant algal species in the dam. Biovolume percentage counts showed that *M. aeruginosa* accounted for 69% of the total species, and *Anabaena* sp. accounted for 22% of the total species (Ololo, 2013). It was noted in Ololo (2013) that the species count of *M. aeruginosa* was lower than

previous studies, citing figures of between 80% and 90%. Thus, N or P removal calculations were based on elemental compositions of *M. aeruginosa*. In addition, elemental composition of *M. aeruginosa* is similar to that of *Anabaena spiroides* (Clay *et al.,* 1991).

As with water hyacinth, algae harvesting methods were not detailed in progress reports, which made estimating tons of algae removed imprecise. The Phase 1 Progress Report simply states that "concentrated algae clouds" were physically removed "with the aid of floating pump stations" which were "pumped out onto adjacent, vacant land" (HDRP, 2012). It may be assumed that the Metsi a Me programme did not use dewatering techniques when harvesting algae biomass as the Phase 1 Progress Report gives the following recommendation:

> "The research and development must carry on finding something to remove the water from the algae while pumping. We are on the brink with the vacuum concept to remove the algae from the top with vacuum; - this will still need more research. The challenge is also to concentrate the algae to certain areas with natural wind actions." (HDRP, 2012)

An estimation of the likely concentrations of algae harvested from the dam was used to calculate algae biomass outputs and is detailed in Section 3.3.2 (a). In addition, an estimation of the upper limit of algae biomass outputs was calculated using a literature-derived dry weight density of *M. aeruginosa*, assuming the algae "soup" was 100% algae and contained no water. This detailed in Section 3.3.2 (b).

3.3.2 (a) Algal biomass output Method 1

A method frequently used to quantify algae abundance is using chlorophyll-*a* concentration (Chutter, 1989). Method 1 of determining N or P removal from algae harvesting assumes a chlorophyll-*a* concentration of 302 000 µg/L from NWIR (1985), which examined water samples of hyperscums on the Hartbeespoort Dam. The study found that chlorophyll-*a* concentration of algae hypercums ranged from 144 400 to 302 000 µg/L. The maximum chlorophyll-*a* concentration was used. Chlorophyll-*a*

concentration was converted to an algae biomass concentration using a modified formula from Raschke (1993) shown by Formula 22.

[Algae biomass (mg/L)] = [chlorophyll-*a* (mg/L)] x 100/1.5 ……..……(22)

The original formula from Raschke (1993) assumed that algae biomass had a constant chlorophyll-*a* concentration of 1.5% of the dry weight. Formula 22 gives a dry weight algae biomass concentration of 20.1 g/L for algae hyperscum on the Hartbeespoort Dam. Formula 22 was also modified to be specific to *M. aeruginosa* and to determine the upper limit of Algae Biomass Output Method 1. Long *et al.* (2001) found that the smallest chlorophyll-*a* content of *M. aeruginosa* detectable in their study was 5.64 ± 0.79 mg/g of the dry weight (0.564% of the dry wt). Thus a chlorophyll-*a* concentration of 0.5% of the dry weight was used to determine the upper limit (i.e. a dry weight algae biomass concentration of 60.4 g/L).

Estimated N and P weights of the algae "soup" harvested each year were calculated using Formulas 4 and 5, respectively. Formulas 3 and 4 are modified formulas from Park and Craggs (2011). Marginally different algae N and P concentrations from those used by Park and Craggs (2011) were used in Formula 23. Algae N and P concentrations were derived from the literature to represent nutrient concentrations of *M. aeruginosa* specifically. N and P contents in g/L were then converted to kg/m^3 for each year of algae harvesting.

[P or N Content (g/L)] = [Algae biomass (g/L)] x [Algae P or N concentration (dry wt%)]……..……(23)

Algae N and P dry weight concentrations of *M. aeruginosa* from the literature are shown in Table 3.3.2.2. High N and P concentrations of *M. aeruginosa* were associated with high N and P concentrations of the medium that algae cells were grown in (Colman and Santha, 1988). The medium concentrations of the Lee *et al.* (2000) study were substantially lower than those of the Colman and Santha (1988) study, which may explain

the differing elemental cell compositions reported. Krivtsov *et al.* (2005) found the composition of *M. aeruginosa* to be relatively constant in a stratified, eutrophic lake under conditions of nutrient depletion. A possible reason for this is the ability of *M. aeruginosa* to move up and down in the water column, taking up nutrients from the lower parts of the water column and photosynthesising in the epilimnion (Krivtsov *et al.*, 2005).

Table 3.3.2.2: Concentrations of N and P of *M. aeruginosa* from the literature

	Concentration range	**Reference**
P [dry wt]	0.55 – 0.89%	Colman and Santha (1988)
	0.78 ± 0.02 -1.47 ± 0.03 mg/g (0.078 -0.147%)	Lee *et al.* (2000)
	127 (± 5 SE) mmol kg^{-1} (0.39%)	Krivtsov *et al.* (2005)
N [dry wt]	6.36 – 9.01%	Colman and Santha (1988)
	6.07 ± 0.24 - 8.50 ± 0.22 mg/g (0.6 – 0.85%)	Lee *et al.* (2000)

Values of 9.01% N and 0.89% P were chosen to be used in algae output calculations as they were most representative of the eutrophic conditions of the Hartbeespoort Dam. Following from Formulas 22 and 23, the N and P contents of dense *M. aeruginosa* scum was calculated as having a N content of 1.81 – 5.44 kg/m^3 and a P content of 0.179 – 0.538 kg/m^3. These values were multiplied with the yearly cubic metres of algae removed in Table 3.3.2.1.

3.3.2 (b) Algal biomass output Method 2

Method 2 used a dry mass algae composition of 0.87 g/cm^3 (i.e. 0.87 t/m^3) from Hu (2014) to estimate the upper limit of N or P removal from algae harvesting. Hu (2014) calculated cell density by dividing dry weight (g/cell) by individual cell volume (cm^3). Hu (2014) found that *M. aeruginosa* had an average dry weight of 1.21 ± 0.09 x 10^{-11} g/cell and an average size of 2.99 ± 0.61 μm. Hu's (2014) *M. aeruginosa* density findings were congruous with findings from Kim *et al.* (2012), who used oven-drying methods,

and determined that the moisture content of *M. aeruginosa* was 10.58% (i.e. 0.106 t/m^3). Formula 24 describes the calculations made in Method 2. The same N or P dry weight concentrations used in Method 1 were used.

[Upper limits of N or P removed from algae harvesting (t/a)] = [algae harvested (m^3/a)] x [algae dry weight (t/m^3)] x [algae N or P dry weight composition (t/m^3)] ……(24)

3.3.3. Fish biomass output

In response to Parliamentary question 2936 of 7 October 2015 (available at https://pmg.org.za/committee-question/1267) the kilograms of fish biomass removed by the Metsi a Me programme were reported and are presented in Table 3.3.3.1. The total catch over the life of the programme was 317 t, an average of 42.3 t/a. The largest yield over a year period was 2011/12 when 80 t of fish biomass was caught.

Table 3.3.3.1: Kilograms of fish removed each year by the Metsi a Me programme as reported in response to Parliamentary question 2936 of 7 October 2015.

Year	**Catfish (kg)**	**Carp (kg)**	**Bi-catch (kg) (Unintended species)**	**Total (kg)**
Feb '08 - Dec '09	37527.25	24361.59	3915.31	65804.15
2010/11 (April '10 – March '11)	9159.30	14416.70	89.30	23665.30
2011/12 (April '11 – March '12)	34991.10	45856.20	76.50	80923.80
2012/13 (April '12 - March '13)	16878.60	35311.80	18.80	52209.2
2013/14 (April '13 to March '14)	20186.6	29278.5	18.8	49483.9
2014/15 (April '14 to March '15)	9592.4	28280.1	10.8	37883.3
2015/16 (April '15 to end July)	756.1	6556.1	0	7312.2
Total	129091.35	184060.99	4127.51	**317279.85**

NIWR (1985) estimated that 695 t/a of fish biomass was removed from the Hartbeespoort Dam from 1982 to 1984 by anglers. These fish biomass outputs are shown in Table 3.3.3.2. The report noted that low dam levels during that period could have made fish more accessible to anglers, causing the fish catch volumes to be larger than periods with high dam levels.

Table 3.3.3.2: Mean annual yield fish biomass removed by anglers from the Hartbeespoort Dam from 1982 to 1984 (NIWR, 1985)

	C. carpio (Carp)	*O. mossambicus* (Mozambique tilapia)	*C. gariepinus* (Catfish)	Total
Mean annual yield (t)	449	144	102	695

3.3.3.(a). N removal from fish biomass estimation method

Ramseyer *et al.* (2002) developed a linear regression equation to estimate whole body nitrogen from whole fish weight. The regression equation is shown in Formula 25. The formula was used to estimate fish biomass outputs from both the Metsi a Me programme and from anglers. Ramseyer *et al.* (2002) examined a broad range of species and found that regression parameters were similar for most species, making it appropriate for use in this study.

$$\log_{10}(\text{fish N}) = 1.03 \times \log_{10}(\text{fish wet weight}) - 1.65 \quad \text{.....(25)}$$

3.3.3.(b). P removal from fish biomass estimation method

A standard of 2.3% TP of fish dry weight and dry weight as 22% of wet weight was used to estimate fish biomass removal estimates following from methods used by Hart and Harding (2015). These figures are likely to produce a slight over-estimation of N or P removal as fish dry weights have also been estimated at 16.7% (Hart and Harding, 2015). Formula 26 shows the formula used to estimate P removal from fish biomass harvesting.

[P removed from fish harvesting (t)] = [fish removed (t)] x [fish dry weight (%)] x [fish P dry weight composition (%)] .....(26)

3.3.4 Denitrification output

When O_2 is limited denitrifying bacteria will switch from aerobic respiration to anaerobic respiration, reducing nitrate and nitrite to gaseous forms of nitrogen (Skiba, 2008). In lakes, denitrification mainly takes place at the sediment surface (Ahlgren *et al.*, 1994). Nitrate, organic matter, P concentrations, pH, temperature, oxygen concentration of the overlying water and toxic compounds from anthropogenic sources affect denitrification rates (Seitzinger, 1990, Finlay *et al.*, 2013). In addition, many of these factors are interrelated, making denitrification temporally and spatially complex (Seitzinger, 1990). Eutrophic lakes have higher denitrification rates than oligotrophic to moderately eutrophic lakes, and low P concentration is associated with low N removal (Seitzinger, 1990, Finlay *et al.*, 2013). Thus the Hartbeespoort Dam is likely to have high denitrification rates since it is hypertrophic with high P inputs. Denitrification rates reported in the literature were used to estimate how much N would be lost from the Hartbeespoort Dam through denitrification. Denitrification rates of 0.10–3.72 mol N $m^{-2}.a^{-1}$ and 303–841 t/a reported in Piña-Ochoa and Álvarez-Cobelas (2006) and NWIR respectively were used to estimate how much N could be lost from the Hartbeespoort Dam through denitrification every year. Formula 27 describes how N denitrification outputs for the Hartbeespoort Dam were calculated.

[Denitrification output (t/a N)] = [areal flux ($g/m^2/a$ N)$\times 10^{-6}$ (estimated from the literature)] x [surface area of dam (m^2)]…….(27)

3.3.5. Atmospheric deposition inputs

Atmospheric deposition is the process by which gasses and particles from the atmosphere are transported to the aquatic and terrestrial surface (Pacyna, 2008). Atmospheric deposition can occur in the form of wet scavenging or dry deposition (Pycna *et al.*, 2008). Rates reported in the literature were used to make an estimation of N and P fluxes to the Hartbeespoort Dam. Formula 28 shows how rates from the literature were used to make this estimation. In addition, papers reporting concentrations of N and P in rainfall were converted to wet deposition flux using Formula 29. Surface area of the dam (20 km^2) was

multiplied with average annual rainfall to find the total average volume of water falling directly on the Hartbeespoort Dam in litres in a year. This was then multiplied with concentration in mg/L before being divided by 10^9 to convert mg to tons. Atmospheric deposition rates of 0.062 g P $m^{-2}.a^{-1}$ and 8–19 kg N $ha^{-1}.a^{-1}$ from Tipping et al. (2014) and Galy-Lacaux et al. (2003) respectively were used to estimate deposition fluxes

[Atmospheric deposition influx (t/a N or P)] = [areal flux (kg/m^2/a N and P)×10^{-3} (from the literature)] x [surface area of dam (m^2)]……..……..…..(28)

[Wet deposition flux (t/a N or P)] = [concentration of N or P in rainfall (mg/L) (from the literature)] x [average annual rainfall (mm)] x [surface area of dam (m^2)]×10^{-9} .....(29)

3.3.6. N fixation input

Nitrogen fixation is the process by which inert atmospheric nitrogen is converted to ammonia and then assimilated by a specialized group of prokaryotes (Wagner, 2011). NWIR (1985) found that N fixation rates at the Hartbeespoort Dam were not detectable in any of the water or sediment samples examined. This was expected since normally, N fixation only occurs in N-limited impoundments (Howarth *et al.*, 1988). In addition, the dominant algae species is *M. aeruginosa,* which is not an N fixing species (Monchamp *et al.*, 2014). Nevertheless, an N fixation rate of 0.2–9.2 g N $m^{-2}.a^{-1}$ reported in Howarth et al. (1988) for eutrophic lakes was converted to N influx using equation 30.

[N fixation influx (t/a N)] = [areal flux (g/m^2/a N)×10^{-6} (from the literature)] x [surface area of the dam (m^2)]……..……...….(30)

3.3.7. Groundwater input and output

Groundwater and surface water are often interlinked but their interaction is challenging to measure because of the heterogeneity of aquifers (Abiye *et al.*, 2015). In the case of the Hartbeespoort Dam, the degree to which the groundwater inputs interact with surface

water, and therefore the degree to which the rivers contaminate aquifers, has not been investigated fully. Extensive mixing of surface and groundwater occurs in the Upper Crocodile catchment (Abiye *et al.*, 2015). However, groundwater closer to the Hartbeespoort Dam may be unaffected by contamination (Davis, 2017).

A significant portion of P is removed before it reaches the water table (Spiteri *et al.*, 2007). Phosphates can move through soil, however, although slowly. For example, in a calcareous geological setting (which is the case of the Hartbeespoort Dam since the area is dominated by dolomites), a P plume takes 20 years to travel 10 m from a point source (Spiteri *et al.*, 2007). It will therefore be assumed that the groundwater P coming into the Hartbeespoort Dam is negligible as it is likely to have been sorbed into sediments and not transported in groundwater. The release of dissolved P from the sediment-water interface plays an increasing role with high P loading (Hupfer and Lewandowski, 2008). Thus the groundwater P outflow was assumed to have the same water chemistry as canal water. Nitrgen is mobile in the subsurface and is generally only removed by denitrification, requiring anoxic conditions, or pyrite/organic matter oxidation (MacQuarrie *et al.*, 2001). The N content of the groundwater flowing into the Hatbeespoort Dam was assumed to have the same chemistry as the river water. The N concentration of water leaving the dam though groundwater was assumed to have the same concentrations as canal water. To calculate N and P input and output fluxes in g/s, Formula 2 was used. These fluxes were then converted to flux in t/a.

3.3.8 Sedimentation

Lake bottoms act as sinks for nutrients, and not sources in the long-term (Peimin *et al.*, 2000). Thus, even though there is sometimes a flux of nutrients from the sediment into the water column, there is a net accumulation in the sediment (Peimin *et al.*, 2000). A number of methods exist for determining sedimentation rates, including theoretical models, using sediment cores, sediment traps and mass balances. Using sediment traps, NWIR (1985) calculated that P deposition flux to the sediment was 660 t/a, which exceeded the total annual P load by almost three times (average P inflow for 1980/81 to

1983/4 was 270 t/a), indicating that re-suspension played a major role in gross P sedimentation (NWIR, 1985). Using mass balance techniques, Chutter and Rossouw (1991) determined that between 60% 85% of the incoming P load is sedimented each year in the Hartbeespoort Dam. NWIR (1985) found that net sedimentation losses were highly variable, with no seasonal patterns. In addition, no spatial separation of different sediments could be made (NWIR, 1985).

Chutter and Rossouw (1991) determined the mass of P sedimented each year in the Hartbeespoort Dam by subtracting the outflow mass and the difference in the mass of P in the dam water from the inflow, shown by Formula 31. On average, the difference of the mass in the dam water column was 10 t P (Chutter and Rossouw, 1991). Determining the whole lake average P concentration, which is needed to calculate the mass of P in the dam, was beyond the scope of this study. Although the difference of the mass of nutrients in the dam water column may vary from year to year, because it is a relatively small number in comparison to the inflow flux, this study will assume it to zero. Thus P and N sedimentation fluxes were calculated using Formula 32.

[Sedimented P (t)] = [inflow mass P (t)] – [outflow mass P (t)] – [Δ mass in dam]…..(31)
where: [Δ mass in dam (t)] = [mass in dam on 1 October (t)] – [mass in dam on 1 September the following year (t)]

[N or P Net sedimentation flux] = Σ[N or P Inputs (river influx + atmospheric deposition influx + groundwater influx + *N fixation influx in the case of N*)] – Σ[N or P Outputs (river outflux + water hyacinth outflux + algae outflux + fish outflux + groundwater outflux + *denitrification in the case of N)*] …….(32)

CHAPTER 4: RIVER FLUX RESULTS

Chapter 4 examines fluxes and trends of river components to meet objectives 1 and 2 of the study. Three flux calculation methods are compared.

4.1. Annual P and N river inflows and outflows

Table 4.1.1 shows the annual river P inflow and outflow using three calculation methods. An average of between 578 and 610 t/a P from the Crocodile and Magalies rivers flowed into the Hartbeespoort Dam during hydrological years 2010/11 until 2016/17. Approximately 175 - 234 t P left the Hartbeespoort Dam each year from the river outflows of the dam during the same period. Approximately 30 to 39% of the incoming P from the rivers left the dam through the river outflows each year, meaning the remaining 61 – 70% (358 - 403 t/a) left the water column through biomass harvesting or sedimentation (discussed in chapter 5 and 6).

Table 4.1.1: Annual river P inflow and outflow of the Hartbeespoort Dam using the three flux calculation methods for hydrological years 2010-2011 until 2016-2017

	Spot Flow Method		Daily Average Flow Method		Two-Weekly Flow Method	
Hydrological Year	P Inflow (t)	P Outflow (t)	P Inflow (t)	P Outflow (t)	P Inflow (t)	P Outflow (t)
2010-2011	343	197 (57%)	418	169 (41%)	434	148 (34%)
2011-2012	511	116 (23%)	470	87 (19%)	519	156 (30%)
2012-2013	470	168 (36%)	441	129 (29%)	405	200 (49%)
2013-2014	1134	157 (14%)	946	135 (14%)	667	232 (35%)
2014-2015	594	227 (38%)	591	185 (31%)	620	223 (36%)
2015-2016	547	482 (88%)	535	328 (61%)	663	393 (44%)
2016-2017	662	287 (43%)	646	198 (29%)	762	316 (41%)
Average	**610**	**234 (38%)**	**578**	**175 (30%)**	**582**	**224 (39%)**

An average of between 4437 and 4687 t/a N from the Crocodile and Magalies rivers flowed into the Hartbeespoort Dam each year during hydrological years 2010/11 until 2016/17. Approximately 2498 to 1976 t/a N left the Hartbeespoort Dam each year from the outflows of the dam during the same period. Approximately 45 – 53% of the incoming N from the rivers left the dam through the river outflows, meaning the remaining 47 to 55% (2172 - 2461 t) left the water column through biomass harvesting, sedimentation, or denitrification (discussed in Chapter 5 and 6).

Table 4.1.2: Annual N inflow and outflow using the three flux calculation methods for hydrological years 2010-2011 until 2016-2017

	Spot Flow Method		Daily Average Flow Method		Two-Weekly Flow Method	
Hydrological Year	N Inflow (t)	N Outflow (t)	N Inflow (t)	N Outflow (t)	N Inflow (t)	N Outflow (t)
2010-2011	3 198	3 295 (103%)	3 732	2 622 (70%)	4 133	2 403 (58%)
2011-2012	2 758	1 383 (50%)	2 480	940 (38%)	2 595	1 699 (65%)
2012-2013	2 758	1 848 (50%)	3 533	1 464 (41%)	3 639	2 142 (59%)
2013-2014	7 716	2 416 (31%)	6 738	2 107 (31%)	5 485	3378 (62%)
2014-2015	3 967	2 329 (59%)	3 934	1 862 (47%)	4 165	2 282 (55%)
2015-2016	4 338	2 775 (64%)	4 234	2 747 (65%)	5217	2 482 (48%)
2016-2017	6 571	2 992 (46%)	6 407	2 093 (33%)	7 474	3 058 (40%)
Average	**4 607**	**2 434 (53%)**	**4 437**	**1 976 (45%)**	**4 687**	**2 492 (53%)**

4.2. Impact of flow on inflow flux

The Crocodile River is responsible for the vast majority of the nutrient influx to the Hartbeespoort Dam, as shown in section 7.1 in the Appendix. Thus the inflow site on the Crocodile River was chosen to compare inflow flux calculation methods. Table 4.2.1 compares the descriptive statistics of the various P inflow flux calculation methods. Flux

observations are spaced at approximately fortnightly intervals from 2 June 2010 until 25 April 2018.

Figure 4.2.1 compares the mean P fluxes of the various flux calculation methods at the inflow site on the Crocodile River. Shapiro-Wilk normality tests showed that the distributions of the four groups were not normal (*p*-value for all three groups was 0.0001). Log, square root, cube root and inverse transformations were not successful in normalizing the groups. Thus the Kruskal-Wallis test was used to determine if there were statistically significant differences between the four groups. The samples were found not to come from the same population (one tailed *p*-value = 0.037). However, paired comparisons showed no significant differences between each flux calculation method. The *p*-values for each paired difference of the various P flux calculation methods of site 90164 on the Crocodile River are presented in Table 4.2.2. There were no significant differences between any of the flux calculation methods. A Bonferroni comparison test was used to protect against type 1 errors. This means there is added certainty when concluding that the samples were not significantly different.

Table 4.2.3 compares the descriptive statistics of the various N flux calculation methods at the inflow site on the Crocodile River. Figure 4.2.2 compares the mean N fluxes of the various N flux calculation methods at the inflow site on the Crocodile River. Shapiro Wilk normality tests showed that the distributions of all three groups were not normal (*p*-value = 0.0001 for all three groups). Log, square root, cube root and inverse transformations were not successful in normalizing the data. Thus the Kruskal-Wallis test was used to determine if there were statistically significant differences between the three groups. The samples were found to come from the same population (one tailed *p*-value = 0.0548). Paired comparisons showed no significant differences between each flux calculation method. The *p*-values for each paired differences of the various P flux calculation methods of the inflow site on the Crocodile River are presented in Table 4.2.4. There were no significant differences between any of the three flow calculation methods.

Table 4.2.1: Descriptive statistics of the various P flux calculation methods of the inflow site on the Crocodile River

Flux calculation method	*n*	Mean (t/a)	Std.Dev (t/a)	Min (t/a)	Max (t/a)
Spot Flow	178	589	973	107	12 873
Daily Average Flow	177	564	648	106	8 214
Two-Weekly Flow	178	577	292	138	1 710

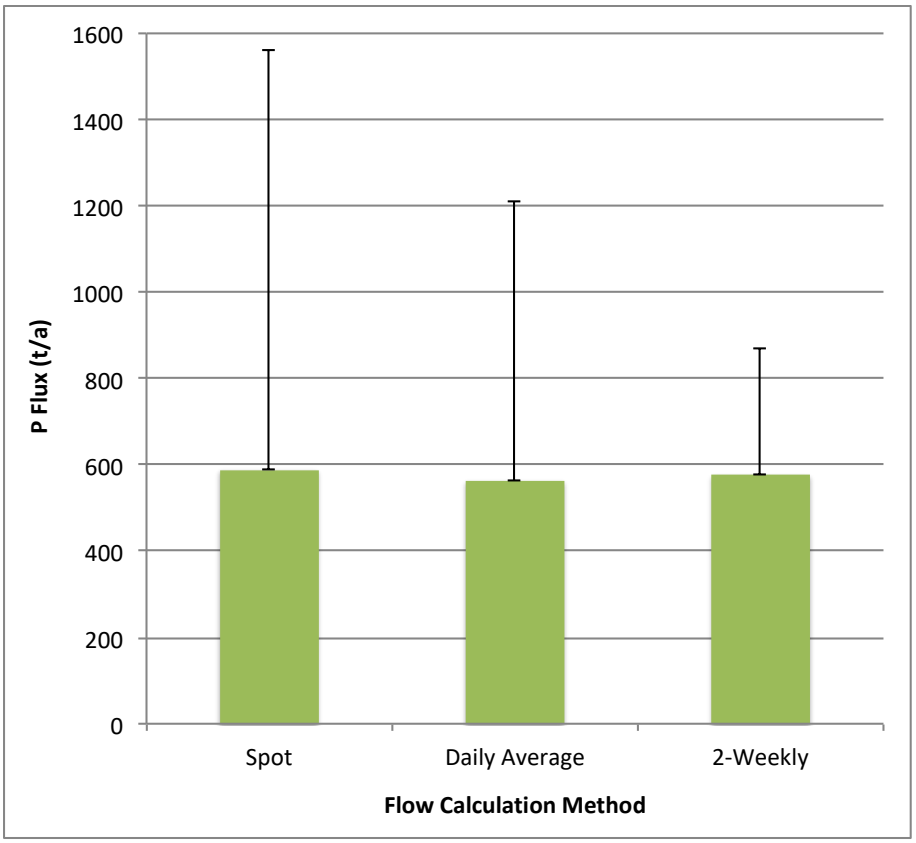

Fig. 4.2.1: Mean P flux (t/a) of the different flow calculation methods at the inflow site on the Crocodile River. Bars represent means. Error bars represent standard deviations.

Table 4.2.3: Descriptive statistics of the various N flux calculation methods of site 90164 on the Crocodile River

Flux calculation method	*n*	Mean (t/a)	Std.Dev (t/a)	Min (t/a)	Max (t/a)
Spot Flow	190	4423	4925	307	64 355
Daily Average Flow	189	4293	3556	315	41 066
Two-Weekly Flow	190	4617	2390	323	13 398

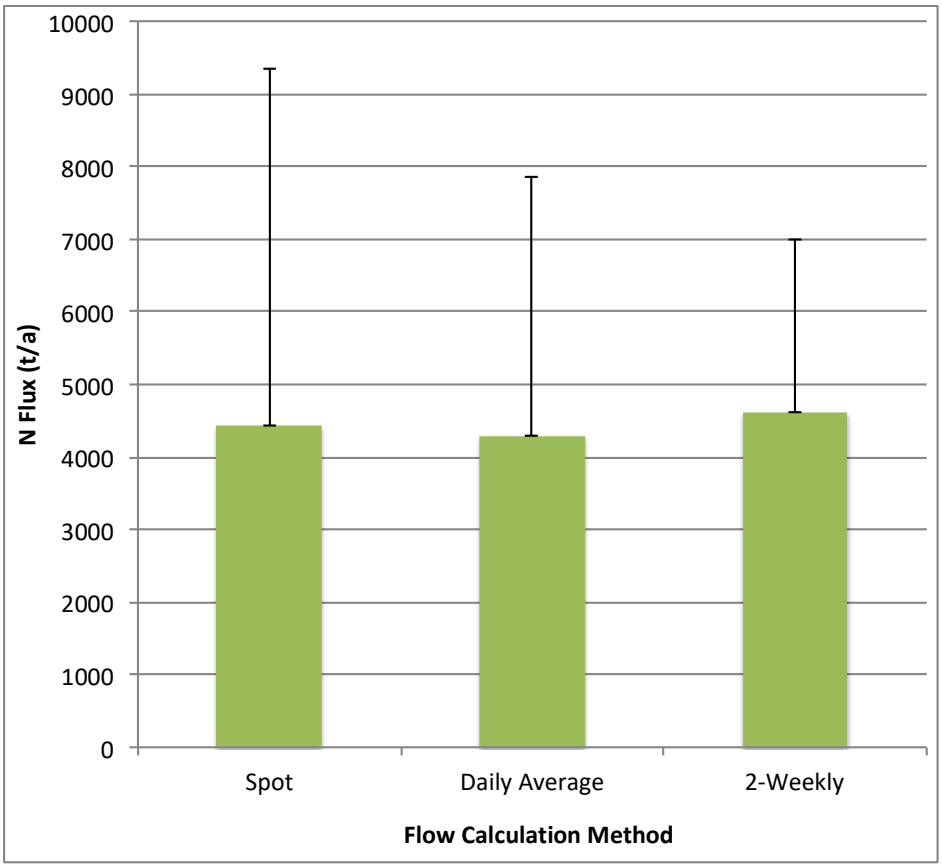

Fig. 4.2.2: N flux (t/a) of the different flow calculation methods at the inflow site on the Crocodile River. Bars represent means. Error bars represent standard deviation.

Table 4.2.2: Pairwise comparison of *p*-values for the various P flux calculation methods at the inflow site on the Crocodile River (no significant differences).

	Spot	**Daily Average**	**Two-Weekly**
Spot	**1.000**	0.947	0.0340
Daily Average	0.947	**1.000**	0.0402
Two-Weekly	0.0340	0.0402	**1.000**

Bonferroni corrected significance level: 0.0167

Table 4.2.4: Pairwise comparison of *p*-values for the various N flux calculation methods at the inflow site on the Crocodile River (no significant differences).

	Spot	**Daily Average**	**Two-Weekly**
Spot	**1.000**	0.920	0.0351
Daily Average	0.920	**1.000**	0.0275
Two-Weekly	0.0351	0.0275	**1.000**

Bonferroni corrected significance level: 0.0167

4.3. Impact of flow on outflow flux

The flux calculation methods from the two abstraction canals and radial sluices are compared in this section. Unlike the inflow data comparisons in Section 4.2, where data from only one site were compared, the outflow data examines three sites where observations were taken on different days. Thus for comparability, outflow flux observations (i.e. flow values multiplied by nutrient concentrations) were spaced at monthly intervals instead of fortnightly intervals (i.e. the average of two fortnightly flux observations). Outflow flux observations were taken from June 2010 until April 2018.

Table 4.3.1 compares the descriptive statistics of the various P outflow flux calculation methods. Figure 4.3.1 compares the means of the various flux calculation methods used to determine outflow P flux. Shapiro-Wilk normality tests showed that the distributions of the three groups were not normal (*p*-value = 0.0001). Log, square root, cube root and inverse transformations were not successful in normalizing the data. Thus the Kruskal-

Wallis test was used to determine if there were statistically significant differences between the three groups. The samples were found not to come from the same population (one tailed *p*-value = 0.0003). Table 4.3.2 compares the *p*-values for each paired difference of the different flow calculation methods used to determine outflow P flux. There was no significant difference between the Spot Flow and Two-Weekly Flow fluxes. However, Daily Average Flow flux was significantly different from both Spot Flow Flux and Daily Average Flow flux.

Table 4.3.3 compares the descriptive statistics of the various N outflow flux calculation methods. Figure 4.3.2 compares the means of the various flow calculation methods used to determine outflow N flux. Shapiro-Wilk normality tests showed that the distributions of the three groups were not normal (*p*-value = 0.0001 for all three groups). Log, square root, cube root and inverse transformations were not successful in normalizing the data. Thus the Kruskal-Wallis test was used to determine if there were statistically significant differences between the three groups. The samples were found not to come from the same population (one tailed *p*-value = 0.0001). Table 4.3.4 compares the *p*-values for each paired difference of the various flux calculation methods used to determine N outflow flux. There was no significant difference between Spot Flow flux and Two-Weekly Flow flux. However Daily Average Flow flux was significantly different from both Spot Flow flux and Daily Average Flow flux.

Table 4.3.1: Descriptive statistics of the various P outflow flux calculation methods based on monthly averages

Flux calculation method	*n*	Mean (t/a)	Std.Dev (t/a)	Min (t/a)	Max (t/a)
Spot Flow	93	239	259	57	2449
Daily Average Flow	92	183	168	39	1429
Two-Weekly Flow	93	260	195	46	1328

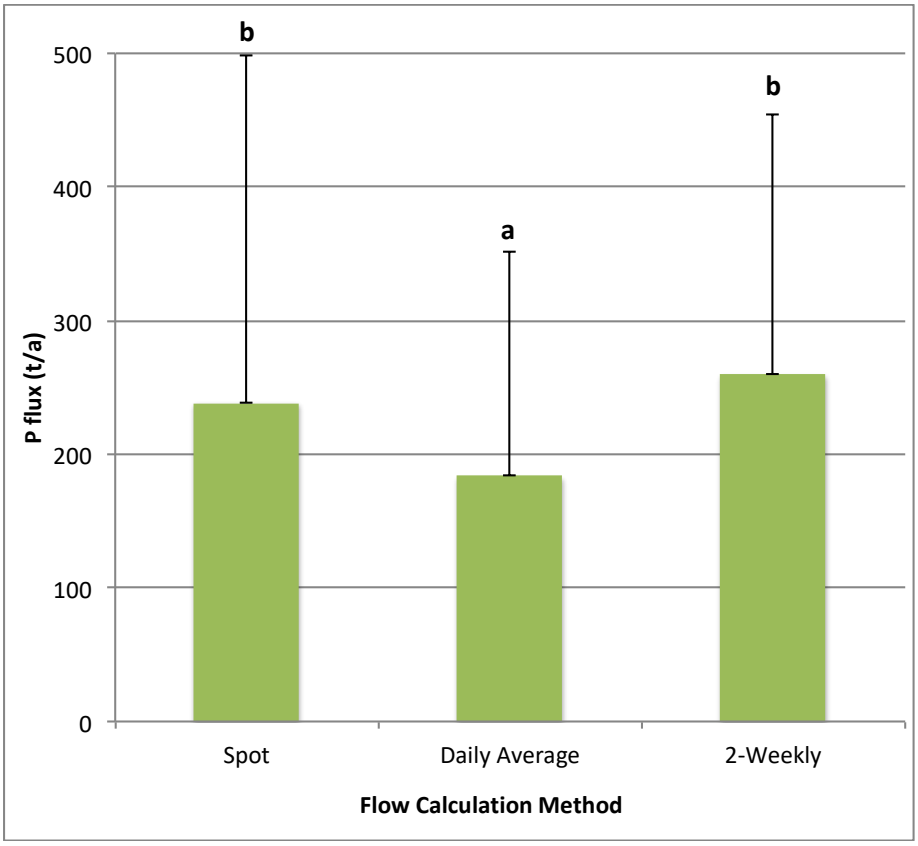

Fig. 4.3.1: Mean P outflow flux (t/a) of the various flux calculation methods. Bars represent means, error bars represent standard deviation and letters indicate significant differences.

Table 4.3.3: Descriptive statistics of the various N outflow flux calculation methods based on monthly averages

Flux calculation method	*n*	Mean (t/a)	Std.Dev (t/a)	Min (t/a)	Max (t/a)
Spot Flow	92	2447	1278	547	8 404
Daily Average Flow	88	1982	1379	292	10 212
Two-Weekly Flow	92	2681	1394	507	7 755

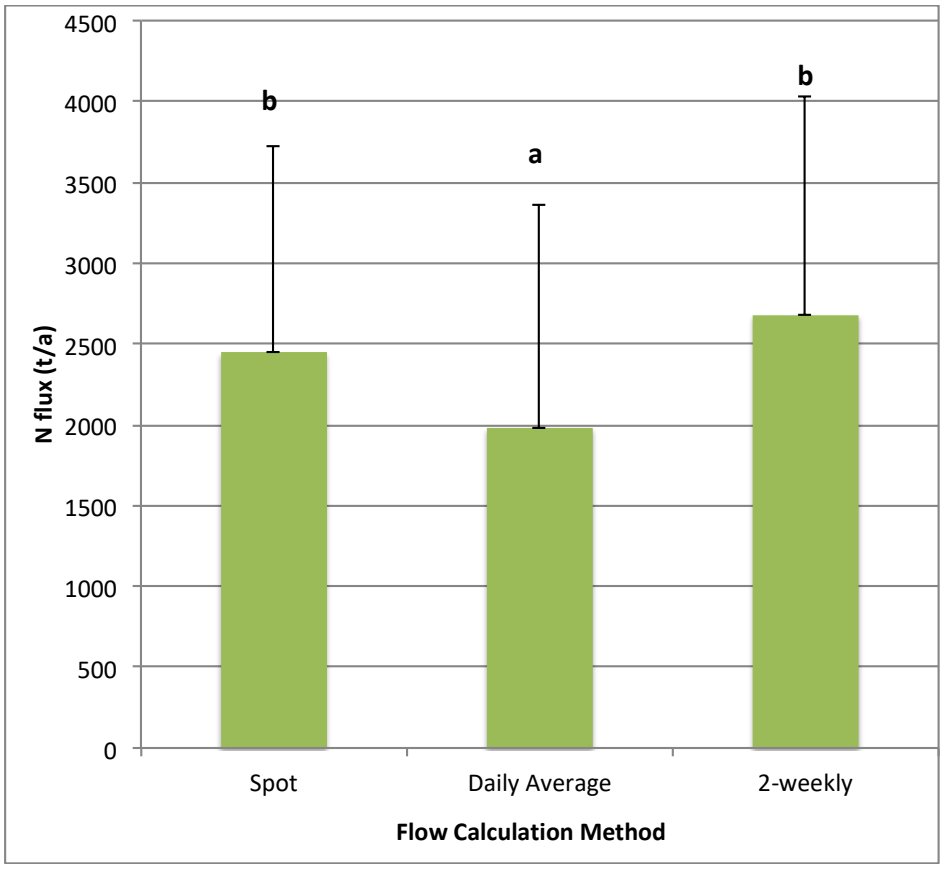

Fig. 4.3.2: Comparison of the mean outflow N flux (t/a) of the various flux calculation methods. Bars represent means, error bars represent standard deviation and letters indicate significant differences.

Table 4.3.2: Pairwise comparison of *p*-values for the various P outflow flux calculation methods ("*" indicates significant difference).

	Spot	**Daily Average**	**Two-Weekly**
Spot	**1.000**	0.006*	0.220
Daily Average	0.006*	**1.000**	0.0001*
2-Weekly	0.220	0.0001*	**1.000**

Bonferroni corrected significance level: 0.0167

Table 4.3.4: Pairwise comparison of *p*-values for the various N outflow flux calculation methods ("*" indicates significant difference).

	Spot	**Daily Average**	**Two-Weekly**
Spot	**1.000**	0.0009*	0.159
Daily Average	0.0009*	**1.000**	0.0001*
Two-Weekly	0.159	0.0001*	**1.000**

Bonferroni corrected significance level: 0.0167

4.4. P seasonal time series and trends

Figure 4.4.1 compares the seasonal P inflow from the Crocodile and Magalies rivers with the seasonal P outflow from the left canal, right canal and radial sluice from June 2010 until April 2018 using spot flow values. Table 4.4.1 shows the descriptive statistics of the seasonal P river inflow and outflow of the Hartbeespoort Dam using spot flow values. Both seasonal inflow and outflow have one major positive outlier. The Shapiro-Wilk normality test showed that the distributions of both the seasonal P inflow and outflow were not normal (*p*-value = 0.0001 for both inflow and outflow) and attempts to normalise both inflow and outflow using log, square root, cube root and inverse transformations were not successful. Thus, the non-parametric Wilcoxon signed rank test was used to detect a difference between the distributions of the seasonal inflow and outflow groups. The two samples were significantly different (*p*-value = 0.001). The

Durbin-Watson test showed that the residuals were not auto-correlated ($U = 2$, p-value = 0.499).

Table 4.4.1: Descriptive statistics of seasonal P inflow and outflow (Spot Flow Method)

	n	Mean (t/season)	Std.Dev (t/season)	Min (t/season)	Max (t/season)
P Inflow (Spot flow)	31	145	93	57	601
P Outflow (Spot flow)	31	63	50	17	282

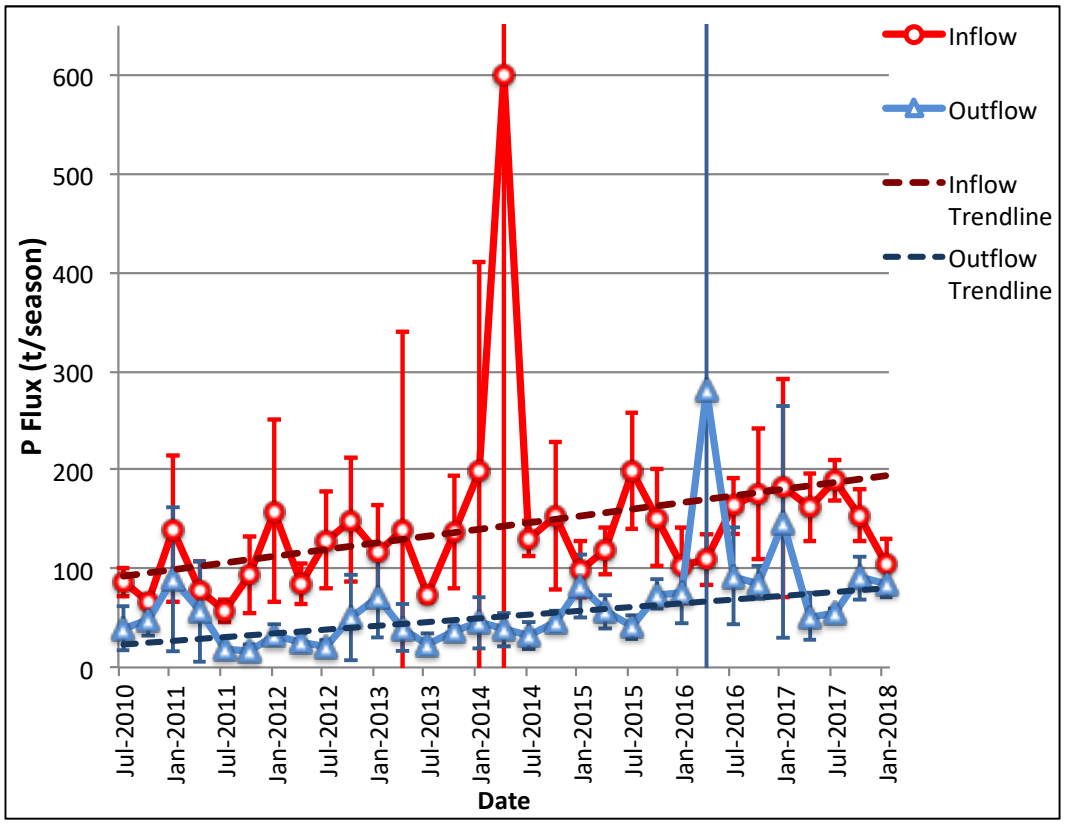

Fig. 4.4.1: Seasonal river flux of P into and out of the Hartbeespoort Dam (t/season) from June 2010 until February 2018. Calculations based on Spot Flow values. Error bars represent standard deviations.

Figure 4.4.2 compares the seasonal P inflow from the Crocodile and Magalies rivers with the seasonal P outflow from the left canal, right canal and radial sluice from June 2010 until January 2018 using Two-Weekly flow values. Table 4.4.2 shows the descriptive statistics of the seasonal P river inflow and outflow using Two-Weekly flow values. The

Shapiro-Wilk normality test showed that the distributions of the seasonal P inflow and outflow were normal (p-value = 0.470 for inflow, p-value = 0.598 for outflow). Thus a two sample paired t-test was used to detect a difference between the inflow and outflow groups. There was a significant difference between the seasonal inflow and outflow groups (p-value = 0.0001).

Table 4.4.2: Descriptive statistics of seasonal P inflow and outflow (Two-Weekly flow method)

	n	Mean (t/season)	Std.Dev (t/season)	Min (t/season)	Max (t/season)
P Inflow (Two-Weekly flow)	31	142	45	64	228
P Outflow (Two-Weekly flow)	31	57	24	16	109

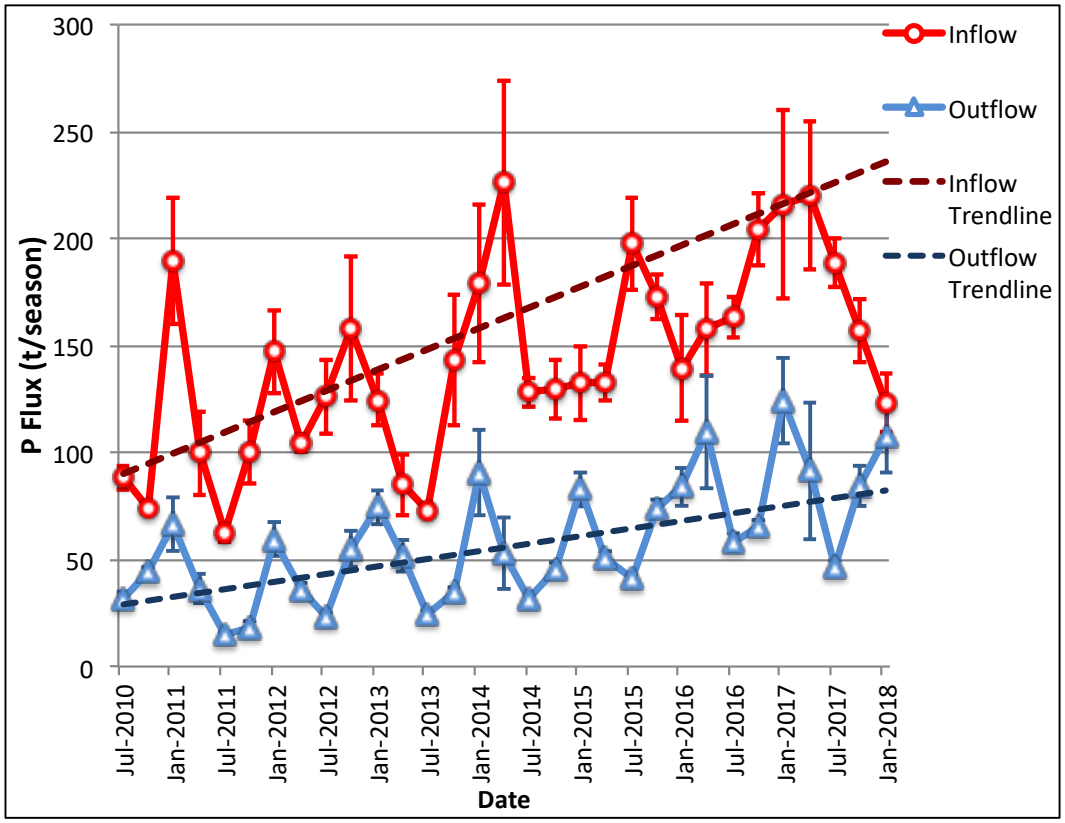

Fig. 4.4.2: Seasonal river TP fluxes into and out of the Hartbeespoort Dam (t/season) from June 2010 until February 2018. Calculations based on Two-Weekly Flow values. Error bars represent weighted standard deviations.

Figure 4.4.3 illustrates the annual P (t/a) inflow, outflow and difference of hydrological years 2010/2011 until 2016/2017 using two-weekly flow values. Figure 4.4.3, which depicts annual trends, is presented here for comparison with Figure 4.4.2, which depicts seasonal trends. Hydrological year 2016/2017 experienced the greatest P inflow (762 t) and 2010/2011 experienced the smallest P inflow (434 t). Hydrological year 2016/17 experienced the greatest P outflow (316 t) and 2010/11 experienced the smallest P outflow (148 t). Hydrological year 2016/17 experienced the greatest difference between inflow and outflow (446 t) and 2012/13 experienced the smallest difference (205 t).

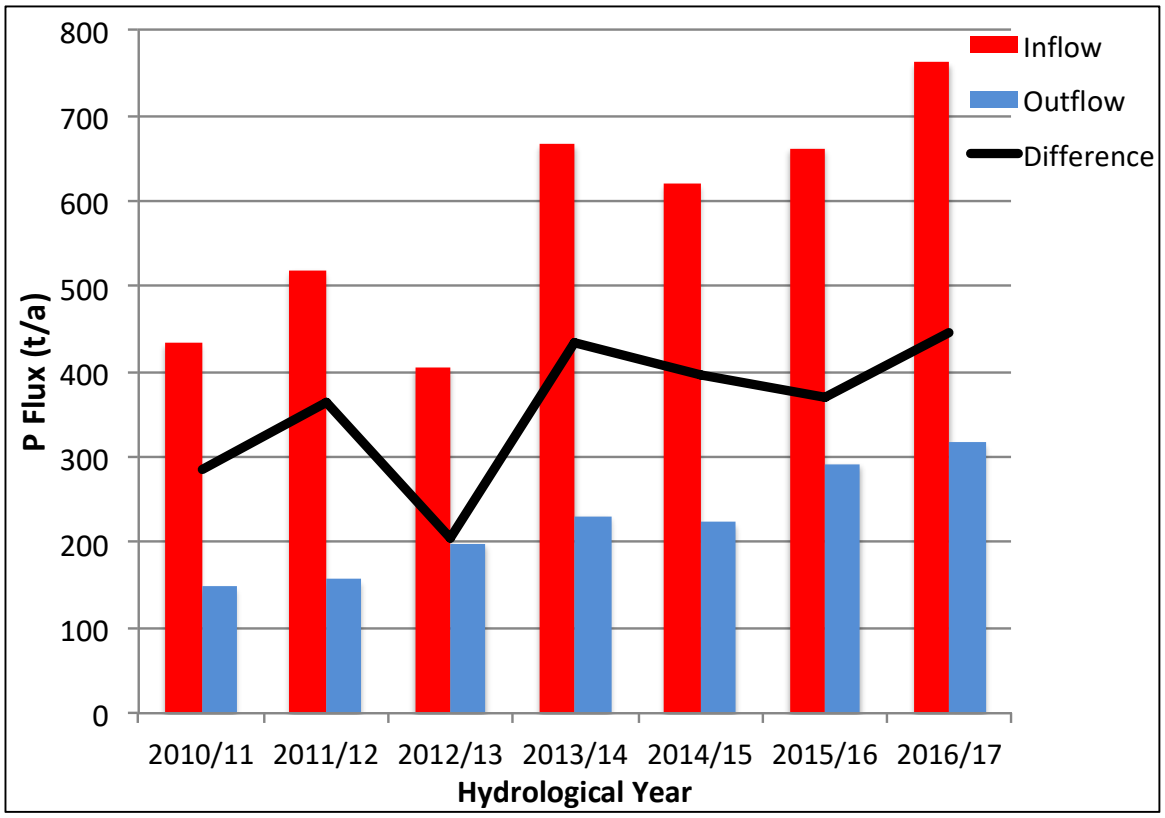

Fig. 4.4.3: Annual P (t/a) inflow, outflow and difference (inflow minus outflow) for hydrological years (October – September) at the Hartbeespoort Dam using two-weekly values.

The seasonal Mann-Kendall test was used to test if there was a trend in the P inflow and outflow fluxes of the various flux calculation methods whilst taking into account

seasonality over a 12-month period. All P river inflow and outflow fluxes had a significant trend in the series as shown by the *p*-values in Table 4.4.3. Table 4.4.3 shows that between June 2010 and April 2018, P inflow flux increased by between 54.2 and 77.8 t year on year, while P outflow flux increased by between 28.4 and 32.4 t per year.

Table 4.4.3: Sen's Slope and seasonal Mann-Kendall *p*-values of inflow and outflow P fluxes for the various flux calculation methods (asterisk indicates statistical significance)

	Inflow P Flux			Outflow P Flux		
	Sen's Slope (t/a)	*p*-value	*n*	Sen's Slope (t/a)	*p*-value	*n*
Spot Flow	54.2	0.0054*	31	30.1	0.0085*	31
Daily Average Flow	54.2	0.0199*	31	32.4	0.0053*	31
Two-Weekly Flow	77.8	0.0034*	31	28.4	0.0001*	31

4.5. N Seasonal time series and trends

Figure 4.5.1 compares the seasonal N inflow from the Crocodile and Magalies rivers with the average seasonal nitrogen outflow from the left canal, right canal and radial sluice from June 2010 until April 2018 using Spot Flow values. Table 4.5.1 shows the descriptive statistics of the seasonal N river inflow and outflow of the Hartbeespoort Dam using spot flow values. Seasonal N outflow has no outliers while average seasonal inflow has one major positive outlier. The Shapiro-Wilk normality test showed that the distributions of the seasonal N inflow and outflow were not normal (*p*-value = 0.0001 for inflow, *p*-value = 0.021 for outflow) and attempts to normalise the data using log, square root, cube root and inverse transformations were not successful. Thus, the non-parametric Wilcoxon signed rank test was used to detect a difference between the distributions of the inflow and outflow groups. The two samples were significantly different (*p*-value = 0.001).

Table 4.5.1: Descriptive statistics of seasonal N inflow and outflow (Spot flow method)

	n	Mean (t/season)	Std.Dev (t/season)	Min (t/season)	Max (t/season)
N Inflow (Spot flow)	31	1 126	567	395	3 365
N Outflow (Spot flow)	31	642	241	225	1 198

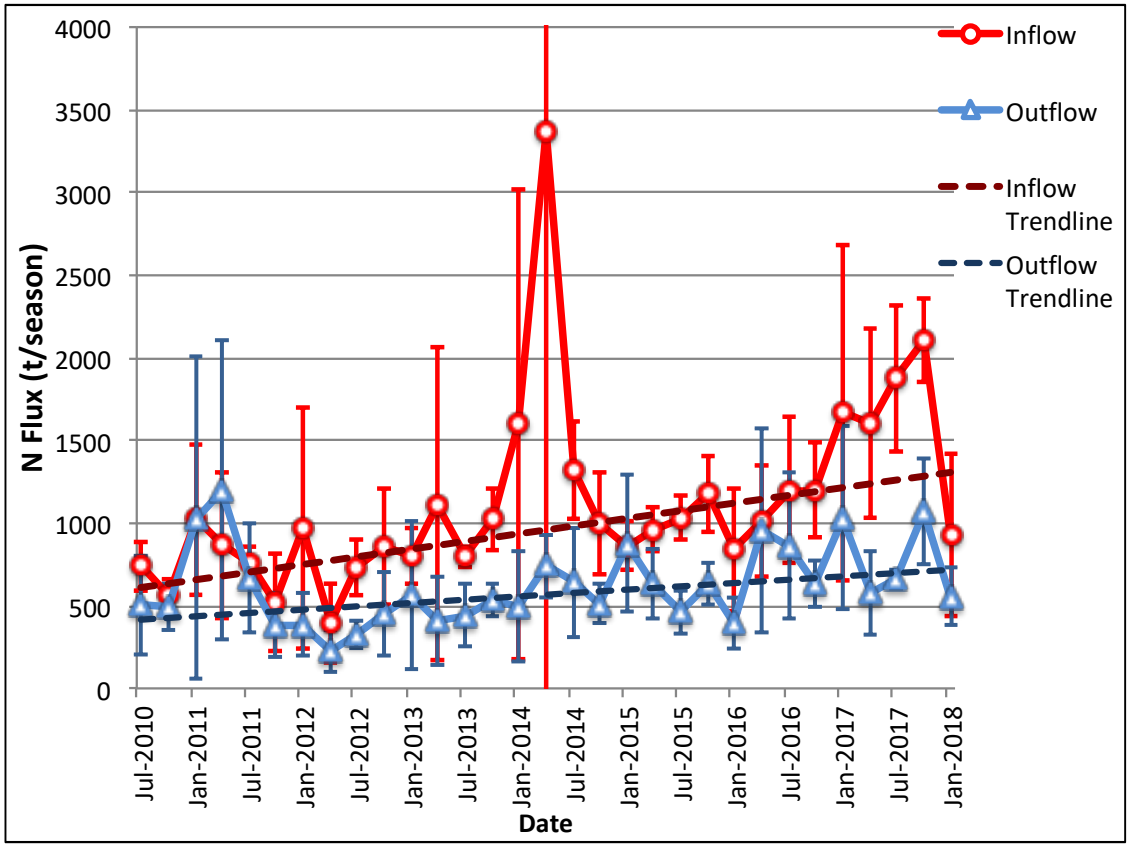

Fig. 4.5.1: Seasonal N river fluxes into and out of the Hartbeespoort Dam (t/season) from June 2010 until February 2018. Calculations based on spot flow values. Error bars represent standard deviations. Outflow trend line not significant.

Figure 4.5.2 compares the seasonal N inflow from the Crocodile and Magalies rivers with the seasonal N outflow from the left canal, right canal and radial sluice from June 2010 until January 2018 using Two-Weekly Flow values. Table 4.5.2 shows the descriptive statistics of the seasonal N river inflow and outflow using Two-Weekly flow values. The Shapiro-Wilk normality test showed that the distribution of the seasonal N inflow was normal (*p*-value = 0.530). The distribution of the seasonal N outflow was not normal (*p*-

value = 0.021). A log transformation was successful in normalising the outflow group (*p*-value = 0.466 for outflow and *p*-value = 0.705 for inflow after log transformations). Thus a two sample paired t-test was used to detect a difference between the inflow and outflow groups after both groups had been log transformed. There was a significant average difference between the inflow and outflow groups (*p*-value = 0.0001).

Table 4.5.2: Descriptive statistics of seasonal N inflow and outflow (Two-Weekly flow)

	n	Mean (t/season)	Std.Dev (t/season)	Min (t/season)	Max (t/season)
N Inflow (Two-Weekly flow)	31	1 148	413	434	2 044
N Outflow (Two-Weekly flow)	31	632	216	313	1 085

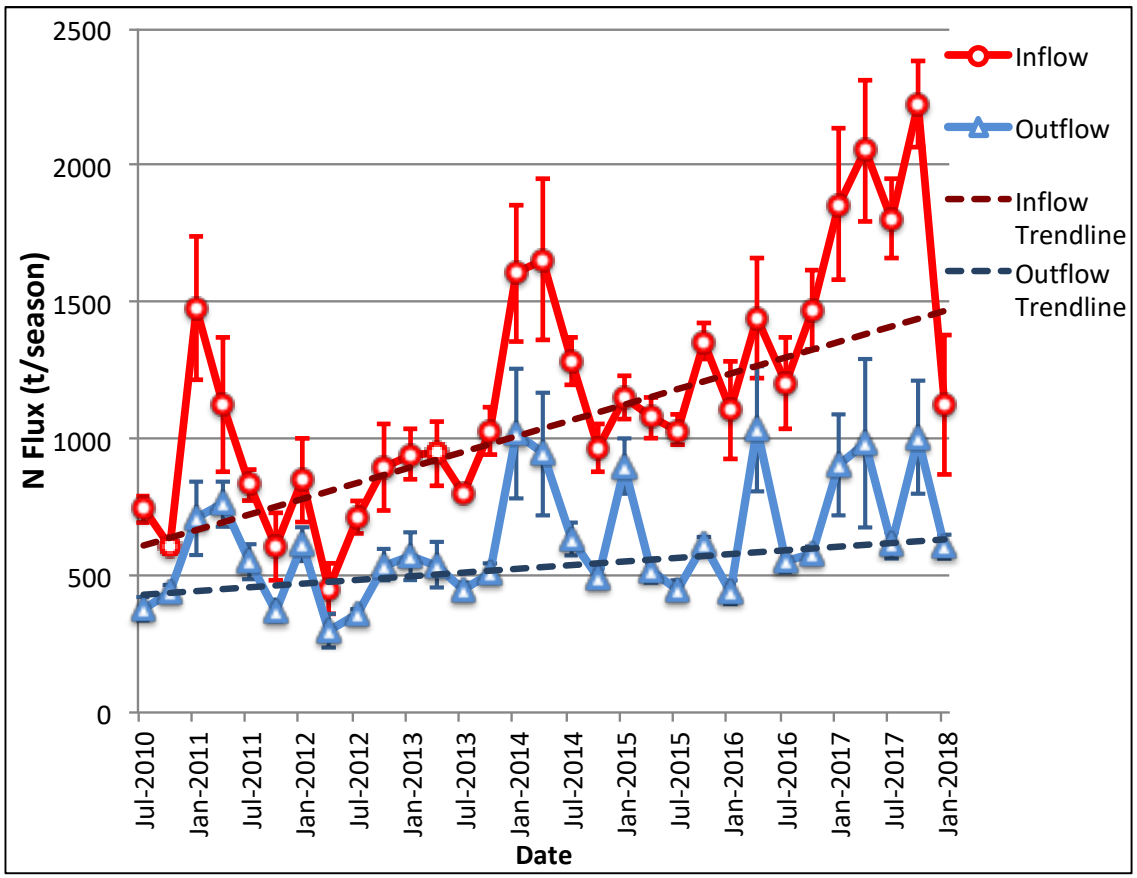

Fig.4.5.2: Seasonal N river fluxes into and out of the Hartbeespoort Dam in tons per season from June 2010 until January 2018. Calculations based on two-weekly flow values. Error bars represent weighted standard deviations.

Figure 4.5.3 illustrates the annual N (t/a) inflow, outflow and difference of hydrological years 2010/2011 until 2016/2017 using two-weekly flow values. Figure 4.5.3, which depicts annual trends, is presented here for comparison with Figure 4.5.2, which depicts seasonal trends. Hydrological year 2016/17 experienced the greatest N inflow (7 574 t) and 2011/12 experienced the smallest N inflow (2 595 t). Hydrological year 2013/14 experienced the greatest N outflow (3 378 t) and 2011/12 experienced the smallest N inflow (1 699 t). Hydrological year 2016/2017 experienced the greatest difference between the inflow and outflow (4 516 t) and 2011/12 experienced the smallest difference (896 t).

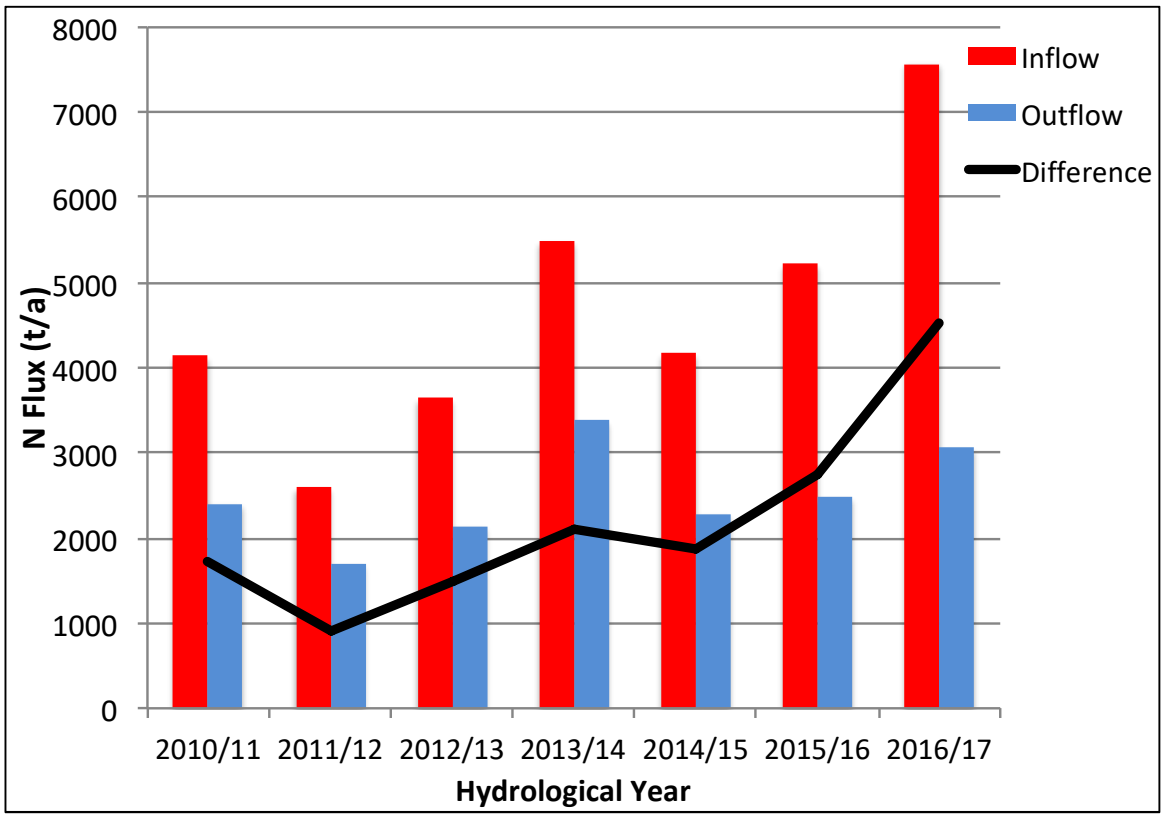

Fig 4.5.3: Annual N (t/a) inflow, outflow and difference (inflow minus outflow) for hydrological years (October – September) at the Hartbeespoort Dam using two-weekly values.

The seasonal Mann-Kendall test was used to test if there was a trend in the N inflow and outflow fluxes of the various flux calculation methods while taking into account seasonality over a 12-month period. All river N inflow and outflow fluxes had a significant trend in the series as shown by the *p*-values in Table 4.5.3. Table 4.5.3 shows that between June 2010 and April 2018, P inflow flux increased by between 296 and 522 t year on year, while P outflow flux increased by between 77 and 134 t.

Table 4.5.3: Sen's Slope and seasonal Mann-Kendall *p*-values of inflow and outflow N fluxes for the various flux calculation methods (asterisk indicates statistical significance)

	Inflow N Flux			Outflow N Flux		
	Sen's Slope (t/a)	*p*-value	*n*	Sen's Slope (t/a)	*p*-value	*n*
Spot Flow	368	0.0034*	31	164	0.0841	31
Daily Average Flow	465	0.0034*	31	115	0.0604	31
Two-Weekly Flow	456	0.0004*	31	110	0.0294*	31

4.6. How representative is the flow on sampling days?

In this section the distributions of the flow values used to calculate nutrient fluxes of the various flux calculation methods (Spot, Daily Average and Two-Weekly) were compared to the complete raw dataset in order to determine if the flow values used were representative. The inflow Site 90164 on the Crocodile River was examined, as it is responsible for the vast majority of the nutrient influx. Table 4.6.1 summarises the descriptive statistics of the complete raw dataset and various flux calculation methods. The non-parametric Kolmogorov-Smirnov (KS) test was used to compare the distributions of the flow values of each flux calculation method against the complete raw flow dataset as the Shapiro-Wilk normality tests showed that none of the datasets followed a normal distribution (*p*-values = 0.0001 for all datasets). The distributions of all the datasets were right skewed. As shown by the *p*-values of the KS tests in Table 4.6.1, the Spot flow and Daily Average flow value distributions were not significantly different to that of the complete raw flow dataset distribution. However, the Two-Weekly

flow distribution was different to the distribution of the complete raw flow dataset. In Table 4.6.1 the KS *p*-values presented for each method of flux calculation (Spot, Daily Average and Two-Weekly) are comparisons with the complete raw flow dataset (e.g. the *p*-value of the KS test comparing the distributions of the Spot flow values and the complete raw flow dataset was 0.468).

Table 4.6.1: Descriptive statistics of the complete raw flow dataset and flow values of the various flux calculation methods of inflow site 90164 on the Crocodile River, and Kolmogorov-Smirnov test *p*-values ('*' indicates significant difference)

	n	Mean (m^3/s)	Std.Dev (m^3/s)	Min (m^3/s)	Max (m^3/s)	KS test *p*-value
Complete Raw Dataset	309 946	17.74	19.2	7.22	594.74	N/A
Spot Flow	178	16.37	19.0	8.32	251.35	0.468
Daily Average Flow	177	16.08	13.6	7.97	160.39	0.594
Two-Weekly Flow	178	17.37	9.8	8.50	85.57	0.0004*

Figure 4.6.1 shows the distribution of the complete raw flow dataset at inflow site 90164 on the Crocodile River. Approximately 43.1% of the observations were between 10 and 13 m^3/s. Cumulatively, 90.9% of the raw flow observations were below 28 m^3/s. Observations above 37 m^3/s made up 5.7% of the total distribution. Observations above 25.27 m^3/s were minor positive outliers and make up 11% of the total observations. Observations above 33.71 m^3/s were major positive outliers and make up 6.64% of the total observations. There were no negative outliers. Figure 4.6.2 shows the distribution of Spot flow values used to calculate nutrient fluxes. Approximately 44.38% of the Spot flow observations were between 10 and 13 m^3/s. Cumulatively, 95.5% of the observations were below 28 m^3/s. Observations above 37 m^3/s made up 2.81% of the total distribution. Figure 4.6.3 shows the distribution of Daily Average Flow values used to calculate nutrient fluxes. Approximately 47.47% of the observations were between 10 and 13 m^3/s. Cumulatively, 94.3% of the Daily Average observations were below 28 m^3/s. Observations above 37 m^3/s made up 3.39% of the total distribution of Daily Average Flow observations. Figure 4.3.4 shows the distribution of the Two-Weekly flow

values used to calculate nutrient fluxes. Approximately 33.71% of the Two-Weekly flow observations were between 10 and 13 m^3/s. Cumulatively, 91.0% of the observations were below 28 m^3/s. Observations above 37 m^3/s made up 5.56% of the observations.

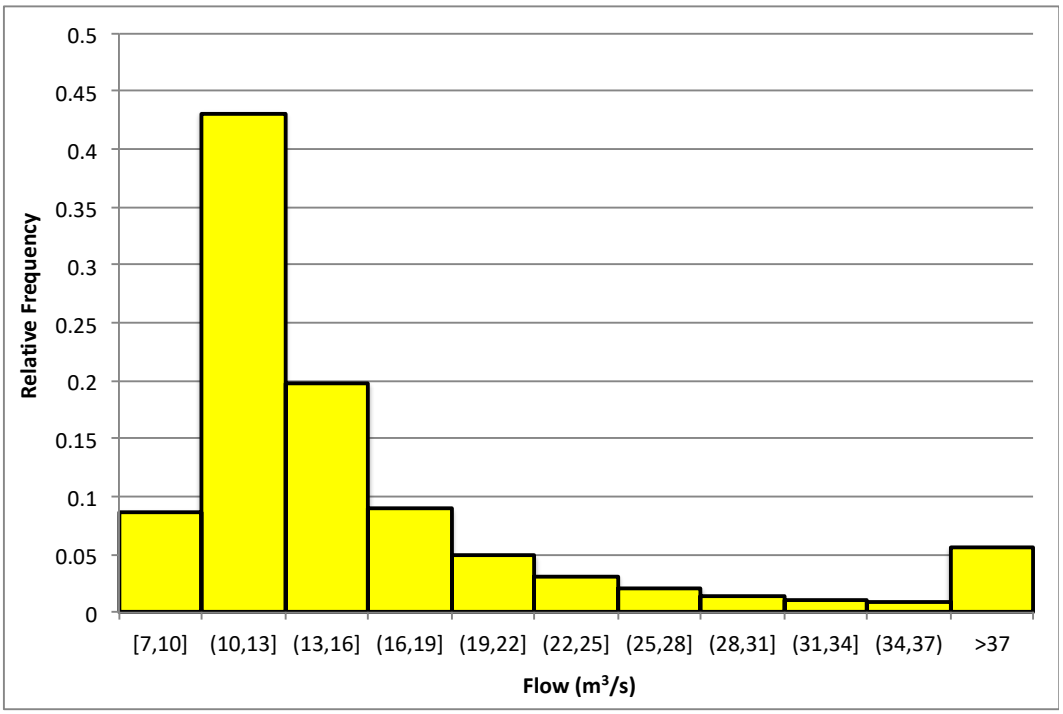

Fig. 4.6.1: Distribution of the complete raw flow dataset from 2 June 2010 until 25 April 2018 at inflow site on the Crocodile River. n = 309 946. On the x-axis a round bracket indicates the range is inclusive and a square bracket indicates the range is exclusive i.e. (10, 13] represents flows between 10 and 12.$\dot{9}$

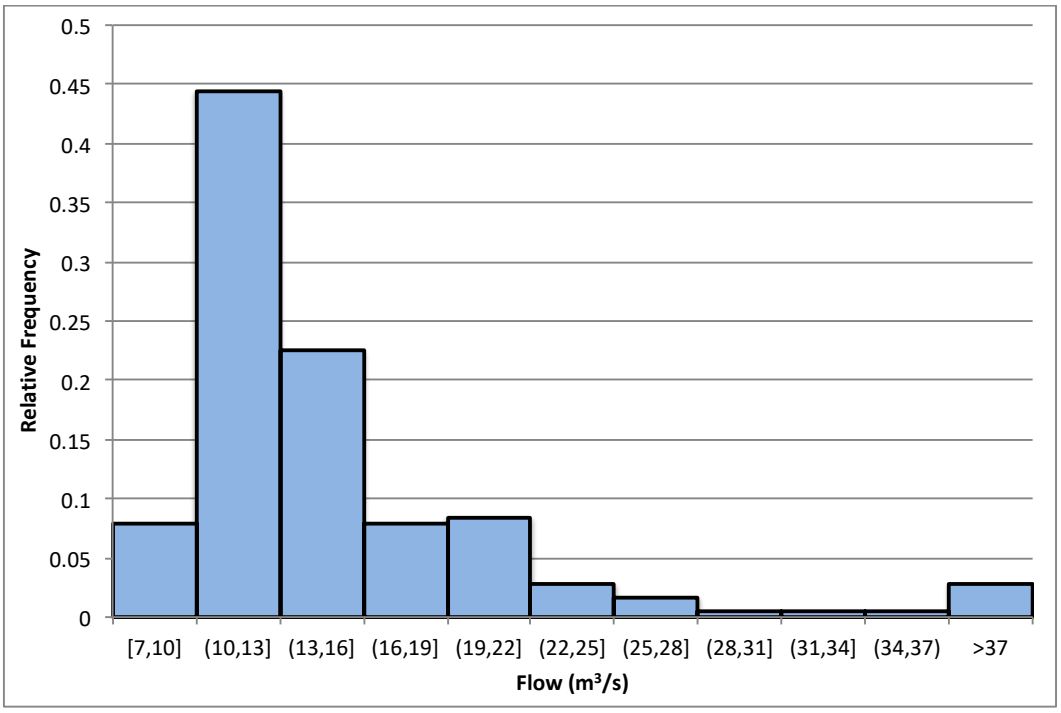

Fig. 4.6.2: Distribution of Spot flow values used to calculate nutrient fluxes at inflow site on the Crocodile River. $n = 178$

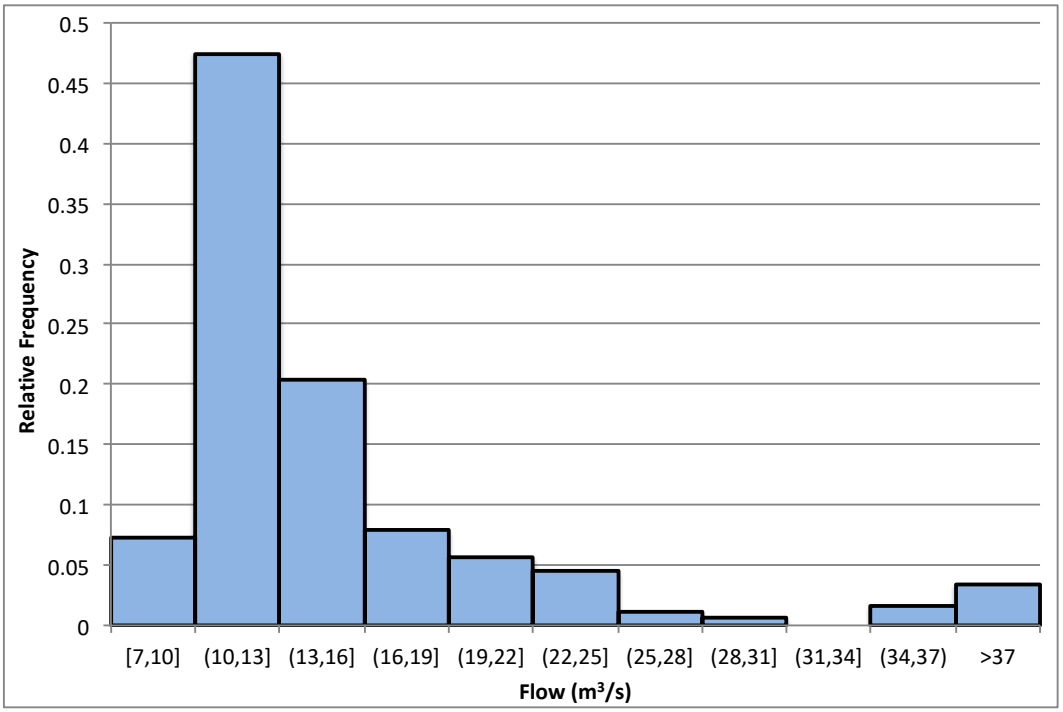

Fig. 4.6.3: Distribution of Daily Average flow values used to calculate nutrient fluxes at inflow Site on the Crocodile River. $n = 177$

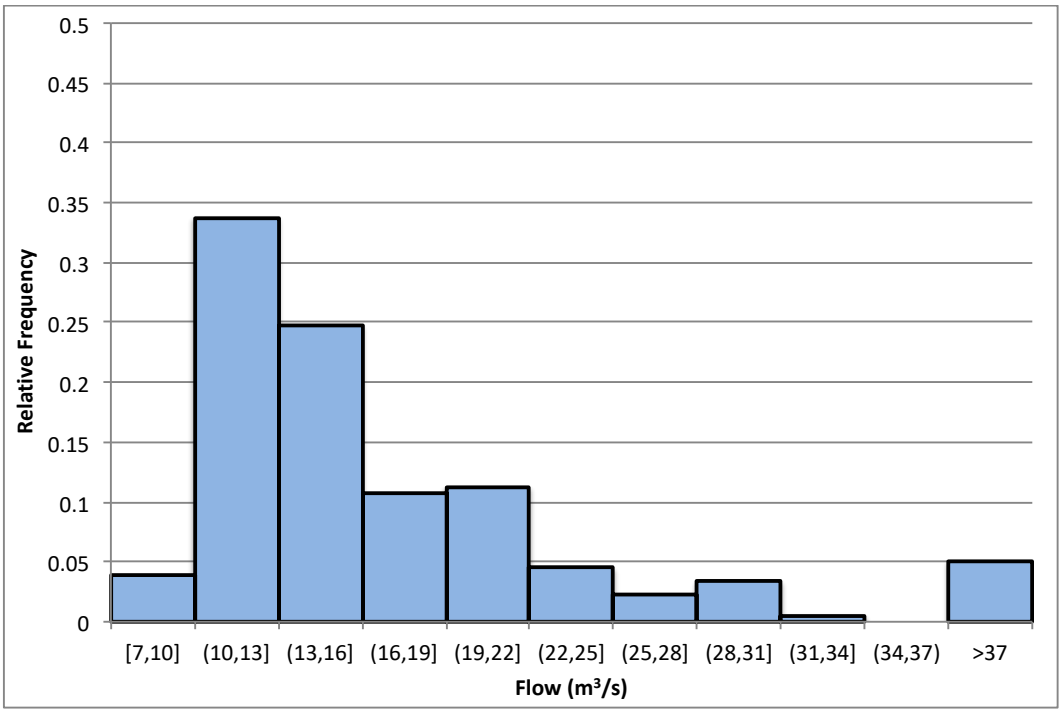

Fig. 4.6.4: Distribution of Two-Weekly flow values used to calculate nutrient fluxes at inflow Site on the Crocodile River. n = 178

4.7. Does flow affect concentration at inflow sites?

Figure 4.7.1 shows the relationship between Spot flow values and P concentrations at the inflow site on the Crocodile River. The descriptive statistics of P concentration on the Crocodile River are shown in Table 4.7.1. P concentration had three minor positive outliers (above 2.604 mg/L). The descriptive statistics of Spot flow are shown in Table 4.6.1 in the previous section. Spot flow had 14 minor positive outliers (above 23.1 m^3/s) and seven major positive outliers (above 30.1 m^3/s) as well as no negative outliers. A Spearman Rank correlation test was used to determine if there was a correlation between the spot flow values and P concentration as the Shapiro-Wilk normality test showed the distributions did not follow a normal distribution (p-value = 0.0001 for both P concentration and Spot flow). On the Crocodile River, there was a weak inverse linear relationship between the variables (-0.380) (p-value <0.0001). The p(F) of the linear regression model was 0.682, thus there was not a significant relationship between spot

flow and P concentration at the inflow site. Spearman's rho was 0.114, which indicates that 11.4% of the data were explained by the model.

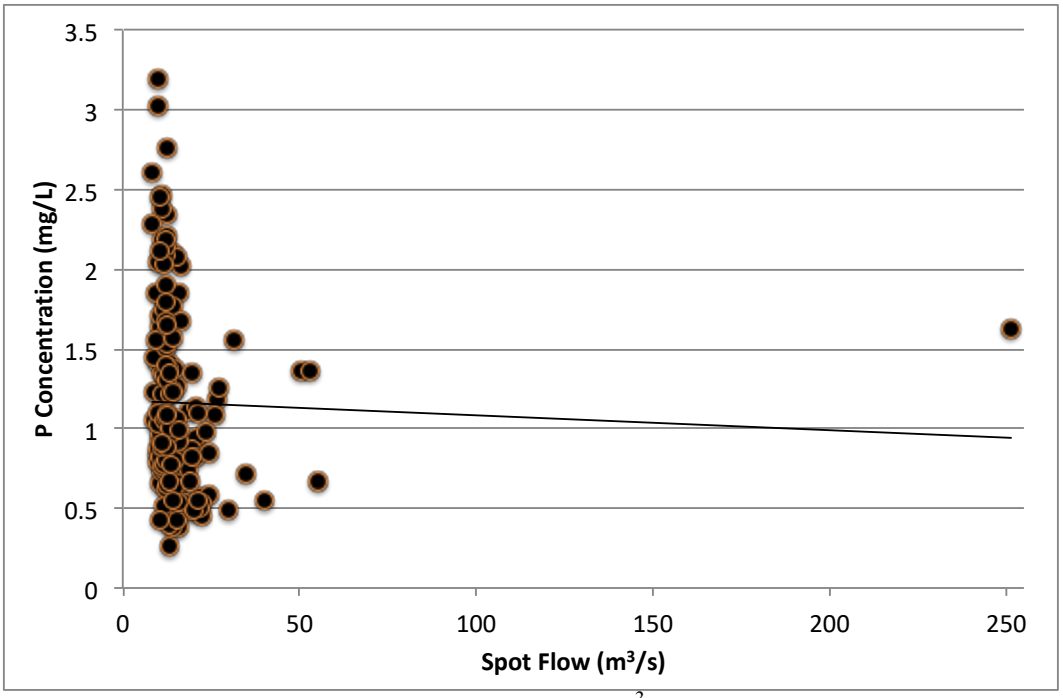

Fig. 4.7.1: Relationship between Spot flow (m^3/s) and P concentration (mg/L) at the inflow site on the Crocodile River. Straight line represents linear relationship (not significant).

Figure 4.7.2 shows the relationship between Spot flow and P concentration at the inflow site on the Magalies River. The descriptive statistics of P concentration and Spot flow of the Magalies River are shown in Tables 4.7.1 and 4.7.2, respectively. P concentration had 29 minor positive outliers (above 0.227 mg/L) and 20 major positive outliers (above 0.350 mg/L). Spot flow had 23 minor positive outliers (above 1.54 m^3/s) and 17 major positive outliers (above 2.33 m^3/s) as well as no negative outliers. Two observations were major positive outliers on both the x- and y-axis. A Spearman Rank correlation test was used to determine if there was a correlation between Spot flow and P concentration as the Shapiro-Wilk normality test showed the data did not follow a normal distribution (*p*-value = 0.0001 for both P concentration and Spot flow). On the Magalies River, there was a weak positive linear relationship between the variables (0.333) (*p*-value = 0.0001). The *p*(F) of the linear regression model was 0.004, thus there was a significant relationship

between Spot flow and P concentration at the inflow site on the Magalies River. Spearman's rho was 0.111, which indicates that 11.1% of the data were explained by the model.

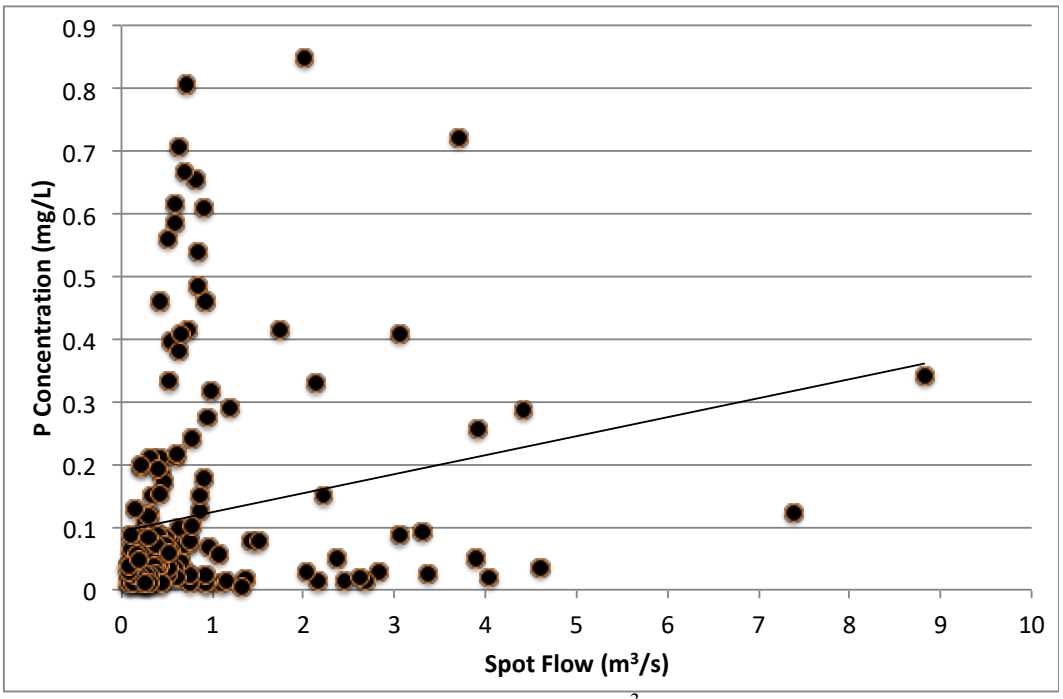

Fig. 4.7.2: Relationship between Spot flow (m^3/s) and P concentration (mg/L) at The inflow site on the Magalies River. Straight line represents linear relationship (significant).

Table 4.7.1: Descriptive statistics of P concentrations (mg/L) at river inflow sites from June 2010 until April 2018

	n	Mean (mg/L)	Std.Dev (mg/L)	Min (mg/L)	Max (mg/L)
Crocodile River (Site 90614)	178	1.162	0.575	0.261	3.189
Magalies River (Site 90615)	195	0.118	0.170	0.006	0.851

Table 4.7.2: Descriptive Statistics of flow (m^3/s) at inflow the inflow site on the Magalies River from June 2010 until April 2018

	n	Mean (m^3/s)	Std.Dev (m^3/s)	Min (m^3/s)	Max (m^3/s)
Magalies River (Site 90615)	195	0.792	1.175	0.063	8.818

4.8. Can water chemistry of the Left Canal be used to infill missing data of the Right Canal and vice versa?

Figure 4.8.1 shows the distribution of the P and N concentration in the water at the left and right canals on days where both sites were sampled on the same day. N and P water chemistry observations from the left canal were used to infill missing data of the right canal and vise versa, making it important to evaluate whether the two canals had similar water chemistries. Shapiro-Wilk normality tests showed that N and P concentrations of both the left and the right canals did not have normal distributions thus the non-parametric Wilcoxon signed rank test was used to compare the medians of the left and right canals. P concentrations for the left and right canal were the same (two tailed *p*-value = 0.150). N concentrations of the left can right canals were also the same (two-tailed *p*-value = 0.443). Thus it may be concluded that the two canals have sufficiently similar chemistry to infill missing data for each other.

Table 4.8.1: Descriptive statistics of N and P concentrations (mg/L) of the left and right abstraction canals when nutrient concentrations were measured on the same day

	n		Mean (mg/L)		Std.Dev (mg/L)		Min (mg/L)		Max (mg/L)	
	P	N	P	N	P	N	P	N	P	N
Left Canal	58	58	0.402	4.316	0.197	0.910	0.154	2.677	0.891	8.705
Right Canal	58	58	0.396	4.414	0.175	0.899	0.136	2.366	0.889	7.892

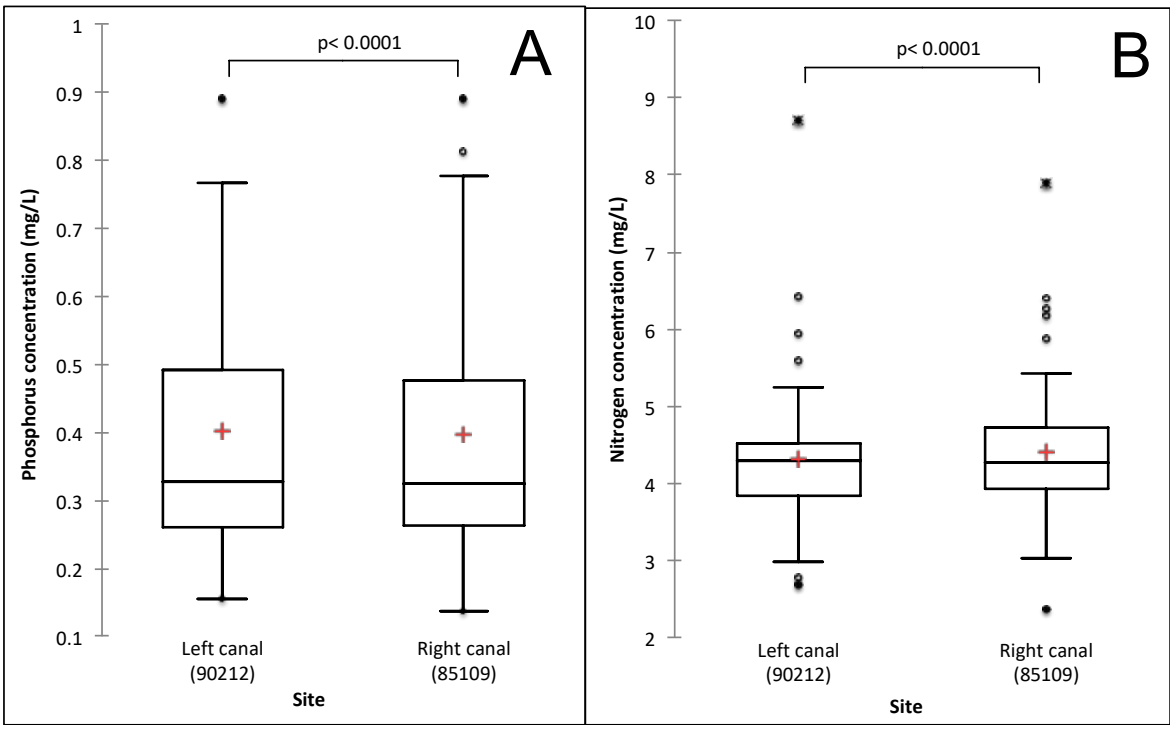

Fig. 4.8.1: Box-and-whisker plots comparing the data spread of P concentration (mg/L) (A) and N concentration (mg/L) (B) of the left and right canals on days where both sites were measured on the same day. The 'box' represents the inter-quartile range. The lower and upper box limits represent the first and third quartiles, respectively. The dividing line represents the median. The red cross represents the mean. The lines above and below each 'box' represent the Tukey limits, which separate the data from potentially extreme data points. Dots above or below the whiskers represent outliers. n = 58 for all sample groups.

CHAPTER 5: OTHER FLUX CONTRIBUTORS

Chapter 5 presents estimations of all other flux components (biomass, denitrification, sedimentation, atmospheric deposition, N fixation and groundwater) to meet Objective 3 and 4 of the study.

5.1. Water hyacinth biomass output

N and P removal estimates from water hyacinth harvesting assuming hyacinth densities of 168 kg/m^3 and an upper theoretical limit of 1000 kg/m^3 are presented in Table 5.1. Lower and upper ranges of both densities were calculated using minimum dry weight and minimum N or P contents and maximum equivalents respectively. Mean annual P yield was estimated to be between 0.7 and 12.5 t. Mean annual N yield was estimated to be between 6.2 and 68.3 t. Figure 5.1 depicts hyacinth harvesting at the Hartbeespoort Dam. A 'best estimation' of nutrients removed annually from water hyacinth harvesting was 2.1 t P and 11.5 t N. Water hyacinth best estimates were based on the upper limit of the more likely hyacinth density, 168 kg/m^3.

Table 5.1: Total, mean and largest annual yield estimates of P and N removed from the Harbeespoort Dam from water hyacinth removal during the Metsi a Me programme

	Assuming a 168 kg/m^3 density of hyacinth (Bagnall, 1982)		Assuming 1000 kg/m^3 density of hyacinth - upper limit	
	P (tons)	N (tons)	P (tons)	N (tons)
Total yield	6.2 – 18.9	55.5 – 103.3	37.0 – 112.4	330.6 – 614.8
Mean annual yield	0.7 – 2.1	6.2 – 11.5	4.1 – 12.5	36.7 – 68.3
Largest annual yield (2013/2014)	1.4 – 4.1	12.1 –22.5	8.4 – 25.4	74.8 – 139.1

5.2. Algae biomass output

N and P removal estimates from algae harvesting using Methods 1 and 2 calculations are presented in Table 5.2. The lower limit of Method 1 was calculated using an algae biomass dry weight concentration of 20 g/L while the upper limit was calculated using an

algae biomass dry weight concentration of 60 g/L. Method 2 assumes the algae "soup" removed was 100% algae. The average annual yield of P was estimated to be between 1.3 and 57 t. The average annual yield of N was estimated to be between 13.3 and 576 t. Figure 5.2 shows the algae being harvested at the Hartbeespoort Dam. A 'best estimation' of algae harvesting was 4.0 t P and 40 t N. Best estimations were based on the upper limit of the more likely algae concentration, Method 1.

Table 5.2: Total, mean annual and largest annual yield estimates of P and N removed from the Harbeespoort Dam from algae removal during the Metsi a Me programme

	Method 1: Assuming a chlorophyll-*a* concentration of 302 mg/L (NWIR, 1985)		Method 2: Assuming a dry wt concentration of 0.87 t/m^3 (Hu, 2014) - upper limit	
	P (tons)	N (tons)	P (tons)	N (tons)
Total yield	11.8 – 29.6	120 – 360	512	5 187
Mean annual yield	1.3 – 4.0	13.3 – 40.0	57	576
Largest annual yield (2014/2015)	2.7 – 8.2	27.7 – 83.5	119	1 202

5.3. Fish biomass output

Table 5.3.1 shows annual N and P removal estimates from fish biomass harvesting from anglers and the Metsi a Me programme in the Hartbeespoort Dam. An estimated 3.6 t P and 20 t N were removed through fish biomass harvesting from the Hartbeespoort Dam each year.

Table 5.3.1: N and P removal estimates from fish biomass harvesting from Anglers and the Metsi a Me programme in the Hartbeespoort Dam

	Metsi a Me Programme	Anglers (NIWR, 1985)	Total
Average annual N yield (t)	1.06	18.9	**20**
Average annual P yield (t)	0.12	3.5	**3.6**

5.4. Denitrification output

Denitrification rates from the literature are given in Table 5.4.1. Wilkins (2019) found that denitrification N loss could be explained by first order kinetics modeled on TON concentration. NWIR (1985) reported that $NO_2 + NO_3$ inputs to the Hartbeespoort Dam were 1367, 1174 and 687 t for hydrological years 1980/81, 1981/82 and 1982/83, respectively. On average, 54% of the $NO_2 + NO_3$ component of the annual N input was denitrified (61.5% in 1980/81, 56.5% in 1981/82 and 44.1% in 1982/83) (NWIR, 1985). In this study, the $NO_2 + NO_3$ comprised 68% of N inputs (i.e. approximately 3000 t/a). The concentration of $NO_2 + NO_3$ in the main basin of the Hartbeespoort Dam during 1980 to 1983 was 590 – 2700 µg/L (mean not given) (NWIR, 1985). During 2010 until 2018, DWS data showed the range was 25 – 22 888 µg/L (mean of 2.88 mg/L). Thus it is likely there was an increase in $NO_2 + NO_3$ concentration from the NWIR (1985) study to the current study.

Thus, if approximately 54% of the $NO_2 + NO_3$ annual inputs is denitrified, in the current study, 1600 t N would have left the dam through the process of denitrification each year between 2010/11 and 2017/18. Given these findings, an estimated 1000 – 1600 t N leaves the Hartbeespoort Dam through denitrification each year. The upper limit of Piña-Ochoa and Álvarez-Cobelas (2006) was chosen to represent the lower limit of this study as the Hartbeespoort Dam is hypereutrophic and is not P limited, making high denitrification rates likely (Seitzinger, 1990; Finlay *et al.*, 2013).

Table 5.4.1: Denitrification rates from the literature. Range of tons removed from Hartbeespoort Dam given in brackets.

Denitrification Rate	**Notes**	**Source**
0.10 – 3.72 mol N m^{-2} y^{-1} **(26.4 – 981.0 t/a)**	Meta-analysis. Denitrification rate of lakes, mostly in Northern Hemisphere.	Piña-Ochoa and Álvarez-Cobelas (2006)
20 – 315 μmol N m^{-2} h^{-1} **(303 – 841 t/hydrological year)**	Acetylene block technique. Denitrification rate of sediments at Hartbeespoort Dam.	NWIR (1985)

5.5. Atmospheric deposition input

Tables 5.5.1 and 5.5.2 present P and N atmospheric deposition flux rates reported in the literature and the equivalent annual flux for the Hartbeespoort Dam. Anthropologically modified locations have N deposition rates in the upper range (Galy-Lacaux *et al*, 2003). Given these findings, it was estimated that nutrient fluxes to the Hartbeespoort Dam from atmospheric deposition were 1.2 t P and 30 to 40 t N per annum.

Table 5.5.1: Atmospheric deposition P fluxes from the literature. Range of flux to the Hartbeespoort Dam given in brackets

P Atmospheric Deposition Flux	Notes	Source
0.19 kg/ha/yr **(0.38 t/a)**	Wet Flux at Pella, 62 km north of Cape Town, SA	Brown *et al.*, (1984)
0.03 – 0.05 mg/L PO_4 **(0.13 – 0.22 t/a)**	March – April rains (wet flux) in the Magaliesburg, SA	Pope (2015)
0.062 g/m^2 **(1.2 t/a)**	Mean wet + dry deposition in Africa. Studies primarily located in west Africa and east Africa	Tipping *et al.* (2014)

Table 5.5.2: Atmospheric deposition N fluxes from the literature. Range of flux to the Hartbeespoort Dam given in brackets

N Atmospheric Deposition Flux	Notes	Source
3.80 – 4.62 kg/ha/year **(7.6 – 9.2 t/a)**	Wet + dry flux of the United States	Holland *et al.* (2005)
8.27 – 10.95 kg/ha/year **(16.5 – 21.9 t/a)**	Wet + dry flux of Europe	Holland *et al.* (2005)
8 – 19 kg/ha/year **(16 – 38 t/a)**	Wet + dry flux of Africa	Galy-Lacaux *et al.* (2003)
2.2 mg/L TN **(29 t/a)**	Mean rainfall concentration (wet flux) measured at Rietvlei Dam, SA	Ashton (1981)

5.6. N Fixation input

Nitrogen fixation rates from the literature are given in Table 5.6.1. Given these findings, an estimated 0 to 4 t N is fixed each year. The lower end of the N fixation range from Howarth *et al.* (1988) was chosen to represent the upper limit as the Hartbeespoort Dam was not N limited.

Table 5.6.1: N fixation rates from the literature. Range flux to the Hartbeespoort Dam given in brackets.

N fixation rate	**Notes**	**Source**
0.2 – 9.2 g N m^{-2} y^{-1} **(3.8 – 174.8 t/a)**	Meta-analysis. N fixation rates of eutrophic lakes	Howarth *et al.* (1988)
Not detectable **(0 t/a)**	Study of Hartbeespoort Dam.	NWIR (1985)

5.7. Groundwater Input and Output

Groundwater fluxes were estimated using flow data from Davis (2017) and mean river (in the case of inflow) and canal (in the case of outflow) concentrations of rivers. Groundwater flow rates and annual N and P flux estimations are given in table 5.7.1. Groundwater nutrient influx estimates were 193 t N and 0 t P. Groundwater outflux estimates were 67 t N and 6.4 t P.

Table 5.7.1: Groundwater flow and N or P flux estimations of inflows and outflow

	Flow (m^3/s) (Davis, 2017)	**N conc. (mg/L)**	**P conc. (mg/L)**	**P (t/a)**	**N (t/a)**
Magalies Groundwater Inflow	0.469	1.87	N/A	**0**	**28**
Crocodile Groundwater Inflow	0.562	9.28	N/A	**0**	**165**
Groundwater Outflow	0.449	4.36	0.45	**67**	**62**

5.8. Sedimentation and mass balances

Sedimentation rates were assumed to make up the difference between all other flux estimates, using water hyacinth and algae outflux best estimates and Two-Weekly flow fluxes. The Two-weekly means are closer to the raw data mean for the study period, justifying the Two-Weekly flow as being the most suitable for flux calculations in this study. In addition, no correlation between concentration and flow was observed, indicating no apparent bias in using flows averaged over the whole sampling interval. Approximately 341 t P and 674 - 1288 t N were sedimented annually in the Hartbeespoort Dam from 2010 until 2017. Conceptual diagrams of the P and N mass balances are shown in Figure 5.8.1. Annual N sedimentation had a larger range, and therefore margin of error, as denitrification ranges are large.

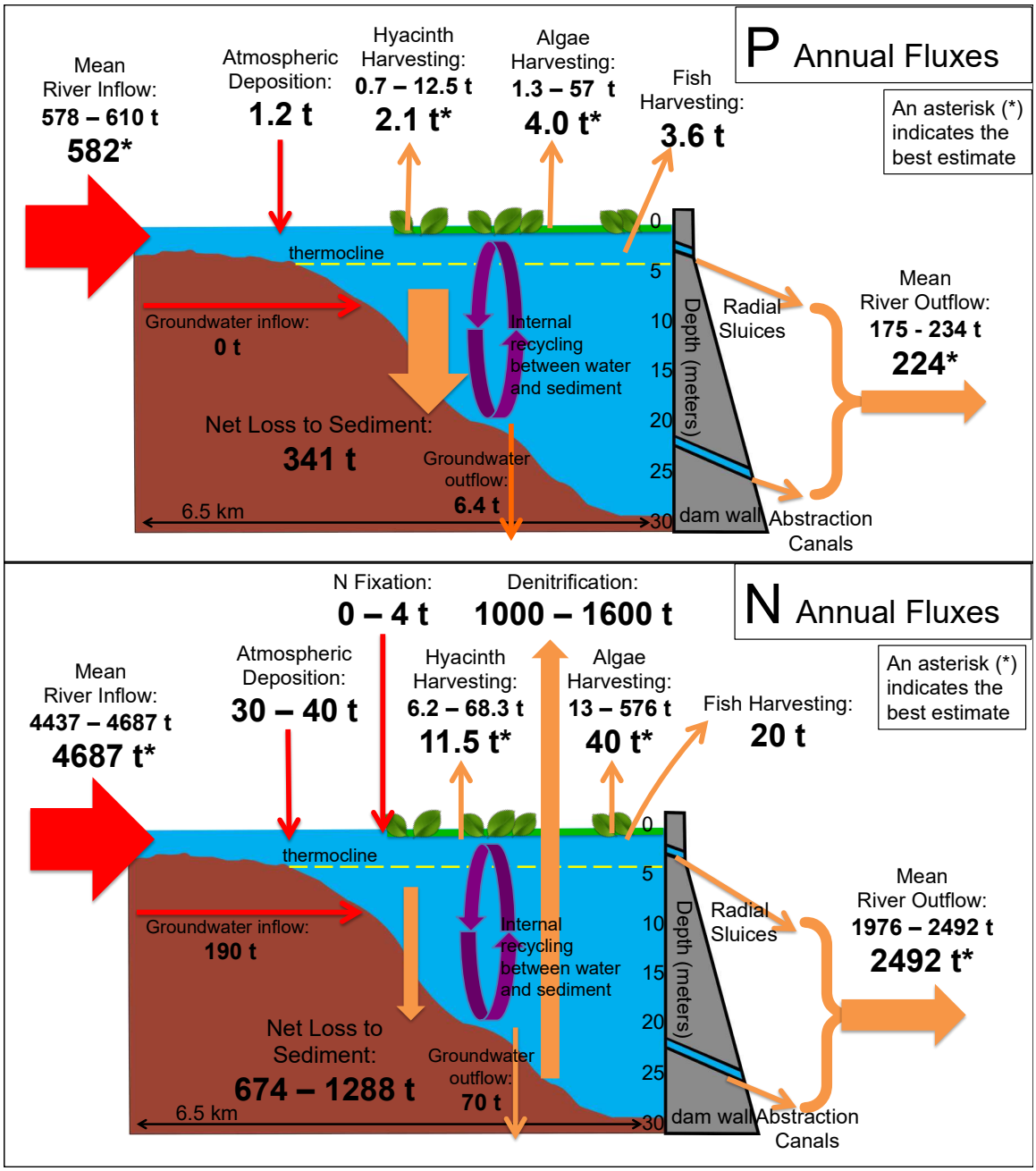

Fig. 5.8.1: Conceptual diagram of annual P (above) and N (below) fluxes in the Hartbeespoort Dam during 2010 to 2017. Red arrows represent nutrient inputs. Orange arrows represent nutrient outputs. Widths of input and output arrows represent approximate relative flux contributions. Purple arrow represents recycling.

CHAPTER 6: CONCLUSIONS AND LIMITATIONS

6.1. Overview of mass balances

Between 2010 and 2017, the range of P to the Hartbeespoort Dam from inflowing rivers was 578 to 610 t/a and the range of N was 4437 to 4687 t/a. This is almost double the P flux estimated by the Institute of Natural Resources in 2010 (INR, 2010). Despite differences in methods, this study closely matches the results from Mitchell and Crafford (2016) for the overlapping period 2010/11, but indicates a major increase in influxes in the later years covered by this study.

Approximately 40% of the incoming P and 50% of the incoming N flowed out of the Hartbeespoort Dam from the abstraction canals and radial sluices. The data in this report indicate that 358 to 403 t P and 2172 to 2461 t N was retained in the dam from river flow each year. Biomass harvesting removes a small portion of P and N from the dam. The 'best estimation' of nutrients removed from water hyacinth harvesting was 1.2 t P and 11.5 t N. A 'best estimation' of algae harvesting was 4.0 t P and 40 t N. Thus algae and hyacinth harvesting combined removed approximately 1% of nutrient influx. In the long term, lake bottoms act as a sink of nutrients, and not a source (Peimin *et al.*, 2000). The largest portion of incoming P will be sedimented. This has important management implications: in the short-term, resuspension and P release from the sediment will affect symptoms of eutrophication in the dam but in the long-term much of the P influx will settle out of the water column and be buried at the lake-bottom. Denitrification plays a significant role in N removal from the dam and about half of the N that is retained within the dam will be sedimented.

6.2. Sources of nutrient influxes

There are a number of indicators that WWTWs are the dominant source of nutrient inputs to the Hartbeespoort Dam. The first indication is that total phosphorus input is largely comprised of orthophosphate (see Section 7.4 of the Appendix). Approximately 90% of the phosphorus flux from WWTWs is soluble, reactive orthophosphate while phosphorus

used in agricultural fertilisers tends to attach to soil particles and is predominately transported to rivers with surface runoff as "bound", unavailable P (Harding, 2015; Berg *et al.*, 2018). The second indication is that there was no significant relationship between concentration and flow at the Crocodile River inflow site, as shown by Figure 4.7.1. One would expect nutrient inputs from agricultural and urban runoff to be correlated with flow as fertilisers are transported to rivers during storm events. Thus the lack of correlation further indicates that agricultural fertilisers were not the major source of nutrients in the Crocodile River. It is interesting to note that the Magalies River does have a significant relationship between flow and concentration, although Spearman's Rho is small. Even though the Magalies River contributes less than 1% of the annual nutrient flux to the Hartbeespoort Dam, the significant relationship between flow and concentration indicates that nutrient flux in the Magalies catchment was primarily caused by agricultural runoff rather than WWTW effluent or leaking sewage pipes. The third indication was the exceptionally high *E.coli* counts in the majority of the major rivers around Johannesburg (Dube *et al.*, 2017). This would indicate fecal contamination sources. The cause of the high *E.coli* counts is collapsed and malfunctioning sewage systems as widely found in South Africa (Herbig and Meissner, 2019).

6.3. Trends

Nutrient fluxes show a trend of increasing flux over time. On average, the P inflow flux increased by 54.2 to 77.8 t/a and the N inflow flux increased by 368 to 456 t/a each year from 2010 until 2018. These trends cannot be attributed to an increase in flow as there was no significant increase in flow over the time period (see Section 7.3 of Appendix). In addition, there was a weak relationship between concentration and flow. This implies that there is a significantly increasing trend in flux. Harding (2008) found that the Hartbeespoort Dam showed a long-term decreasing trend in P. Thus the increasing nutrient flux is a recent trend, and a reversal of earlier improvements made. In addition, this study found that nutrient influxes were increasing at a faster rate than outfluxes, meaning that storage in the dam (sedimentation of nutrients) must be increasing.

The Spot flow method of flux calculation showed a high input flux of note in spring 2014. A high flow event was recorded on the 3rd of March 2014, which was coupled with a high nutrient concentration event. This event can be traced to a pollution event caused by a brief breakdown at Northern Works WWTW (Eybers, 2016). In addition, during early 2016 there was a three-month period where a blocked pipe close to Leeukop Prison resulted in a steady discharge of untreated sewage to the Crocodile River. The large spike in the outflow nutrient flux of autumn 2016 observed in the Spot flow method trend graphs can be attributed to an exceptionally large outflow from the Radial Sluices on the 10th of March 2016 (the spot flow reading was 240 m^3/s while the median flow was 5 m^3/s).

Nutrient inflow fluxes have greater variability than outflow fluxes, as seen by the comparatively larger error bars of the inflow fluxes (Section 4.4). This can be attributed to both a greater variability in stream flow and of nutrient concentrations of the inflow. The outflow fluxes appear to display seasonality, with fluxes dropping in winter and increasing in summer. This may be caused by greater demand for irrigation water during summer months or outflow flux being controlled to match a natural flow regime by dam managers. Inflow fluxes do not appear to display a seasonal pattern. Outflows (i.e. opening sluices) are managed, while inflows are largely influenced by rainfall patterns. This further indicates that WWTWs are the primary source of nutrients in the Hartbeespoort Dam since one would expect seasonal nutrient flux trends mimicking those of rainfall patterns to be visible in agriculturally-dominated catchments.

6.4. Flux uncertainties

While it is unclear which method of estimating river flux (Spot, Daily Average or Two-Weekly) is the most appropriate, the three methods produced a range. The actual flux is likely to be between the largest and smallest estimates. The three methods produced similar results, especially when comparing inflow flux estimates, which were not significantly different from each other. The Two-Weekly figures tend toward the median value while the Spot figures capture extreme events. However, the average P and N

inflow flux estimates of the three methods are within 5% and 4% of each other respectively. The outflow river flux had a greater range of uncertainty as the Daily Average Flow method produced average outflow flux estimates that were 25% and 21% lower than both the Spot and Two-Weekly Flow method for P and N annual estimates, respectively. This may have been caused by sampling bias, with low flow days being disproportionately sampled. The algae and hyacinth biomass outputs both produced estimates with large margins of error. Despite this, even the largest possible estimations of N and P loss from biomass harvesting are trivial in proportion to the inputs, indicating their relative importance was low. Denitrification also hds a large margin of error; as literature data were relied on to make this estimate. In relation to the N river influx estimates, denitrification is likely to play an important role in N removal.

6.5. Limitations of the study

Intermittent, instantaneous grab sampling fails to provide adequate load estimates if the catchments experience flashy hydrology (Cassidy and Jordan, 2011). It is preferable to conduct time series studies with intermittent to weekly grab water quality sampling study over long time spans (Kirchner *et al.*, 2004). This allows for an increased chance in catching extreme hydrological or chemical events (Kirchner *et al.*, 2004). Intense and short rainfall events are not adequately captured and represented in this study, as shown by the infrequency of high flow events in flux calculations (see in Figure 4.7.1). However, the flow values used were not significantly different from those of the data set with flow readings taken every 12 minutes. In addition, the analysis in this study showed that flash events are not likely to be the main flux contributing events. It would have been preferable to conduct the study over a longer time period if it were not for large gaps in the water quality data available. Although annual fluxes should not be considered exact but rather approximations, the average annual flux of the seven-year period is likely to be a more accurate estimation of nutrient fluxes over the time period. Greater continuous monitoring would be more suitable for more reliable load estimates to be made (Cassidy and Jordan, 2011). Groundwater N inputs were challenging to estimate without borehole water quality measurements and a well-established understanding of the groundwater

system. Thus groundwater nutreint inputs could be underestimated in this study. Estimates of river inputs can be considered conservative as nutrient inputs from the Swartspruit River and the golf courses adjacent to the Hartbeespoort Dam could not be accounted for. However, these inputs contribute a trivial proportion of the total inputs (Mitchell and Crafford, 2016).

6.6. The way forward

The desired load to the Hartbeespoort Dam is 68 t/a (Mitchell and Crafford, 2016). In order to achieve this condition, a load reduction of at least 88% is required. "Minimising waste generation at source is a central tenet of South Africa's Pollution Control and Waste Management legislation" (Harding, 2015). Reducing N and P flux to the Hartbeespoort Dam from leaking and/overflowing sewers and WWTWs is the only long-term solution to controlling the eutrophication problem at the Hartbeespoort Dam. Re-establishing the green drop initiative, and enforcing its compliance, will go a long way to achieve this. This will be an expensive operation as the cost of upgrading all WWTWs in the Hartbeespoort Dam catchment to the desired effluent specification of 0.15 mg/L P is just over R2 billion (Mitchell and Crafford, 2016). In addition, the cost of reducing the nutrient load from diffuse sources, including the rehabilitation of failing pump stations and the refurbishment of sewers is estimated to cost a further R1.5 billion (Mitchell and Crafford, 2016). In comparison, R159 million was spent on bioremediation over the life of the Metsi a Me programme (Mitchell and Crafford, 2016). The bioremediation approaches of the Metsi a Me programme may have achieved some localised improvements in terms of wildlife habitat, clearing water hyacinth to allow water based activities, and water quality, but the mass balance approach used here demonstrates that biomass removal fluxes are trivial compared to the input fluxes and make a minor contribution to nutrient removal from the dam.

CHAPTER 6: REFERENCES

Abiye, T., Mengistu, H., Masindi, K. and Demlie, M. (2015). Surface water and groundwater interaction in the upper Crocodile River basin, Johannesburg, South Africa: environmental isotope approach. *South African Journal of Geology*, 118(2), pp.109-118.

Ahlgren, I., Sornsson, F., Waara, T. and Vrede, K. (1994). Nitrogen budgets in relation microbial transformations in lakes. *Royal Swedish Academy of Sciences*. 23(6) pp. 367-377.

Akendo, I., Gumbe, L., and Gitau, A. (2008). Dewatering and Drying Characteristics of Water Hyacinth (Eichhornia Crassipes) Petiole. Part II. Drying characteristics. Agricultural Engineering International: the CIGR Ejournal Manuscript FP 07 033. Vol. X.

Ashton, P. (1981). Nitrogen fixation and the nitrogen budget of a eutrophic impoundment. *Water Research*, 15(7), pp.823-833.

Ashton, P. (2010). Demise of the Nile crocodile (*Crocodylus niloticus*) as a keystone species for aquatic ecosystem conservation in South Africa: the case of the Olifants River. *Aquatic Conservation: Marine and Freshwater Ecosystems*, 20(5), pp 489-493

Bagnall, L. (1982). Bulk Mechanical Properties of Waterhyacinth. *Journal of Aquatic Plant Management*, 20, pp.49-43.

Balzer, T. (2018). *Water Security and Water Governance in South Africa*. Pretoria: Department of Water and Sanitation, p.14. Available at: https://agbiz.co.za/uploads/2018-Congress/Trevor.pdf [Accessed 16 December 2019].

Bega, S. (2016). Is Hartbeespoort damned? *Pretoria News Weekend*, [online] (7), p.2. Available at: https://www.pressreader.com/south-africa/pretoria-news-weekend/20160611/281719793857631 [Accessed 24 May 2018].

Berg, M., Meehan, M., Franzen, D. and Scherer, T. (2018). *Phosphorus Behavior In the Environment — Publications*. [online] Ag.ndsu.edu. Available at: https://www.ag.ndsu.edu/publications/environment-natural-resources/phosphorus-behavior-in-the-environment [Accessed 21 Nov. 2019].

Binzer, A., Guill, C., Rall, B. and Brose, U. (2015). Interactive effects of warming, eutrophication and size structure: impacts on biodiversity and food-web structure. *Global Change Biology*, 22(1), pp.220-227.

Boehrer, B. and Schultze, M. (2008). Stratification of lakes. *Reviews of Geophysics*, 46(2).

Borsuk, M., Stow, C. and Reckhow, K. (2004). A Bayesian network of eutrophication models for synthesis, prediction, and uncertainty analysis. *Ecological Modelling*, 173(2-3), pp.219-239.

Botha, F. (2015). *Nutrient reduction options in Hartbeespoort Dam catchments to lower in-dam eutrophication status*. M.Sc. North-West University.

Boyd, C. (1976). Accumulation of dry matter, nitrogen and phosphorus by cultivated water Hyacinths. *Economic Botany*, 30(1), pp.51-56.

Brown, G., Mitchell, D. and Stock, W. (1984). Atmospheric Deposition of Phosphorus in a Coastal Fynbos Ecosystem of the South-Western Cape, South Africa. *The Journal of Ecology*, 72(2), p.547.

Bwapwa, J. (2018). Review on Main Issues Causing Deterioration of Water Quality and Water Scarcity: Case Study of South Africa. *Environmental Management and Sustainable Development*, 7(3), p.14.

Carpenter, S. R. *et al.* (1995). Biological control of eutrophication in lakes. *Environmental Science & Technology* 29(3) pp 784-786

Cassidy, R. & Jordan, P. (2011). Limitations of instantaneous water quality sampling in surface-water catchments: Comparison with near-continuous phosphorus time-series data. *Journal of Hydrology*. 405(1-2):182-193. DOI: 10.1016/j.jhydrol.2011.05.020.

Chislock, M. F., Doster, E., Zitomer, R. A. & Wilson, A. E. (2013) Eutrophication: Causes, Consequences, and Controls in Aquatic Ecosystems. *Nature Education Knowledge* 4(4) p10

Chutter, F. (1989). Evaluation of the Impact of 1 mg l^{-1} phosphate-p standard on the water quality and trophic state of Hartbeespoort Dam. WRC report No. 181/1/89 pp. 69. Water Research Commission, Pretoria.

Chutter, F. and Rossouw, J. (1991). *The management of phosphate concentrations and algae in Hartbeespoort Dam*. WRC Report No 289/1/91. xii + 37 pp. Water Research Commission, Pretoria.

Clay S., Sigee D.C. and Bellinger E. (1991). X-ray micro-analytical studies of freshwater biota: changes in the elemental composition of *Anabaena spiroides* during blooms of 1988 and 1989. *Scan Microsc*, 5(1) pp. 207–217.

Claassen, M. (2010). How much water do we have? In: CSIR, A CSIR perspective on water in South Africa. CSIR Report No. CSIR/NRE/PW/IR/2011/0012/A, pp 4-7.

Colman, J. and Santha, C. (1988). Critical concentrations of tissue nitrogen and phosphorus for growth rate and yield in the freshwater blue-green alga *Microcystis aeruginosa* Kütz. in the tropics. *Aquatic Botany*, 32(1-2), pp.167-177.

Conley, D., Paerl, H., Howarth, R., Boesch, D et al (2009). Controlling eutrophication: nitrogen and phosphorus. *Science.* 323 pp 1014–1015

Coser, P. (1989). Nutrient concentration-Flow relationships and loads in the South Pine River, South-eastern Queensland. I. Phosphorus loads. *Marine and Freshwater Research*, 40(6), p.613.

Dabrowski, J., Bruton, S., Dent, M., Graham, M., Hill, T., Murray, K., Rivers-Moore, N. and van Deventer, H. (2013). *Linking Land Use to Water Quality for Effective Water Resource and Ecosystem Management*. WRC Report 1984/1/13. Pretoria: Water Research Commission.

Dabrowski, J. and de Klerk, L. (2013). An assessment of the impact of land use activities on water quality in the upper Olifants River Catchment. *Water SA*. 39(2). pp. 231 – 244.

Dube, R, Maphosa, B., Malan, A., Fayemiwo, D., Ramulondi, D. and Zuma, T. (2017). *Response of Urban and Peri-Urban Aquatic Ecosystems to Riparian Zones Land Uses and Human Settlements: A Study of the Rivers, Jukskei, Kuils and Pienaars.* WRC Report 2339/1/17. Nxt2u (Pty) Ltd. Pretoria: Water Research Commission.

Davis, A. (2017). *Hydrogeological Characteristics of the Hartbeespoort Dam.* M.Sc. University of the Witwatersrand.

Department of Water Affairs and Forestry (DWAF). (1992). Analytical Methods Manual TR 151. Pretoria. [online] Available at: http://www.dwaf.gov.za/iwqs/reports/tr/TR_151_1992_Analytical_methods_manual.pdf

Department of Water Affairs and Forestry (DWAF) (2004). *Crocodile River (West) and Marico Water Management Area: Internal Strategic Perspective of the Crocodile River (West) catchment*: By Goba Moahloli Keeve Steyn (Pty) Ltd, Tlou & Matji (Pty) Ltd and Golder Associates (Pty) Ltd, on behalf of the Directorate: National Water Resource Planning. DWAF Report No. 03/000/00/0303.

Department of Water Affairs and Forestry (DWAF) (2009). *Hartbeespoort Dam Bioremediation Programme: Development and Implimentation of an Integrated Monitoring Programme for Hartbeespoort Dam and upstream catchment: A first order Integrated Monitoring Framework*. Integrated Water Resource Managment and Catchment Strategies, pp.23-25.

DH Environmental Consulting (DHEC) (2004). *Final Report (Volume I)*. Hartbeespoort Dam Remediation Project (Phase 1). [online] Department of Agriculture, Conservation, Environment and Tourism of the North West Province Government (DACET, NWP),

p.26. Available at: http://www.dwaf.gov.za/Harties/documents/ActionPlanVol1Oct04full.pdf [Accessed 9 May 2018].

Edmondson, W. (1970). Phosphorus, Nitrogen, and Algae in Lake Washington after Diversion of Sewage. *Science*, 169(3946), pp 690-691.

Eybers, C., 2016. Sewage Spill Hits Hartbeespoort Dam. *Eyewitness News*, URL: https://ewn.co.za/2016/11/07/sewage-spill-hits-hartbeespoort-dam [Accessed 11 March 2020].

Finlay, J., Small, G. and Sterner, R. (2013). Human Influences on Nitrogen Removal in Lakes. *Science*, 342(6155), pp.247-250.

Garrell, M., Confer, J., Kirschner, D. and Fast, A. (1977). Effects of hypolimnetic aeration on nitrogen and phosphorus in a eutrophic lake. *Water Resources Research*, 13(2), pp.343-347

Galy-Lacaux, C., Al Ourabi, J., Galloway, J., Lacaux, J., Mphepya, K. Pienaar, V. Pont, L., Sigha, and Yoboué, V. (2003). Dry and wet atmospheric nitrogen deposition in Africa, *IGAC Newsl.*, 27 pp. 6– 11.

van Ginkel, C., du Plessis, S. and Bezuidenhout, J. (2010). *Investigating the Applicability of Ecological Informatics Modelling Techniques for Predicting Harmfull Algal Blooms in Hypertrophic Reservoirs of South Africa*. TT 451/10. Pretoria: Water Research Commission, p.142. ISBN 978-1-77005-953-5

Gong, Z. and Xie, P., 2001. Impact of Eutrophication on Biodiversity of the Macrozoobenthos Community in a Chinese Shallow Lake. *Journal of Freshwater Ecology*, 16(2), pp.171-178.

Gupta, S. (2000). *Global environment*. 1st ed. New Delhi: Sarup & Sons, p.497.

Harding, W. (2008). The Determination of Annual Phosphorus Loading Limits for South African Dams. Water Reserch Comission Report 1687/1/08. ISBN 987-1-77005-866-6

Harding, W. (2015). *A Feasibility Study of the Total Maximum Daily (Pollutant) Load (TMDL) Approach for Managing Eutrophication in South African Dams.* Pretoria: Water Research Commission. ISBN: 978-1-4312-0673-5

Harding, W. and Paxton, B. (2001). *Cyanobacteria in South Africa: A Review. TT 153/01* Pretoria: Water Research Commission.

Hart, R. (2006). Food web (bio-)manipulation of South African reservoirs – viable eutrophication management prospect or illusory pipe dream? A reflective commentary and position paper. *Water, SA,* 32 (4), pp. 567-575.

Hart, R. and Harding, W. (2015). Impacts of fish on phosphorus budget dynamics of some SA reservoirs: evaluating prospects of 'bottom up' phosphorus reduction in eutrophic systems through fish removal (biomanipulation). *Water SA*, 41(4), p.432.

Hart, R. and Matthews, M. (2018). Bioremediation of South Africa's hypertrophic Hartbeespoort Dam: evaluating its effects by comparative analysis of a decade of MERIS satellite data in six control reservoirs. *Inland Waters*, 8(1), pp.96-108.

HDRP. (2012). Hartbeespoort Dam Integrated biological remediation programme: Consolidated progress report: Phase 1. December 2012.

Herbig, F. and Meissner, R. (2019). Talking dirty - effluent and sewage irreverence in South Africa: A conservation crime perspective. Cogent Social Sciences, 5(1).

Himmelblau, D. and Riggs, J. (2012). *Basic principles and calculations in chemical engineering*. 8th ed. Texas: Prentice Hall.

Hobbs, P. (2017). TDS load contribution from acid mine drainage to Hartbeespoort Dam, South Africa. *Water SA*, 43(4), p.626.

Hoffman, J. (1976). Removal of *Microcystis* toxins in water purification processes. Water SA, (2), 58-60.

Holland, E., Braswell, B., Sulzman, J. and Lamarque, J. (2005). Nitrogen deposition onto the United States and Western Europe: synthesis of observations and models. *Ecological Applications*, 15(1), pp.38-57.

Howarth, R., Marino, R., Lane, J. and Cole, J. (1988). Nitrogen fixation in freshwater, estuarine, and marine ecosystems. 1. Rates and importance1. *Limnology and Oceanography*, 33(4part2), pp.669-687.

Howarth, R., Chan, F., Conley, D., Garnier, J., Doney, S., Marino, R. and Billen, G. (2011). Coupled biogeochemical cycles: eutrophication and hypoxia in temperateestuaries and coastal marine ecosystems. *Front Ecol Environ*. 9(1), pp18-26. DOI:10.1890/100008

Hu, W. (2014). *Dry Weight and Cell Density of Individual Algal and Cyanobacterial Cells for Algae*. M.Sc. University of Missouri-Columbia.

Hupfer, M. and Lewandowski, J. (2008). Oxygen Controls the Phosphorus Release from Lake Sediments - a Long-Lasting Paradigm in Limnology. *International Review of Hydrobiology*, 93(4-5), pp.415-432. https://doi.org/10.1002/iroh.200711054

Huttula, T. (2012). *Stratification in Lakes.* In: Bengtsson L., Herschy, R., Fairbridge, R. (eds.) *Encyclopedia of lakes and reservoirs*. Dordrecht : Springer Science, 8-10. (Encyclopedia of Earth Sciences Series). ISBN 978-1-4020-4410-6

Institute of Natural Resources (INR) (2010). *Investigation of the positive and negative consequences associated with the introduction of zero-phosphate detergents into South Africa*. TT 446/10. Pretoria: Water Research Commission, p.182. ISBN 978-1-77005-946-7

Jarvie, H., Withers, J. and Neal, C. (2002) Review of robust measurement of phosphorus in river water: sampling, storage, fractionation and sensitivity. *Hydrol Earth Syst Sci*, 6(1), pp.113-131.

Jiang, C., Zhu, L., Hu, X., Cheng, J. and Xie, M. (2011) Reasons and control of Eutrophication in new reservoirs. In: Ansari A., Gill S. (eds) Eutrophication: Causes, Consequences and Control. Springer, Dordrech pp326-340.

Judeel, G. and Hartmann, A. (2008). Ground support at Crocodile River Mine located in the Brits graben of the western limb of the Bushveld Complex. Abstracts, 6th International Symposium on Ground Support in mining and Civil Engineering Construction, Capetown 30 March–3 April 2008, pp.525-544. DOI:10.13140/RG.2.1.1006.7689

Khan, M and Mohammed, F (2014). Eutrophication: Challenges and Solutions. In: Ansari, A., Gill, S. (eds) Eutrophication: causes, consequences and control. Springer, Dordrecht, pp 1–15. ISBN 978-94-007-7814-6

Kim, J., Chae, G., Seo, H., Chaudhary, N., Yoon, Y., Shin, T. and Kim, M. (2012). Bioalcohol Production with Microalgae, *Microcystis aeruginosa*. *KSBB Journal*, 27(6), pp.335-340.

King, J., Mitchell, S., and Pienaar, H., (2011) 1: Water supply and demand. In: King, J & Pienaar, H. (Eds.) *Sustainable use of South Africa's inland waters. A situation assessment of Resource Directed Measures 12 years after the 1988 National Water Act.* WRC Report Number TT 491/11, Water Research Commission, Gezina, South Africa, pp1-16

Kirchner, J., Feng, X., Neal, C. & Robson, A. (2004). The fine structure of water-quality dynamics: the(high-frequency) wave of the future. *Hydrological Processes*. 18(7):1353-1359. DOI: 10.1002/hyp.5537.

Krivtsov, V., Bellinger, E. and Sigee, D. (2005). Elemental composition of *Microcystis aeruginosa* under conditions of lake nutrient depletion. *Aquatic Ecology*, 39(2), pp.123-134.

Kuo, J., Hsieh, M., Lung, W. and She, N. (2007). Using artificial neural network for reservoir eutrophication prediction. *Ecological Modelling*, 200(1-2), pp.171-177.

Laws, E. (2000). *Aquatic Pollution*. 3rd ed. New York: Wiley, p.61.

Lee, S., Jang, M., Kim, H., Yoon, B. and Oh, H. (2000). Variation of microcystin content of *Microcystis aeruginosa* relative to medium N:P ratio and growth stage. *Journal of Applied Microbiology,* 89(1), pp. 323 -329.

Lee, Z., Shang, S., Hu, C., Du, K., Weidemann, A., Hou, W., Lin, J. and Lin, G. (2015). Secchi disk depth: A new theory and mechanistic model for underwater visibility. *Remote Sensing of Environment*, 169, pp.139-149.

Long, B., Jones, G. and Orr, P. (2001). Cellular Microcystin Content in N-Limited *Microcystis aeruginosa* Can Be Predicted from Growth Rate. *Applied and Environmental Microbiology,* 67(1) pp. 278–283

MacQuarrie, K., Sudicky, E. and Robertson, W. (2001). Multicomponent simulation of wastewater-derived nitrogen and carbon in shallow unconfined aquifers. *Journal of Contaminant Hydrology*, 47(1), pp.85-104.

Mashitisho, D. (2017). *Briefing to the Portfolio Committee on Water and Sanitation on the Green Drop Progress Assessment Tool Report*
Matthews, S. (2016). *Remote sensing technology is being developed to keep a better eye on the quality of South Africa's dams,* Water Wheel, Jan/Feb, 2016.

Mattson, M., Godferey, P., Barletta R., and Aiello, A. (2004). *Eutrophication and Aquatic Plant Management in Massachusetts: Final Generic Environmental Impact Report.* Executive Office of Environmental Affairs, Commonwealth of Massachusetts, USA, Massachusetts.

Mitchell, S. and Crafford, J. (2016). *Review of the Hartbeespoort Dam Integrated Biological Remediation Programme (Harties Metsi a Me).* KV 357/16. Pretoria: Water Research Comission

Monchamp, M., Pick, F., Beisner, B. and Maranger, R. (2014). Nitrogen Forms Influence Microcystin Concentration and Composition via Changes in Cyanobacterial Community Structure. *PLoS ONE*, 9(1), p.e85573.

Murphy, S. (2007). *BASIN: General Information on Phosphorus*. [online] Bcn.boulder.co.us. Available at: http://bcn.boulder.co.us/basin/data/NEW/info/TP.html [Accessed 7 Nov. 2019].

Newcombe, G. (2009) *International Guidance Manual for the Management of Toxic Cyanobacteria.* Global Water Research Coalition and Water Quality Research. Australia, London

NWIR, (1985). *The Limnology of the Hartbeespoort Dam.* South African National Scientific Programmes Report No. 110

Oberholster, P. (2009). Impact on ecotourism by water pollution in the Olifants River catchment, South Africa. *SIL News*. 55(1), pp 8 - 9.

Ololo, G. (2013). *A limnological Study of the Factors Affecting Algal biodiversity in the Hartbeespoort Dam*. M.Sc. University of Johannesburg.

Owuor, K., Okonkwo, J., van Ginkel, C. and Scott, W. (2007). *Environmental factors affecting the persistence of toxic phytoplankton in the Hartbeespoort dam*. 1401/3/07. [online] Water Research Commission, p.89. Available at: http://www.wrc.org.za/Knowledge%20Hub%20Documents/Research%20Reports/1401-3-07.pdf [Accessed 9 May 2018]. ISBN: 978-1-77005-623-7

Pacyna, J. (2008). Atmospheric Deposition. *Encyclopedia of Ecology*, pp.275-285.

Paerl, H. and Otten, T. (2013). Harmful Cyanobacterial Blooms: Causes, Consequences, and Controls. *Microbial Ecology*, 65(4), pp.995-1010.

Park, J. and Craggs, R. (2011). Nutrient removal and nitrogen balances in high rate algal ponds with carbon dioxide addition. *Water Science and Technology,* 63(8), pp. 1758-1764

Peimin, P., Guoxiang, W., Chunhua, H., Weiping, H. and Chengxin, F. (2000). Can We Control Lake Eutrophication by Dredging?. *Journal of Lake Sciences*, 12(3), pp.269-279.

Piña-Ochoa, E. and Álvarez-Cobelas, M. (2006). Denitrification in Aquatic Environments: A Cross-system Analysis. *Biogeochemistry*, 81(1), pp.111-130.

Pope, S. (2015). An investigation into acid deposition in central Magaliesberg streams. Unpublished Honours Research Report, GAES, University of the Witwatersrand.

Roux SP, de Lange W, Oelofse SHH (2010) *The rising costs of both sewage treatment and the production of potable water associated with increasing levels of pollution in a portion of the Crocodile-West Marico water management area (a case study).* Available at: http://hdl.handle.net/10204/4209. (Accessed 7 November 2019).

Ramseyer, L. (2002). Predicting Whole-Fish Nitrogen Content from Fish Wet Weight Using Regression Analysis. *North American Journal of Aquaculture,* 64(3), pp. 195-204.

Raschke, R.L., (1993). Diatom community response to phosphorous in the Everglades National Park USA. *Phycologia*, 32(1), pp.48-58

River Health Programme (RHP), (2005). *State-of-Rivers Report: Monitoring and Managing the Ecological State of Rivers in the Crocodile (West) Marico Water Management Area*. Department of Environmental Affairs and Tourism. Pretoria, South Africa. p 23. ISBN: 0-620-34054-1

Rossouw, J., Harding, W. and Fatoki, O. (2008). *A Guide to Catchment-Scale Eutrophication Assessments for Rivers, Reservoirs and Lacustrine Wetlands*. TT 352/08. Pretoria: Water Research Commission. pp.21 – 23. ISBN: 978-1-77005-715-9

Schindler, D. (1974). Eutrophication and Recovery in Experimental Lakes: Implications for Lake Management. Science. 184(4139), pp.897-899.

Schindler, D. (2006). Recent advances in the understanding and management of eutrophication. *Limnology and Oceanography*, 51(1-2), pp.356-363.

Schindler, D. (2012). The dilemma of controlling cultural eutrophication of lakes. *Proceedings of the Royal Society B: Biological Sciences*, 279(1746), pp. 4322-4333.

Schindler, D., Carpenter, S., Chapra, S., Hecky, R. and Orihel, D. (2016). Reducing Phosphorus to Curb Lake Eutrophication is a Success. *Environmental Science & Technology*, 50(17), pp.8923-8929.

Schyns, J., Hoekstra, A. and Booij, M. (2015). Review and classification of indicators of green water availability and scarcity. *Hydrology and Earth System Sciences Discussions*, 12(6), pp.5519-5564.

Seitzinger S. (1990). *Denitrification In Aquatic Sediments*. In: Revsbech N., Sørensen J. (eds) Denitrification in Soil and Sediment. Federation of European Microbiological Societies Symposium Series, vol 56. Springer, Boston, MA

Skiba, U. (2008). *Denitrification.* S.E. Jorgensen, B.D. Fath (Eds.), Encyclopedia of Ecology, Elsevier, Oxford (2008), pp. 866-871

Smith, V. and Schindler, D. (2009). Eutrophication science: where do we go from here? *Trends in Ecology and Evolution* 24(4), pp. 201-207.

Spiteri, C., Slomp, C., Regnier, P., Meile, C. and Van Cappellen, P. (2007). Modelling the geochemical fate and transport of wastewater-derived phosphorus in contrasting groundwater systems. *Journal of Contaminant Hydrology*, 92(1-2), pp.87-108.

Su, W., Sun, Q., Xia, M., Wen, Z. and Yao, Z. (2018). The Resource Utilization of Water Hyacinth (*Eichhornia crassipes* [Mart.] Solms) and Its Challenges. *Resources*, 7(3), p.46.

Tipping, E., Benham, S., Boyle, J., Crow, P., Davies, J., Fischer, U., Guyatt, H., Helliwell, R., Jackson-Blake, L., Lawlor, A., Monteith, D., Rowe, E. and Toberman, H. (2014). Atmospheric deposition of phosphorus to land and freshwater. *Environmental Science: Processes Impacts*, 16(7), pp.1608-1617.

Turton, A. (2012). A South African Perspective on Climate Change, Food Security and Water. Paper presented at the BRICS Academy Forum, New Delhi, March 2012. Available online at: http://anthonyturton.com/assets/my_documents/my_files/A_South_African_Perspective_on_Climate_Change.pdf.

Turton, A. (2008). *The state of water resources in South Africa: what the beverage industry needs to know*. Web document Version 2

Uttormark, P. & Hutchins, M. (1980). Input/output models as decision aids for lake restoration. *Journal of the American Water Resources Association*. 16(3):494-500. DOI: 10.1111/j.1752-1688.1980.tb03903.x.

van Belle, G. & Hughes, J. (1984). Nonparametric Tests for Trend in Water Quality. *Water Resources Research*. 20(1), pp.127-136. DOI: 10.1029/wr020i001p00127.

Verdouw, H., Van Echteld, C. and Dekkers, E. (1978). Ammonia determination based on indophenol formation with sodium salicylate. *Water Research*, 12(6), pp. 399-402.

Vörösmarty, C., McIntyre, P., Gessner, M., Dudgeon, D., Prusevich, A., Green, P., Glidden, S., Bunn, S., Sullivan, C., Liermann, C. and Davies, P. (2010). Global threats to human water security and river biodiversity. *Nature*, 467(7315), pp. 555-561.

Wagner, S. (2011) Biological Nitrogen Fixation. *Nature Education Knowledge*, 3(10), p.15

Walmsley, (2000). *Perspectives on eutrophication of surface waters: policy / research needs in South Africa: a review and discussion document.* WRC report no. KV 129/00. Water Research Commission, Pretoria.

Water Research Comission (WRC) (2012). Water resources of South Africa, 2012 study: Book of Maps. By A.K. Bailey and W.V. Pitman. Royal Haskoning DHV (Pty) Ltd. Pretoria, South Africa.

Wilkins, B. (2019). *Deciphering Soil Nitrogen Biogeochemical Processes Using Nitrogen and Oxygen Stable Isotopes.* PhD, Department of Chemistry, Purdue University.

Wilson, A., Chislock, M., (2013). Ecological control of cyanobacterial blooms in freshwater ecosystems. In : Ferrao Filho,A. (Ed.). Cyanobacteria: Ecol Toxicol Management. Nova Science Publishers, UK. pp. 1-16.

Zamalloa, C., Vulsteke, E., Albrecht, J. and Verstraete, W. (2011). The techno-economic potential of renewable energy through the anaerobic digestion of microalgae. *Bioresource Technology*, 102(2), pp.1149-1158.

Zambrano, L., Scheffer, M. and Martinez-Ramos, M. (2001). Catastrophic response of lakes to benthivorous fish introduction. *Oikos*, 94(2), pp.344-350.

Zhang, F., Lee, J., Liang, S. and Shum, C. (2015). Cyanobacteria blooms and non-alcoholic liver disease: evidence from a county level ecological study in the United States. *Environmental Health*, 14(1).

Zhang, J.-Z., Ortner, P. and Fischer, C. (1997). Determination of nitrite and nitrate in estuarine and coastal waters by gas segmented continuous flow colorimetric analysis, in *Methods for the Determination of Chemical Substances in Marine and Estuarine Environmental Matrices, 2nd ed., EPA/600/R-97/072*, Washington, D. C.: Environ. Prot. Agency.

CHAPTER 7: APPENDIX

7.1. Breakdown of seasonal P fluxes and trends of individual sites

Figures 7.1.1 to 7.1.5 show the seasonal P fluxes of the various inflow and outflow sites. Table 7.1.1 displays the descriptive statistics of the various inflow and outflow sites. It can be concluded that the Crocodile River was responsible for the vast majority of the river inflow flux, upwards of 99%. The left and right canals had similar fluxes and together were responsible for about 42% of the outflow flux. The seasonal Mann-Kendall trend test was used to detect trends in the Spot flow P fluxes of the inflow and outflow sites whilst taking into account seasonality of a 12-month period. The seasonal Mann-Kendall trend test *p*-values and Sen's Slope are shown in Table 7.1.2. All sites had significant trends. The Magalies River inflow site was the only site to have a decreasing trend.

Table 7.1.1: Descriptive statistics of seasonal P fluxes of all river inflow and outflow sites

	n	Mean (t/season)	Std.Dev (t/season)	Min (t/season)	Max (t/season)
Inflow Sites					
Crocodile River	32	147	243	57	590
Magalies River	32	1	3	0.01	6
Outflow Sites					
Left Canal	32	13	11	1	35
Right Canal	32	13	10	2	32
Radial Sluices	32	36	90	6	253

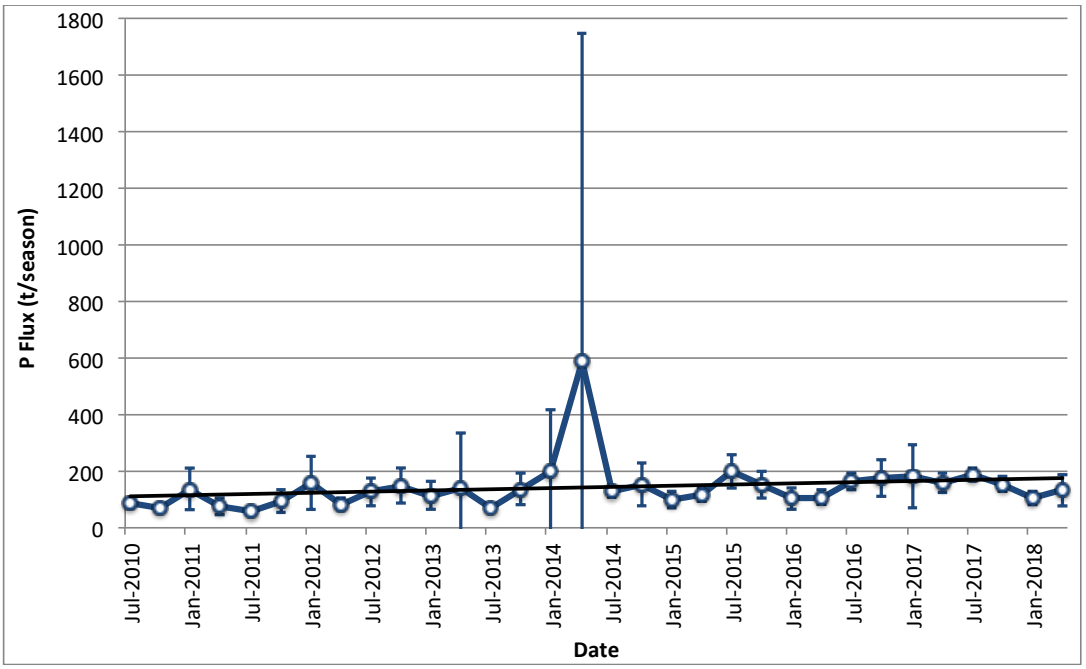

Fig 7.1.1: Seasonal P inflow flux (t/season) of the Crocodile River from July 2010 until April 2018. Calculations based on spot flow values. Error bars represent standard deviations. Straight line represents linear relationship (significant).

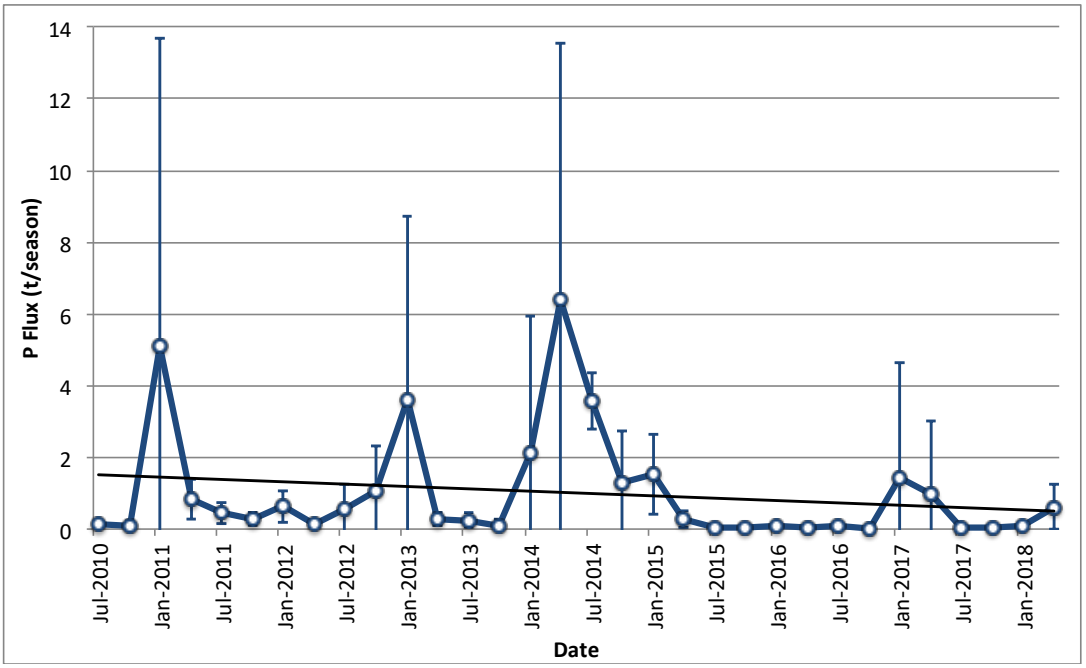

Fig 7.1.2: Seasonal P inflow flux (t/season) of the Magalies River from July 2010 until April 2018. Calculations based on spot flow values. Error bars represent standard deviations. Straight line represents linear relationship (significant)

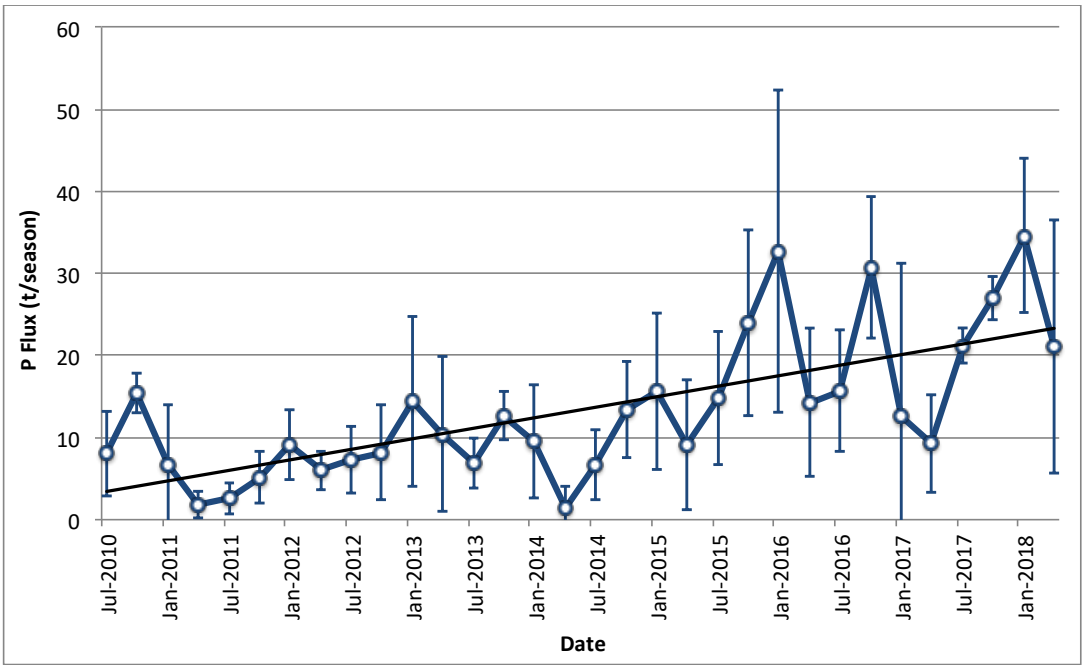

Fig 7.1.3: Seasonal P outflow flux (t/season) of the Left Canal from July 2010 until April 2018. Calculations based on spot flow values. Error bars represent seasonal standard deviations. Straight line represents linear relationship (significant).

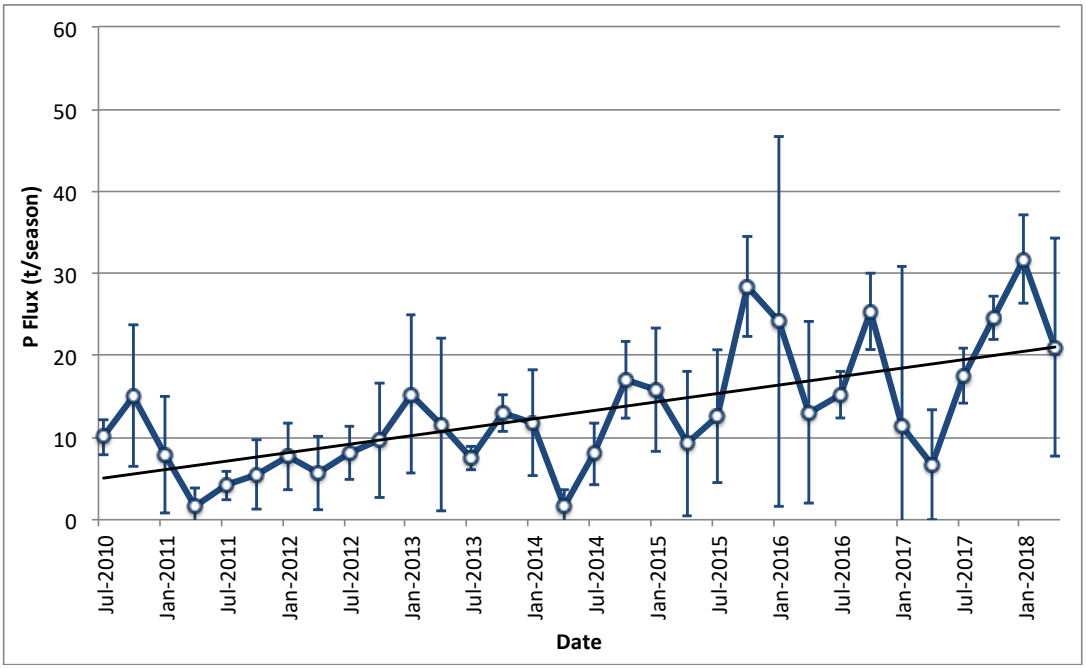

Fig 7.1.4: Seasonal P outflow flux (t/season) of the Right Canal from July 2010 until April 2018. Calculations based on spot flow values. Error bars represent seasonal standard deviations. Straight line represents linear relationship (significant).

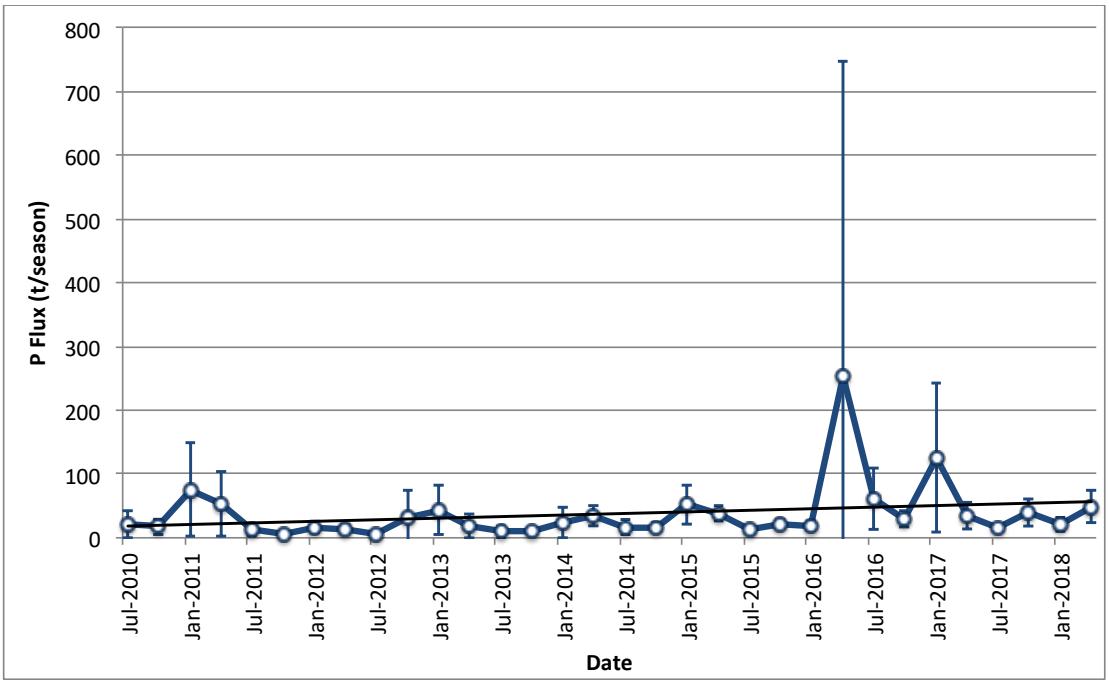

Fig 7.1.5: Seasonal P outflow flux (t/season) of the Radial Sluices from July 2010 until April 2018. Calculations based on Spot flow values. Error bars represent seasonal standard deviations. Straight line represents linear relationship (significant).

Table 7.1.2: Sen's Slope and seasonal Mann-Kendall trend test *p*-values of inflow and outflow sites ('*' indicates significant trend).

	Sen's Slope (t/a)	*p*-value	*n*
Inflows			
Crocodile River	41.4	0.0001*	95
Magalies River	-0.1	0.017*	94
Outflows			
Left Canal	8.3	0.0001*	94
Right Canal	6.5	0.0001*	94
Radial Sluices	6.0	0.006*	96

7.2. Time series of N and P inflow and outflow using Daily Average flow values

Figure 7.2.1 compares the seasonal P inflow from the Crocodile and Magalies rivers with the seasonal P outflow from the left canal, right canal and radial sluice from June 2010 until April 2018 using Daily Average flow values. Table 7.2.1 shows the descriptive statistics of the seasonal P river inflow and outflow using Daily Average flow values. For both the average seasonal inflow and the average seasonal outflow, the maxima are outliers. The Shapiro-Wilk normality test showed that the distributions of both the average seasonal P inflow and outflow were not normal (p-value = 0.0001 for inflow and 0.0002 outflow). A log transformation was successful in normalising the data (p-value = 0.347 for inflow, and 0.937 for outflow). Thus the paired two-sample t-test was used to detect a difference between the log-transformed distributions of the seasonal inflow and outflow groups (n = 32 for both groups). There was a significant difference between the mean seasonal inflow and outflow fluxes (p-value = 0.001).

Figure 7.2.3 compares the seasonal N inflow and from the Crocodile and Magalies rivers with the seasonal N outflow from the left canal, right canal and radial sluices from June 2010 until February 2018 using Daily Average flow values. For both the average seasonal inflow and the average seasonal outflow, the maxima were outliers. The Shapiro-Wilk normality test showed that the distributions of both the average seasonal N inflow and outflow were not normal (p-value = 0.004 for inflow and 0.0003 outflow). A log transformation was successful in normalising the data (p-value = 0.643 for inflow, and 0.795 for outflow). Thus the paired two-sample t-test was used to detect a difference between the log-transformed distributions of the seasonal inflow and outflow groups (n = 31 for both groups). There was a significant difference between mean seasonal inflow and outflow fluxes (p-value = 0.001).

Table 7.2.1: Descriptive statistics of seasonal P inflow and outflow (Daily Average flow)

	n	Mean (t/season)	Std.Dev (t/season)	Min (t/season)	Max (t/season)
P Inflow (Daily Average Flow)	31	140	68	58	436
P Outflow (Daily Average Flow)	31	47	32	13	171

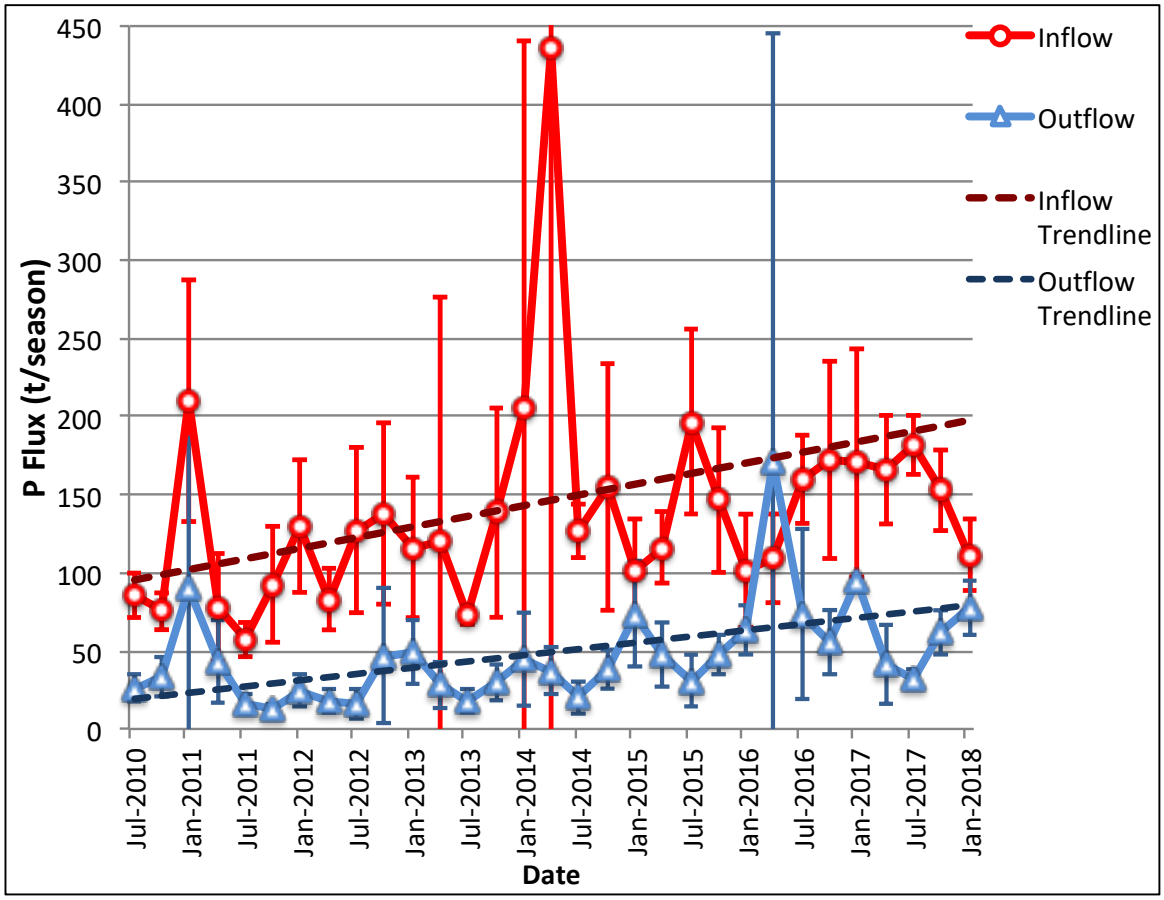

Fig. 7.2.1: Seasonal P river fluxes (using daily average flow) into and out of the Hartbeespoort Dam in tons from June 2010 until April 2018. Error bars represent standard deviations.

Table 7.2.2: Descriptive statistics of seasonal N inflow and outflow (Daily Average flow)

	n	Mean (t/season)	Std.Dev (t/season)	Min (t/season)	Max (t/season)
N Inflow (Daily Average Flow)	31	1098	473	389	2549
N Outflow (Daily Average Flow)	31	508	257	149	1293

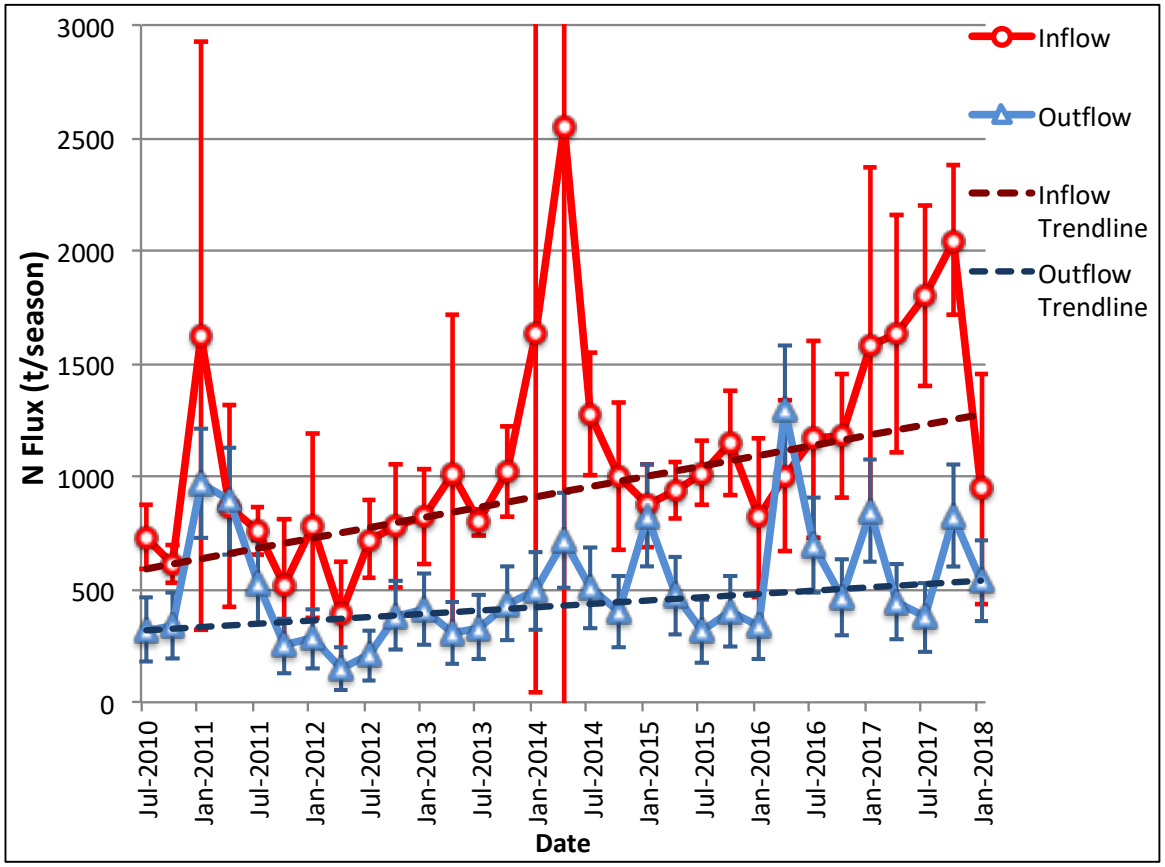

Fig. 7.2.3: Seasonal N river fluxes (using daily average flow) into and out of the Hartbeespoort Dam in tons per annum from June 2010 until February 2018. Error bars represent standard deviations. Outflow trend not significant.

7.3. Did flow increase over the study time period?

The seasonal Mann-Kendall test was used to test if there was a trend in the average monthly flow at Site 90164 on the Crocodile River from June 2010 until March 2018. Average monthly flows were calculated using the complete raw flow dataset. Flow did not show a trend in the series (p-value = 0.319, n = 94). This means that flow did not account for the observed increasing nutrient flux trends. The formula of the linear regression was "flow = 27.20574-0.0002328600*date". The slope of the line is negative and close to zero, which could have indicated a slight decrease in flow over the time period. However, the p(F) of the linear regression model was 0.822. Thus the model is not significant.

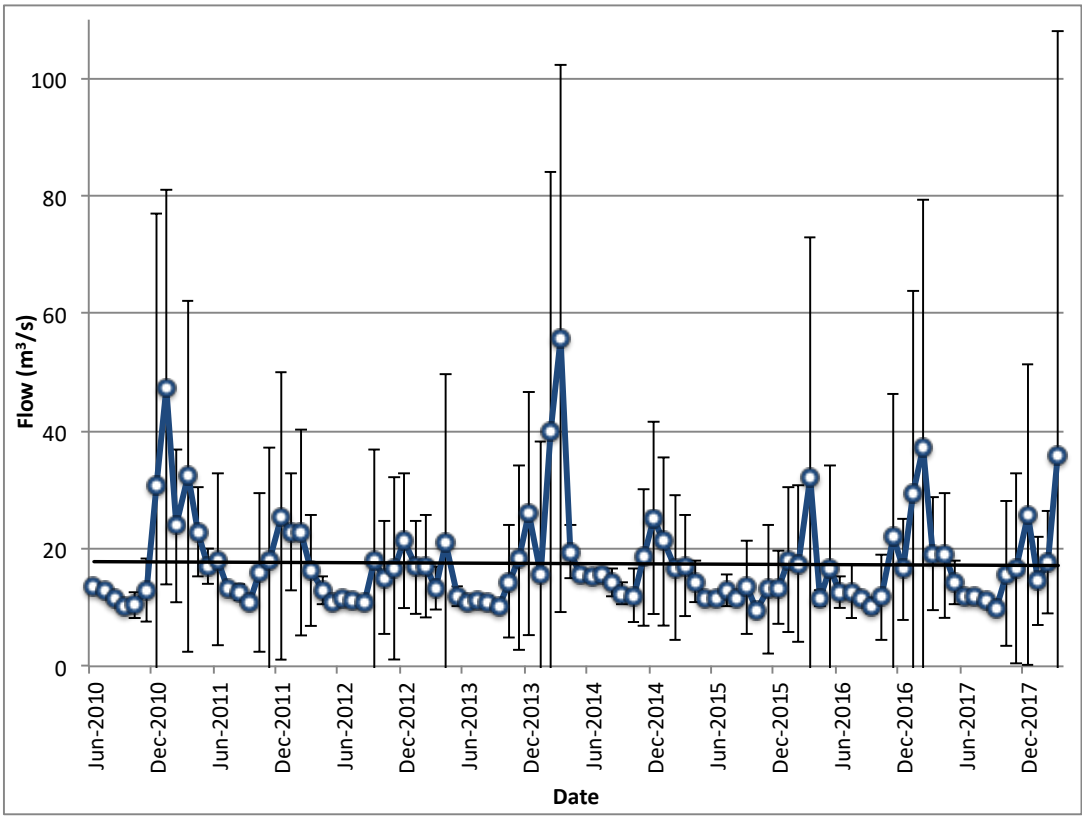

Fig. 7.3.1: Average monthly flow (m^3/s) at site 90164 on the Crocodile River from June 2010 until March 2018. Error bars represent standard deviation. Straight line represents the linear relationship (not significant).

7.4. Relationship between orthophosphate (OP) and total phosphorus (TP)

Figure 7.4.1 shows the relationship between the orthophosphate proportion of total phosphorous in relation to flow. The minimum percentage composition of orthophosphate in total phosphorus was 0.73% and the maximum 99.7%. The mean was 69.22%, the median is 70.56% and the standard deviation is 18.06%. There were two major negative outliers. A Spearman Rank correlation test was used to determine if there was a correlation between the OP/TP ratio and spot flow. There was a weak inverse linear relationship between the variables (-0.312) (*p*-value <0.0001). Spearman's rho was 0.097 which means that 9.7% of the data was explained by the model.

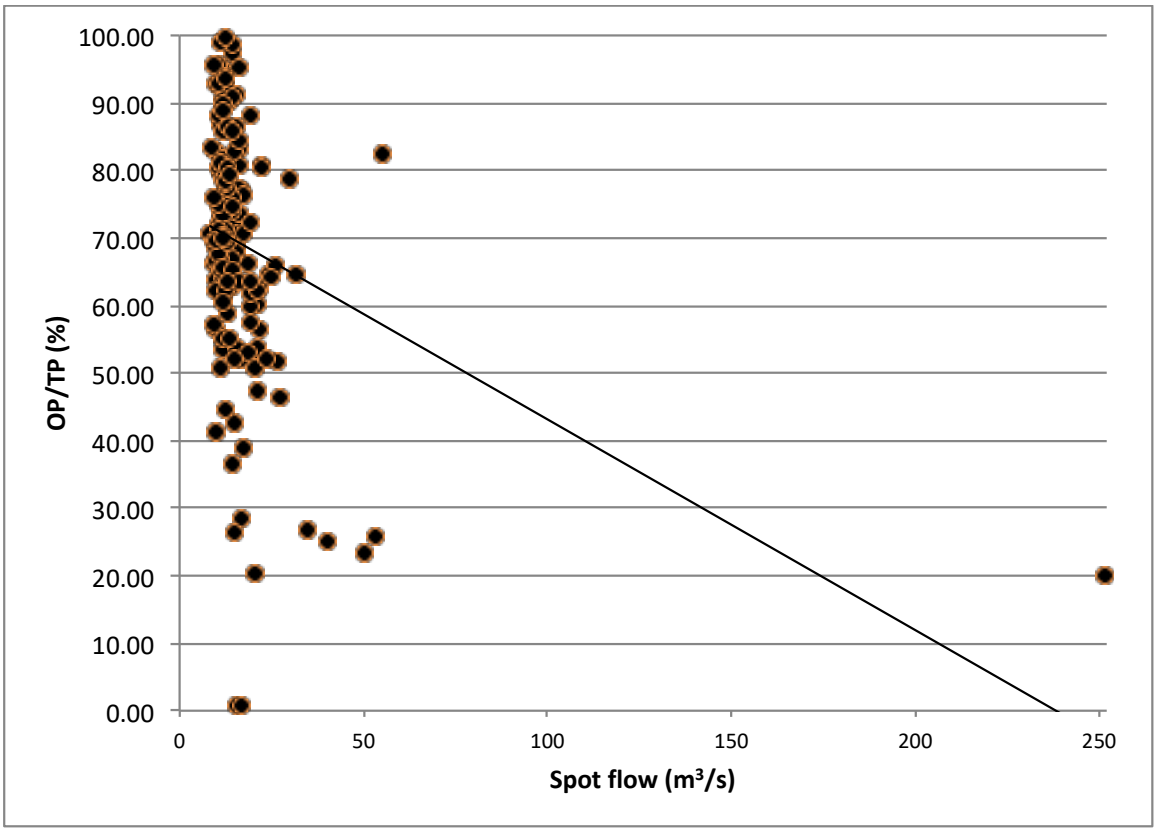

Fig. 7.4.1: Relationship between the percentage component of orthophosphate (OP) comprised in total phosphorous (TP) relalative to spot flow (m^3/s) at site 90164 on the Crocodile River (*n* = 177). The straight line represnts the linear relationship.